Euscorpius

Occasional Publications in Scorpiology

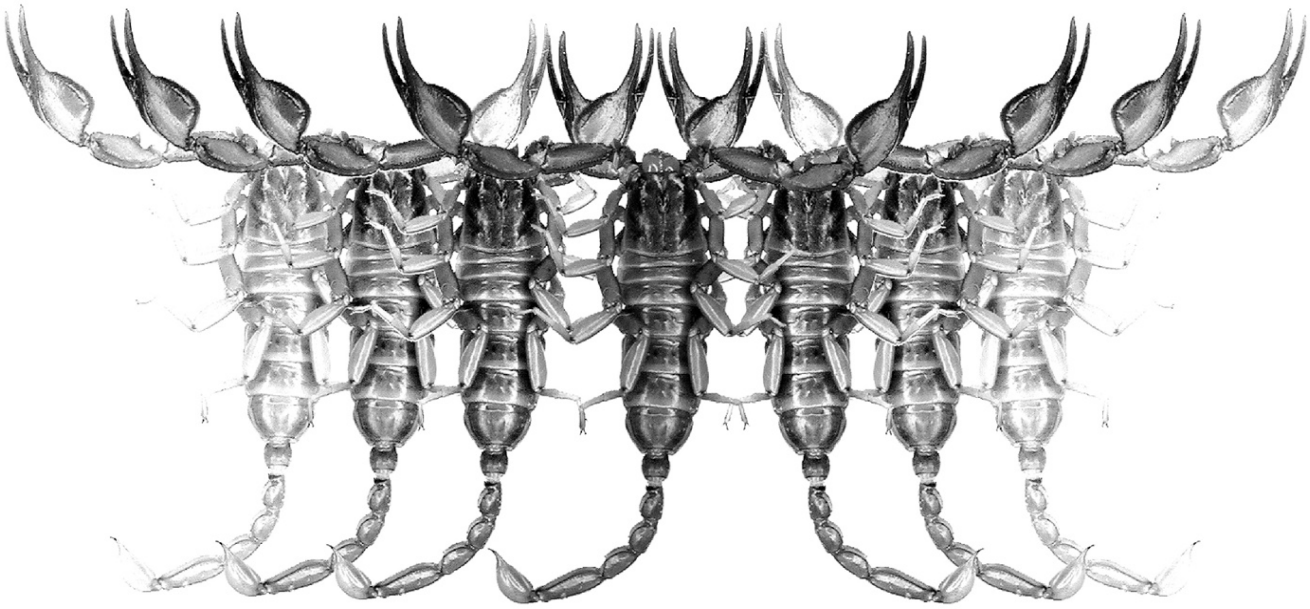

Description of the adult male *Scorpiops tongtongi* Tang, 2022, with further comments on the genus *Scorpiops* Peters, 1861 in China (Scorpiones: Scorpiopidae)

Victoria Tang

September 2023 — No. 377

Euscorpius

Occasional Publications in Scorpiology

EDITOR: **Victor Fet**, Marshall University, **'fet@marshall.edu'**

ASSOCIATE EDITOR: **Michael E. Soleglad, 'msoleglad@gmail.com'**

TECHNICAL EDITOR: **František Kovařík, 'kovarik.scorpio@gmail.com'**

Euscorpius is the first research publication completely devoted to scorpions (Arachnida: Scorpiones). ***Euscorpius*** takes advantage of the rapidly evolving medium of quick online publication, at the same time maintaining high research standards for the burgeoning field of scorpion science (scorpiology). ***Euscorpius*** is an expedient and viable medium for the publication of serious papers in scorpiology, including (but not limited to): systematics, evolution, ecology, biogeography, and general biology of scorpions. Review papers, descriptions of new taxa, faunistic surveys, lists of museum collections, and book reviews are welcome.

Derivatio Nominis

The name ***Euscorpius*** Thorell, 1876 refers to the most common genus of scorpions in the Mediterranean region and southern Europe (family Euscorpiidae).

Euscorpius is located at: https://mds.marshall.edu/euscorpius/
Archive of issues 1-270 see also at: http://www.science.marshall.edu/fet/Euscorpius

(Marshall University, Huntington, West Virginia 25755-2510, USA)

ICZN COMPLIANCE OF ELECTRONIC PUBLICATIONS:

Electronic ("e-only") publications are fully compliant with ICZN (*International Code of Zoological Nomenclature*) (i.e. for the purposes of new names and new nomenclatural acts) when properly archived and registered. All ***Euscorpius*** issues starting from No. 156 (2013) are archived in two electronic archives:

- **Biotaxa,** http://biotaxa.org/Euscorpius (ICZN-approved and ZooBank-enabled)
- **Marshall Digital Scholar**, http://mds.marshall.edu/euscorpius/. (This website also archives all *Euscorpius* issues previously published on CD-ROMs.)

Between 2000 and 2013, ICZN ***did not accept online texts*** as "published work" (Article 9.8). At this time, *Euscorpius* was produced in two ***identical*** versions: online (*ISSN 1536-9307*) and CD-ROM (*ISSN 1536-9293*) (laser disk) in archive-quality, read-only format. Both versions had the identical date of publication, as well as identical page and figure numbers. ***Only copies distributed on a CD-ROM*** from ***Euscorpius*** in 2001-2012 represent published work in compliance with the ICZN, i.e. for the purposes of new names and new nomenclatural acts.

In September 2012, ICZN Article 8. What constitutes published work**,** has been amended and allowed for electronic publications, disallowing publication on optical discs. From January 2013, ***Euscorpius*** discontinued CD-ROM production; only online electronic version (ISSN 1536-9307) is published. For further details on the new ICZN amendment, see http://www.pensoft.net/journals/zookeys/article/3944/.

Publication date: 4 September 2023

http://zoobank.org/urn:lsid:zoobank.org:pub:50D83584-CFB9-4170-B27C-45C86C94B741

Euscorpius — Occasional Publications in Scorpiology. 2023, No. 377

Description of the adult male *Scorpiops tongtongi* Tang, 2022, with further comments on the genus *Scorpiops* Peters, 1861 in China (Scorpiones: Scorpiopidae)

Victoria Tang

Zhangyang Rd. 200120, Pudong New District, Shanghai, China; email: jibril.flueqel@gmail.com

http://zoobank.org/urn:lsid:zoobank.org:pub:50D83584-CFB9-4170-B27C-45C86C94B741

Summary

Adult male *Scorpiops tongtongi* Tang, 2022 is described based on recently collected specimens, which revealed a strong sexual dimorphism in the pedipalp finger lobe of this species (present in males, absent in females), lending more support to the separation from its geographic neighbors, *S. jendeki* Kovařík, 1994, *S. shidian* (Qi et al., 2005), *S. zhangshuyuani* Ythier, 2019, and *S. beccaloniae* (Kovařík, 2005). The morphological studies of Chinese *Scorpiops* are further discussed. A refined mensurational method of *Scorpiops* pedipalp chela is proposed. Morphological comparisons of both quantitative and qualitative characters for all *Scorpiops* from Yunnan are provided, along with a dichotomous key to those species.

Introduction

The genus *Scorpiops* Peters, 1861 is the most speciose genus in China, with 31 species (including the dubious records of two species, *S. hardwickii* (Gervais, 1843) and *S. petersii* Pocock, 1893). Among those, the Yunnan Province accommodates 10 species (excluding the two unidentified populations mentioned in Tang (2022c)). The remaining 21 species were described/recorded from Xinjiang, Chongqing, Hubei, and Xizang Provinces (Tang, 2022c; Lv & Di, 2022; Lv et al., 2023). In Xinjiang, the genus is represented by a single species, *S. taxkorgan* Lourenço, 2018.

Scorpiops tongtongi Tang, 2022 was described from Yingjiang County, Dehong Prefecture, Yunnan Province, China. In the original description, Tang (2022b) conducted a preliminary review on this genus in Yunnan in order to confirm the validity of that new species as only a single adult female specimen was available. During that investigation, the author first pointed out the problems, confusion, and inconsistency in the previous descriptions of Yunnan *Scorpiops* by different authors. Then, new morphological characters proposed by Kovařík et al. (2020) were summarized in terms of their applications in Yunnan *Scorpiops*. Finally, supplementary data on six previous species were obtained from the new material, based on which the utility and problems of several morphological characters were discussed. The Yunnan population of *S. kubani* Kovařík, 2004 was subsequently found to be a misidentification, and a new species, *S. lowei* Tang, 2022 was described (Tang, 2022c).

The present study supplements the description of adult male *S. tongtongi* based on recently collected specimens. The morphological identification of *Scorpiops* and the taxonomy of Chinese *Scorpiops* are further discussed, with an emphasis on chela length and width measurement. New dichotomous key to the *Scorpiops* of Yunnan is also provided, along with diagnostic tables for both quantitative and qualitative characters.

Methods, Material & Abbreviations

Morphology. Nomenclature and measurements mostly follow Stahnke (1970), Soleglad & Sissom (2001), Kovařík (2009), and Kovařík & Ojanguren-Affilastro (2013), except for trichobothriotaxy (Vachon, 1974), chelicera (Soleglad & Fet, 2003a), sternum (Soleglad & Fet, 2003a) and pedipalp patellar and femur carinae (Prendini et al., 2021). Hemispermatophore terminology generally follows Kovařík et al. (2020) and Monod et al. (2017). See below for further explanation. Finger dentition color markings: inner accessory denticles = yellow, median denticles = green, inner denticles = blue, outer denticles = red. STP. files (in ZIP.) of caliper modification are available for download on ResearchGate: https://www.researchgate.net/publication/373093259_Caliper_modification.

Materials. Four of five specimens of *Scorpiops tongtongi* were dead when the author received them. To avoid decomposition, they were instantly immersed into the embalming fluid (purchased from Beijing Jiaying Art Insectarium, China) that stiffens the specimen by denaturing the protein molecules in the tissues and membranes; therefore, the specimens were pinned on a foam board at desired angles with needles prior to the immersion for the convenience of subsequent observation and photography (Fig. 96). The single living adult male was not killed for inspection (Fig. 55). However, it was anaesthetized with carbon dioxide in order to record the diagnostic data.

The detailed description of the adult male *S. tongtongi* was solely based on the dead specimen, but the diagnosis included data (chela L/W, telson L/D, PTC, trichobothria and finger dentitions) of both male specimens. Membranous paraxial organs enveloping the hemispermatophores were hydrolyzed in trypsin solution and then manually dissected with forceps. Photos of minute structures of pectines, cuticle surface and hemispermatophore capsule were taken by Mitutoyo M Plan Apo 10X objective lens connected to Raynox DCR-150 lens.

Abbreviations. D, depth; L, length; W, width; PTC, pectinal tooth count; IAD, inner accessory denticle; MD, median denticle; ID, inner denticle; OD, outer denticle. Other abbreviations explained in the text.

Specimen Depositories. VT (Personal collection of Victoria Tang, Shanghai, China).

Comparative material. *Scorpiops jendeki* Kovařík, 1994, **China**, Yunnan Province, Dehong Prefecture, Lianghe County, 24°49'07"N 98°17'44"E (24.8185189°N 98.2954599°E), 1038 m a. s. l., 5 August 2023, 1♂5♀, leg. Qingquan Jia; VT.

Scorpiops xui (Sun & Zhu, 2010), **China**, Yunnan Province, Menglian County, Nayun Town, 22°18'16" N 99°35'02" E (22.304578°N 99.583786°E), 954 m a. s. l., 13 February 2023, 1♂4♀ (Figs. 61–62), leg. Qiu Hang; VT.

Scorpiops yangi (Zhu et al., 2007), **China**, Yunnan Province, Wenshan Prefecture, Maguan County, Gulinqing Township, 22°47'58" N 103°57'01" E (22.79942559°N 103.95028024°E), 1538 m a. s. l., 16 July 2023, 1♂1♀ (Figs. 63–64), leg. Qingquan Jia; VT.

Other material from Yunnan listed in Tang (2022b, 2022c); materials from Xizang (Tibet Autonomous Region) lacked information and were used only as demonstrative illustrations for discussing morphological study methods (see text).

Systematics

Scorpiopidae Kraepelin, 1905
Scorpiops Peters, 1861
Scorpiops tongtongi Tang, 2022

(Figures 1–56, 96, 113–116; Tables 1–3)

http://zoobank.org/urn:lsid:zoobank.org:act:7A317530-A04C-48E8-8061-B99958D3DED6

Type locality and type depository. Holotype ♀, **China**, Yunnan Province, Dehong Prefecture, Yingjiang County, 24°37'39"N 97°38'27"E, 1451 m a. s. l; VT.

New material examined. **China**, Yunnan Province, Dehong Prefecture, Yingjiang County, near Chashanzhai, 24°37'07"N 97°39'11"E (24.618553°N 97.652983°E), 1380 m a. s. l., 19 June 2023, 1♂ (alive when received; Fig. 55), near Rongshuwang, 24°40'18"N 97°36'20"E (24.671558°N 97.605458°E), 950 m a. s. l., 10 July 2023, 1♂3♀ (dead when received; Fig. 96), leg. Chenkai Tang; VT.

Diagnosis (modified from Tang, 2022b). Total length ca. 40–45 mm for females and 44 mm for male. Base color uniformly reddish brown to brownish black, telson and parts of legs brown to brownish yellow. Pectinal teeth number 5–6 in females and 7 in males; fulcra absent; pectines form one compact unit with an incomplete furrow between areas where marginal and middle lamellae are usually delimited. Patella of pedipalp with 17–18 external and 6–7 ventral trichobothria. Chela with 4 *V* series trichobothria located on ventral surface. Chelal trichobothrium Eb_3 located in middle of manus between trichobothria *Dt* and *Est*. Dentate margin of movable fingers of pedipalps not obviously undulate (no proximal lobe present) in female but strongly undulate in male (proximal lobe present) and create prominent gap when closed (in combination with the strong ventral incision on dentate margin of fixed finger). Chela length to width ratio 2.9–3.17 in females and 2.71–2.91 in males. Pedipalp movable finger with ca. 39–52 IAD, which have the same size as MD (ca. 86–96 in number) and create a second row of denticles; there are also 3–5 ID and 10–12 OD present. Tarsomere II of leg III with 5–9 stout median ventral spinules in a single row, and two pairs of flanking setae. Metasoma I with 10 carinae, II–IV with 8 carinae, V with 7 carinae. Telson relatively short and bulbous, and densely covered with fine granules, length to depth ratio 2.8–3.4 in females and 2.63–2.84 in males; annular ring developed (circumference constricted at vesicle-aculeus juncture).

Description (of adult male). The hereby description of adult male *S. tongtongi* (Figs. 1–2) is modified from the original description for the holotype female, with coloration disregarded. Both white light and UV light (except for the overall habitus) photos are provided. Figures of pectines, trichobothria and finger dentitions of the females, the living male and the left pedipalp patella of the dead male are available on ResearchGate as supplementary files (in ZIP.).

Prosoma and mesosoma (Figs. 3–12, 31–34). *Prosoma*: Carapace with 3 pairs of lateral eyes of which two are larger and one is smaller. Superciliary carinae of the median ocelli smooth, short and compact, closely spaced. Median dorsal part of the carapace (ca. half of total area) planar, from anterior to posterior margins; lateral surfaces slanting downwards. Lateral surfaces with a pair of shallow central lateral sulci and prominent posterior lateral sulci; posterior marginal sulcus obvious. Entire carapace generally smooth, sparsely covered with small to moderate sized granules; distinct carinae absent. Anterior margin of carapace with a prominent median notch (emargination) leading to a deep, wide, smooth anteromedian sulcus. Circumocular sulcus is connected with anteromedian sulcus anteriorly, and with posteromedian sulcus posteriorly. Larger granules concentrated at edges flanking anteromedian sulcus, and above and posterior to lateral ocelli. Chelicerae with dorsal surface smooth and ventral surface setose; macrosetae localized on fixed finger. Dorsal distal, ventral distal and distal denticles of cheliceral fingers very long. *Mesosoma*: tergites sparsely covered with smaller to moderate granules, becoming slightly denser and larger closer to posterior margins, with one very weak median carina indicated (concealed by random

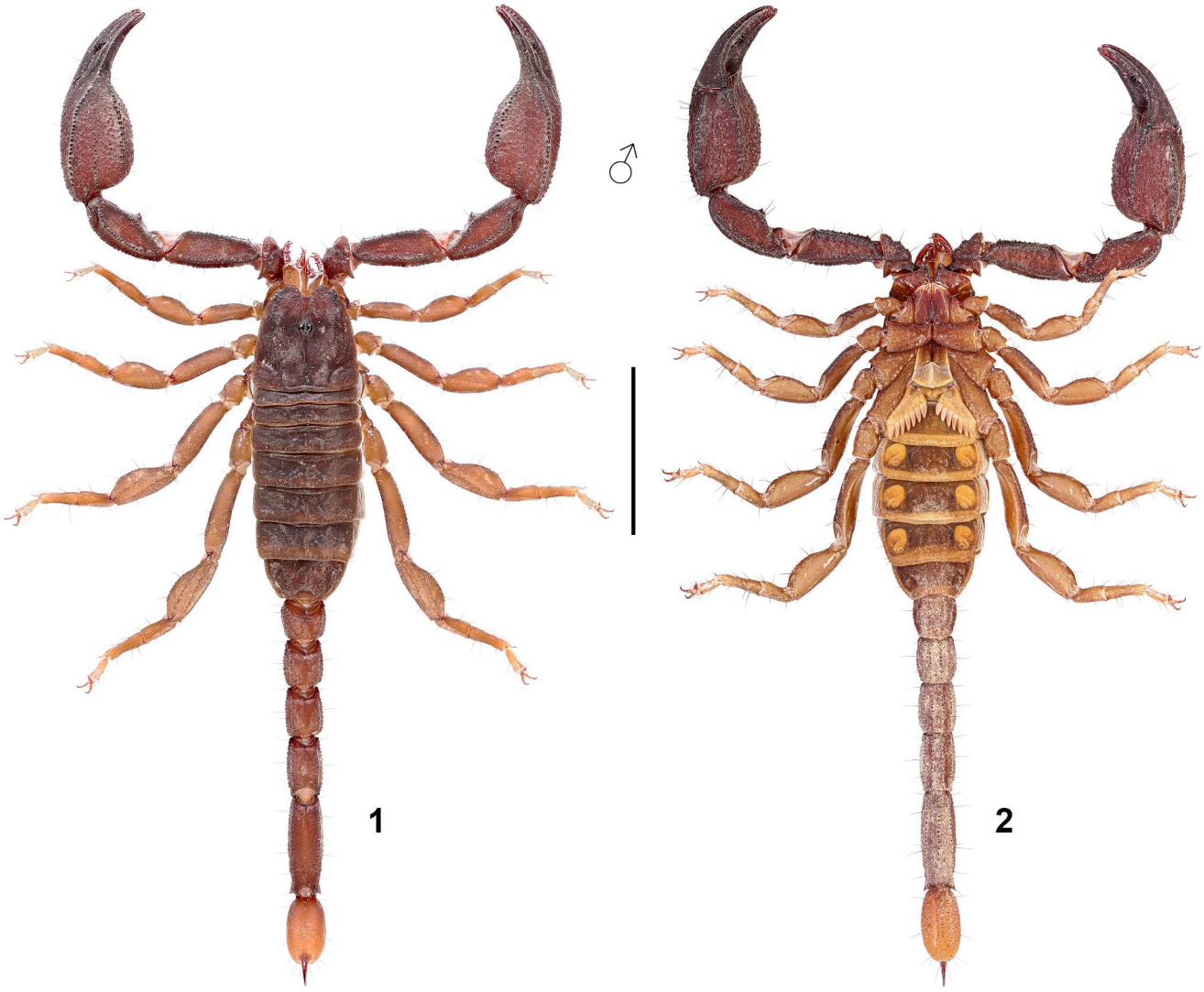

Figures 1–2. *Scorpiops tongtongi*, male, habitus in dorsal (1) and ventral (2) views, under white light. Scale bar = 10 mm.

granules on VII). Tergite VII pentacarinate. Sternites smooth with sparse macrosetae and fluorescent microsetae; sternites IV–VI with two axisymmetric, curved furrows furnished with lattice microstructure (shattered on VII), sternite VII with four weakly granulate carinae; respiratory spiracles suboval. Genital operculum divided into two halves, with a pair of genital papillae at the base. Pectines form one compact unit with incomplete furrow between areas where marginal and middle lamellae are usually delimited; pectine teeth number 7; area of peg sensilla with cover the majority of each pectinal tooth; fulcra absent; fluorescent microsetae stout.

Metasoma and telson (Figs. 39–46). Metasoma sparsely hirsute and granulated; carinae with relatively large granules. Metasomal segment I with 10 carinae, II–IV with 8 carinae, and V with 7 carinae. Median lateral carina of metasoma II–IV incomplete, presented by several posterior granules. Granules relatively smaller and thinner on dorsosubmedian (I–IV), median lateral (V) and dorsolateral (V) carinae, larger and rounded on dorsolateral (I–IV), median lateral (I), ventrolateral (I–III) and ventrosubmedian (I–III) carinae. becoming conspicuously sharper on ventrolateral (IV–V), ventrosubmedian (IV) and ventromedian carinae (V). Anal arch armed with sharp granules. Telson proportionally short and bulbous; dorsal surface smooth, lateral and ventral surfaces with dense, fine granulation; annular ring developed. Vesicle sparsely covered with fluorescent microsetae and few macrosetae; lateral surface with one longitudinal sulci close to dorsal surface, ventral surface with two parallel longitudinal sulci, all four sulci shallow and basically smooth (covered with extremely minute granules). Aculeus smooth, weakly curved (tip broken).

Pedipalps (Figs. 13–30, 35–38). Pedipalps sparsely hirsute, intercarinal surfaces scattered with small to moderate granules and patches of squamous/lattice microstructures; fluorescent microsetae show weak iridescence under white light, visible under high magnification. Patella with 17–18 external (4–5 *et*,

Figures 3–4. *Scorpiops tongtongi*, male, prosoma and mesosoma in dorsal view, under white (3) and UV (4) light. Scale bar = 10 mm.

4 *est*, 2 *em*, 2 *esb*, 5 *eb*) and 6–7 ventral trichobothria. Chela with 4 *V* series trichobothria located on ventral surface. Chelal trichobothrium Eb_3 located in middle of manus between trichobothria *Dt* and *Est*. Femur and patella granulated. Femur with 6 granulose carinae; promedian carina incomplete, composed of several large, discrete granules; retroventral carina incomplete, deconstructed into small, random granules; granules larger on prodorsal, retrodorsal, retromedian and proventral carinae, especially the retromedian carina. Patella with 5 granulose carinae, composed of large granules; granules larger and denser on retrodorsal, retromedian and retroventral carinae, discrete on prodorsal and proventral carinae; prolateral surface with two small internal apophyses. Manus dorsally with fine, rounded granules; largest granules constitute digital, dorsal marginal and ventromedian carinae; moderate size granules present on interomedian carina;

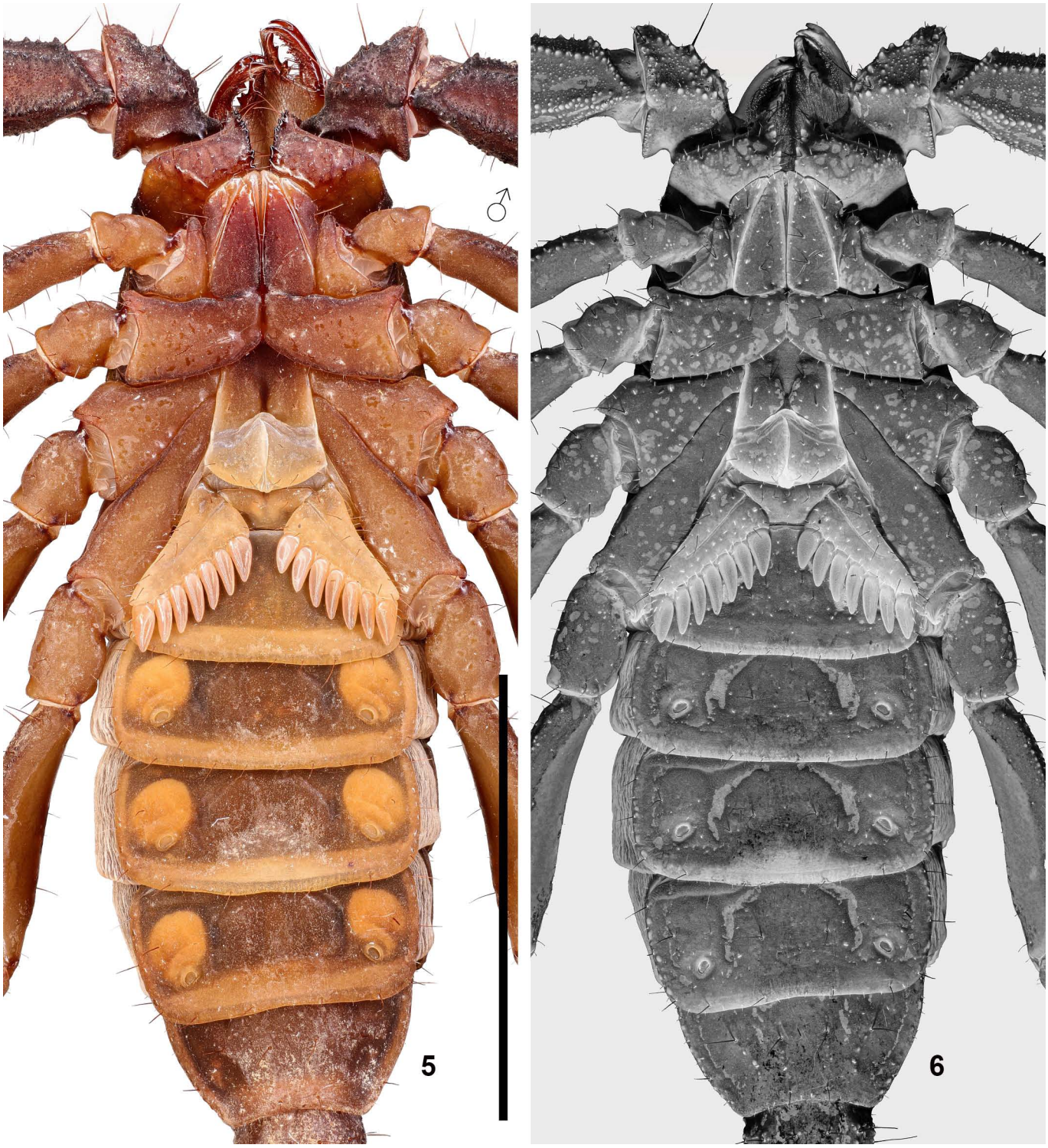

Figures 5–6. *Scorpiops tongtongi*, male, prosoma and mesosoma in ventral view, under white (5) and UV (6) light. Scale bar = 10 mm.

subdigital, dorsal secondary, dorsal internal, ventrointernal, ventroexternal, and external secondary carinae relatively weak, incomplete or obsolete, gradually diffusing to dispersed granules. Dentate margin of movable fingers strongly undulate (proximal lobe present) and create prominent gap when closed (in combination with the strong ventral incision on dentate margin of fixed finger). Movable fingers (left/right) with 52/49 IAD, which have the same size as MD (96/91 in number) and form a second row that terminated at the proximity of lobe; 4/4 ID and 12/11 OD also present, larger than IAD and MD.

Legs (Figs. 47–54). Tibia and tarsomeres of legs with several macrosetae and fluorescent microsetae not arranged into bristle combs. Basitarsi of legs I–II with two rows of short spinules, a pair of pedal spurs present on basitarsi of all legs.

Dimensions (mm)		***Scorpiops tongtongi*** ♂
Carapace	L / W	6.28 / 6.66
Mesosoma	L	14.14
Tergite VII	L / W	3.32 / 5.29
Metasoma + telson	L	23.63
Segment I	L / W / D	2.49 / 2.59 / 2.16
Segment II	L / W / D	2.71 / 2.34 / 2.08
Segment III	L / W / D	2.77 / 2.17 / 2.07
Segment IV	L / W / D	3.58 / 2.12 / 2.03
Segment V	L / W / D	5.66 / 2.05 / 1.94
Telson	L / W / D	6.42 / 2.32 / 2.44
Pedipalp	L	23.33
Femur	L / W	5.82 / 2.13
Patella	L / W	5.79 / 2.66
Chela	L	11.72
Manus	L / W / D	6.84 / 4.03 / 3.88
Fixed Finger	L	4.88
Movable finger	L	6.76
Total	**L**	**44.02**
Pectine Teeth	Left / Right	7 / 7

Table 1. Measurements of a male *Scorpiops tongtongi*. Abbreviations: length (L), width (W, in carapace it corresponds to posterior width), depth (D).

Telotarsi of legs I–IV with a row of short, stout ventromedian spinules that has 2 spinules on both ends and 2–5 spinules in the middle (i.e., 6–9 in total). Ungues moderately long and curved. Femur with 3–4 and patella 4–5 carinae; both femur and patella finely granulated, with sparse setae.

Hemispermatophores (Figs. 56–60). Lamelliform in profile. Distal lamina long, moderately slender; basally constricted, terminally coiled and tapered. Capsule conforms to 2-folds bauplan; distal posterior lobe marginally sclerotized and armed with ca. 9 denticles; lateral hook entirely sclerotized, apically sharpened; terminal membrane of sperm duct spiculate and translucent; basal carina accords with Group 4 (Kovařík et al., 2020: 27), sclerotized and distally expended into a plate with polydentate basal crest bearing crown-like structure. Trunk broad with mid-axial rib dividing it into anterior and posterior halves, distal end of the axial rib connected to the sclerotized distal carina of the capsule by a narrow junction, truncal flexure absent. Pedicel (= foot, in Kovařík et al., 2020) broad, soft and translucent.

Measurements. See Table 1.

Variation. Both males had 7 teeth on each pectine. The examined dead male had one additional trichobothrium in the *et* series and one absent trichobothrium in the *V* series on its left pedipalp patella. The living male had 17 external and 7 ventral trichobothria on both of its patellae, identical with the right pedipalp of the dead male. The 11th OD (on its right movable finger) of the dead male nearly fitted into the MD series but was recognized by the prominent gap it created between two adjacent MDs. Living male with 10/10 OD, 86/89 MD, 50/50 IAD, and 5/5 ID on its left/right movable fingers; right movable finger with one additional enlarged "IAD" (excluded) between the first IAD and third ID.

Note. In the original description, Tang (2022b: 5, 10, fig. 11) considered fulcra to be present in the holotype female. However, based on the current inspection of new materials with improved photographic technologies, it is now confirmed that *S. tongtongi* does lack fulcra. The triangular interdental membrane was mistaken as the fulcrum in the original description, which also appeared fluorescent under UV light. Ambiguous figures in the past literature and contradiction between statements in the papers published by other authors and personal observations also led Tang (2022b: 21, 34, 40) to believe that it is uncertain whether there are *Scorpiops* species that lack fulcra. Later, Lv & Di (2022: figs. 11, 13, 43, 45, 75, 77) well illustrated the pectine morphology of three Tibetan congeners which *S. tibetanus* Hirst, 1911 clearly differed from *S. atomatus* Qi et al., 2005 and *S. lourencoi* Lv & Di, 2022 by the lack of pectinal fulcra.

Sexual dimorphism. The three new females were examined in terms of their chela-L/W, telson L/D, PTC, trichobothria and finger dentition. Ratiometrics of chela and telson are

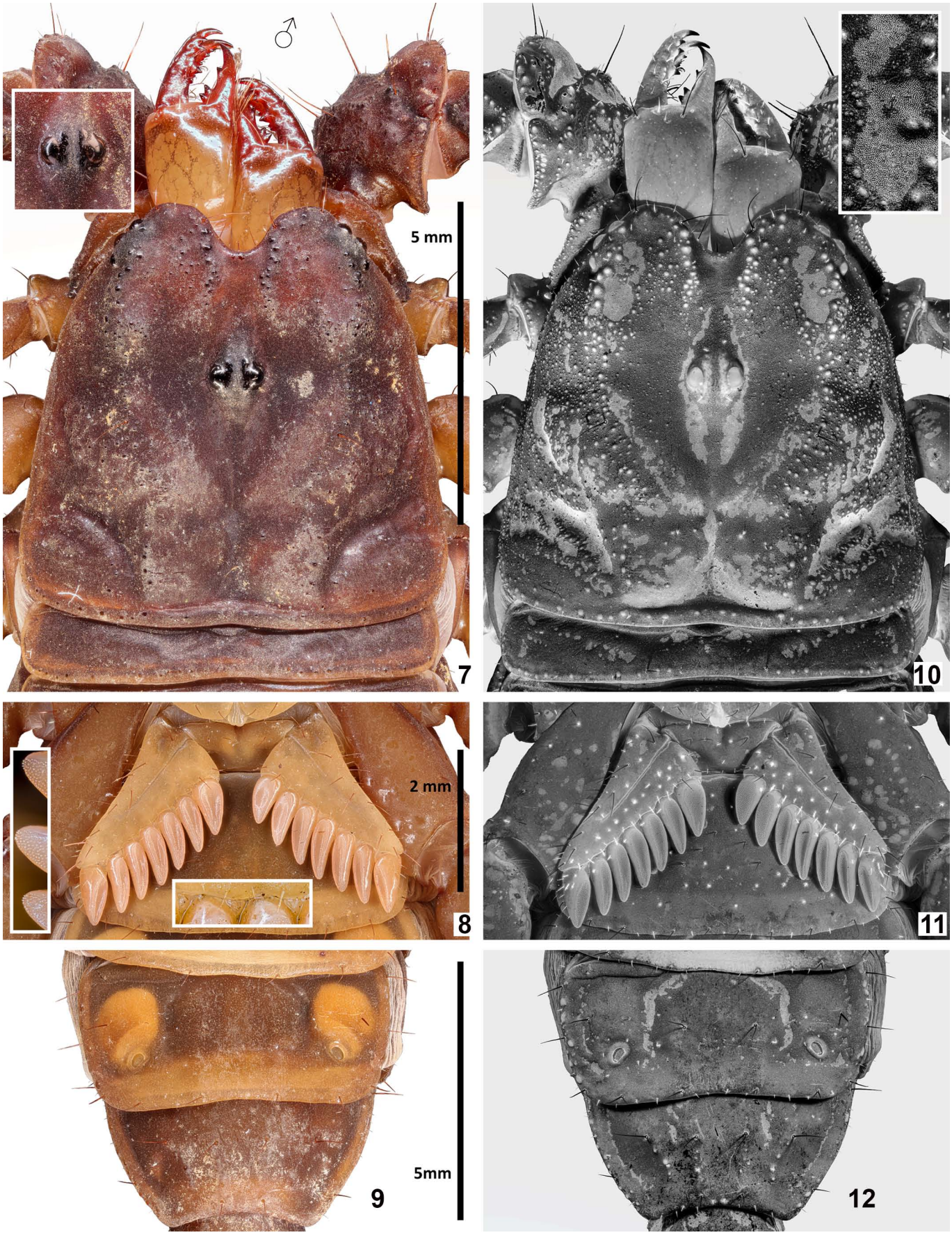

Figures 7–12. *Scorpiops tongtongi*, male, carapace (7, 10), pectines (8, 11) and sternites VI–VII (9, 12). **Figures 7–9**. Under white light. **Figures 10–12**. Under UV light.

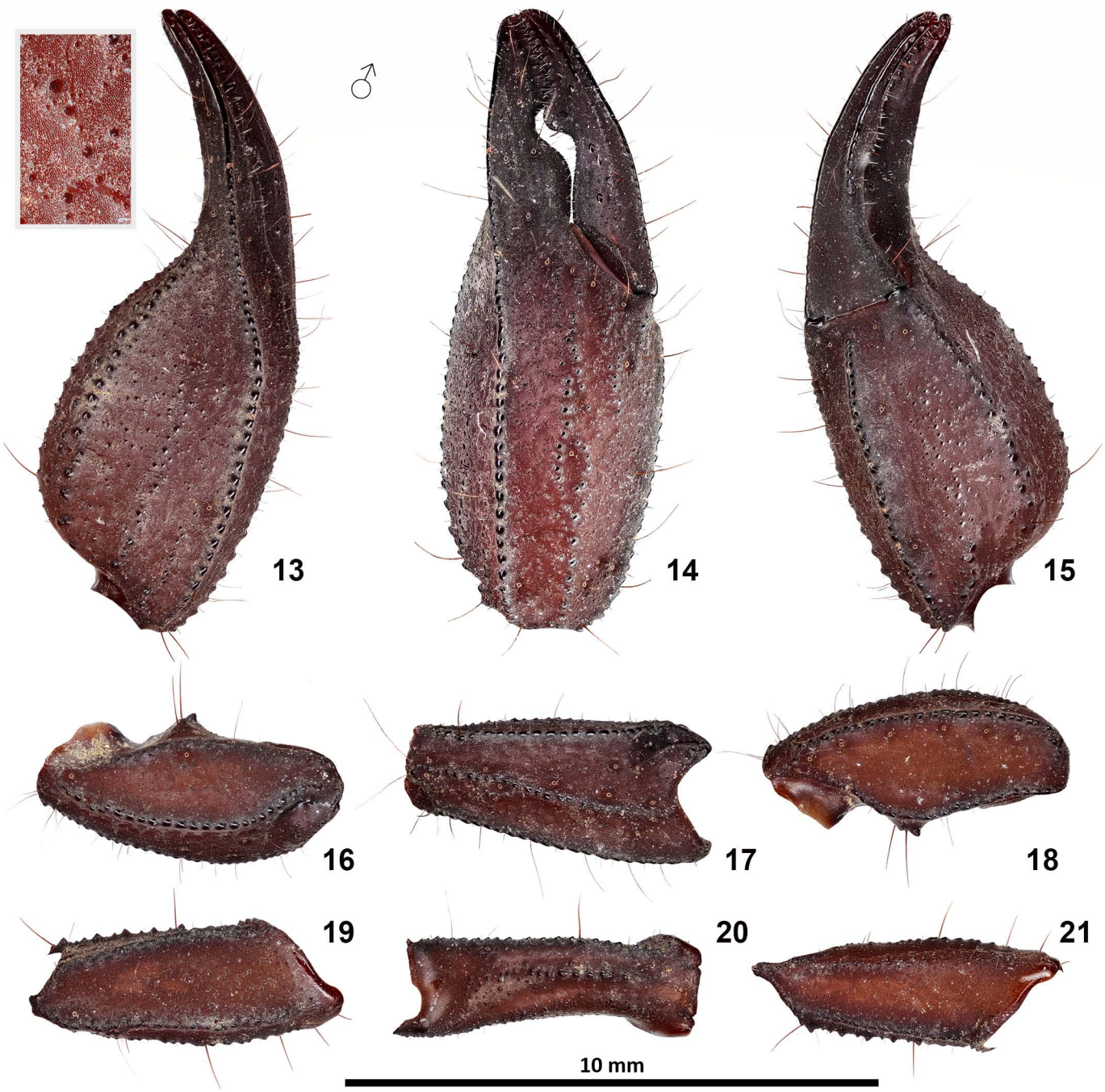

Figures 13–21. *Scorpiops tongtongi*, male, pedipalp chela in dorsal (13), external (14) and ventral (15) views, patella in dorsal (16), external (17) and ventral (18) views, femur in dorsal (19), external (20) and ventral (21) views, under white light. Scale bar = 10 mm.

incorporated in the diagnosis and Table 2. In one single female, only five teeth were observed on its left pectine ("left/right" considered as in ventral view). All three examined females had 17 external and 7 ventral trichobothria on either of their patellae. Geometric configurations of patellar trichobothria generally the same among all examined materials, except that there was a higher variability in the relative position of *em* and *esb* series where the distal *esb* may travel to the same level of *em*. The males of *S. tongtongi* can be easily distinguished from the females by the presence of the proximal lobe on pedipalp movable finger (and a corresponding notch on fixed finger) and a pair of genital papillae at the base of the genital operculum. Pectines of males proportionally longer with longer and larger teeth, adorned with more peg sensilla (sensory area located on distal region in females). In addition, tergal granules are larger and slightly denser in females; this discrepancy appears to exhibit in most Yunnan *Scorpiops* (except for *S. jendeki* where male has apparently denser granulation) and may probably be related to parental care behavior in which females have to provide a more grippable surface for the offspring.

It is also interesting to note that there was a consistent sexual dimorphism in the denticle rows on movable finger.

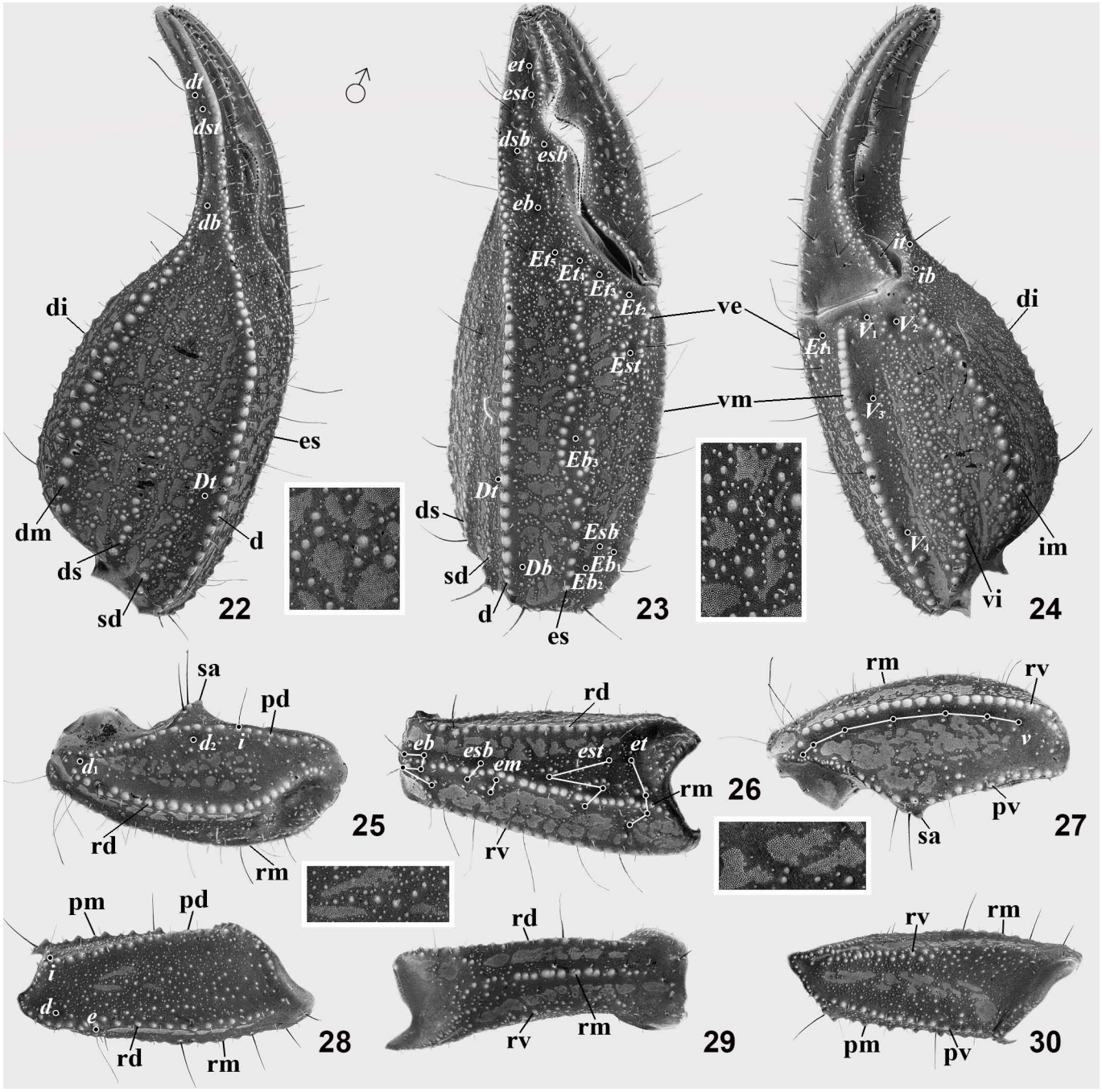

Figures 22–**30**. *Scorpiops tongtongi*, male, pedipalp chela in dorsal (22), external (23) and ventral (24) views, patella in dorsal (25), external (26) and ventral (27) views, femur in dorsal (28), external (29) and ventral (30) views, under UV light. Trichobothrial pattern indicated in Figures 22–28. Carina abbreviations: d = digital, sd = subdigital, ds = dorsal secondary, dm = dorsal marginal, di = dorsal internal, im = interomedian, vi = ventrointernal, vm = ventromedian, ve = ventroexternal, es = external secondary, pd = prodorsal, rd = retrodorsal, rm = retromedian, rv = retroventral, pv = proventral, pm = promedian. sa = spiniform apophysis.

All movable fingers of examined females exhibited the same condition as in the holotype female: IADs did not evidently partition from MDs when they approached proximity of the finger, and random series of denticles continued the entire length of dentate margin. The same method for differentiating MD and IAD was applied: the most proximal IAD was recognized as the one on the same level with the most proximal OD, treating all the more proximal denticles as MDs. This decision was taken as the most proximal OD located near the region where the IADs terminate in males. On the other hand, IADs terminated in the proximal end of the finger lobe in males, and a single row of MDs covered a small section before it again proliferated into random distributions. Given the location where the single row was recognized, this variation may result from the presence of the proximal lobe in males. However, this discrepancy did not give rise to prominent sexual dimorphism in denticle counts. Values (left/right) for three examined females: (1) 10/10 OD, 86/97 MD, 46/46 IAD, 1/≈2 ID; (2)

Figures 31–**38**. *Scorpiops tongtongi*, male. **Figures 31**–**34**. Dorsal (31, 33) and ventral (32, 34) views of left chelicera in opening status (right chelicera in closing status available in original description) under white (31–32) and UV (33–34) light. **Figures 35**–**38**. Left movable finger (35, 37), right movable finger (36, 38), under white (35–36) and UV (37–38) light. Finger dentition indicated in Figures 37–38. Denticle abbreviations: *dd* = dorsal distal, *vd* = ventral distal, *d* = distal, *sd* = subdistal, *m* = median, *b* = basal, *va* = ventral accessory. Scale bar = 2 mm (31–34) and 3 mm (35–38).

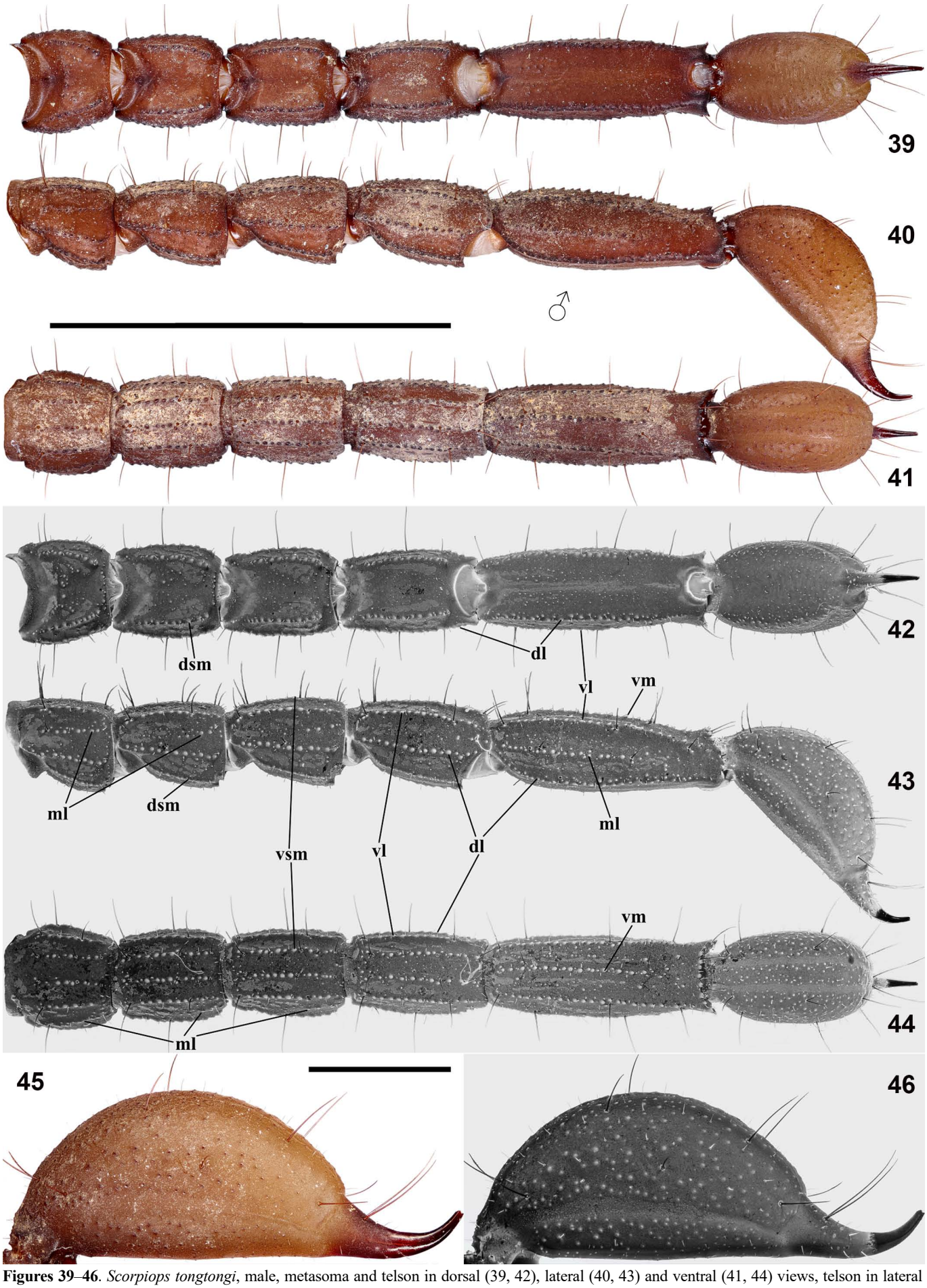

Figures 39–46. *Scorpiops tongtongi*, male, metasoma and telson in dorsal (39, 42), lateral (40, 43) and ventral (41, 44) views, telson in lateral view (45, 46). **Figures 39–41**, **45**. Under white light. **Figures 42–44**, **46**. Under UV light. Carina abbreviations: dsm = dorsosubmedian, dl = dorsolateral, ml = median lateral, vl = ventrolateral, vsm = ventrosubmedian, vm = ventromedian. Scale bar = 10 mm (39–44) and 2 mm (45–46).

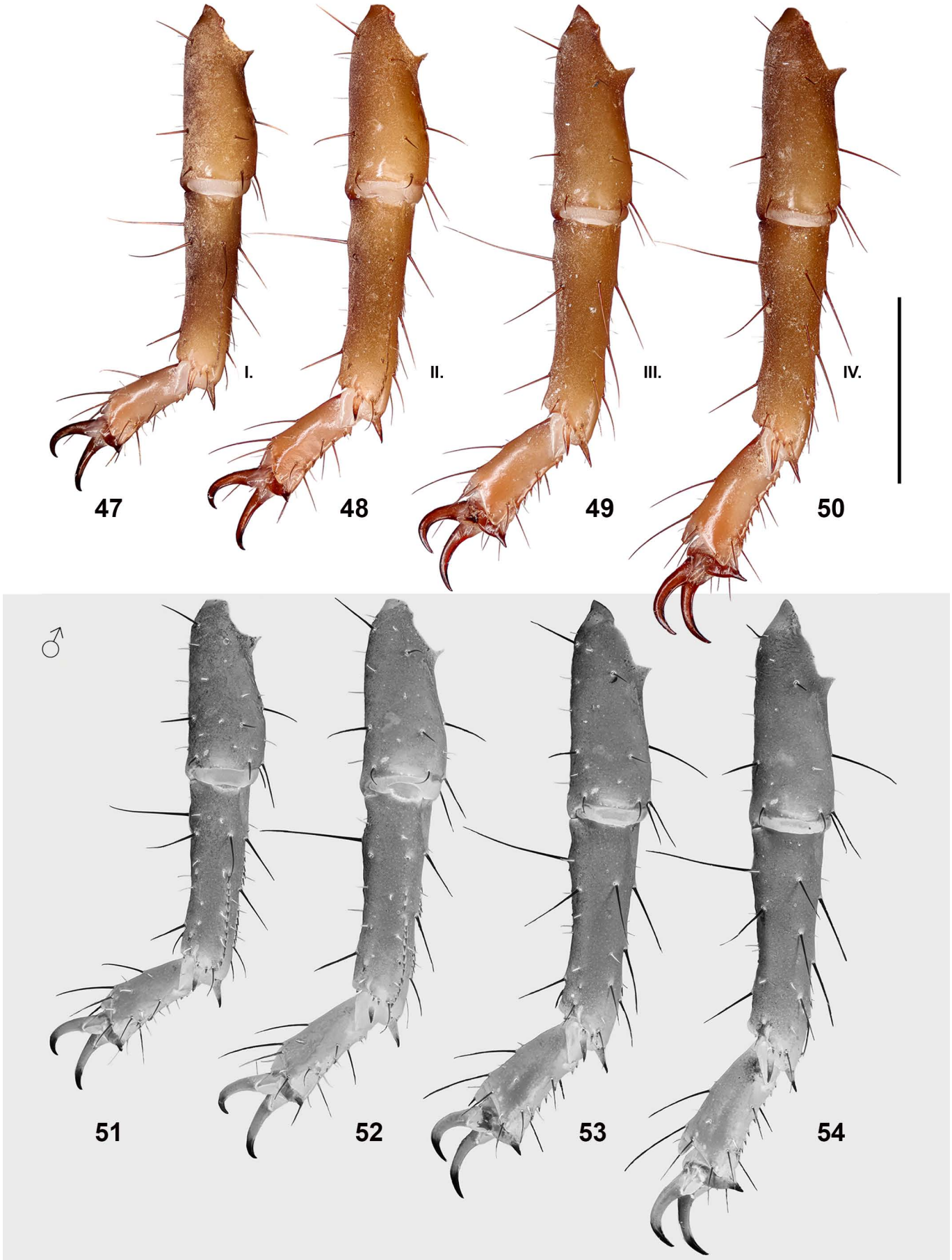

Figures 47–54. *Scorpiops tongtongi*, male, left legs I–IV in retrolateral view. **Figures 47–50**. Under white light. **Figures 51–54**. Under UV light. Scale bar = 2 mm

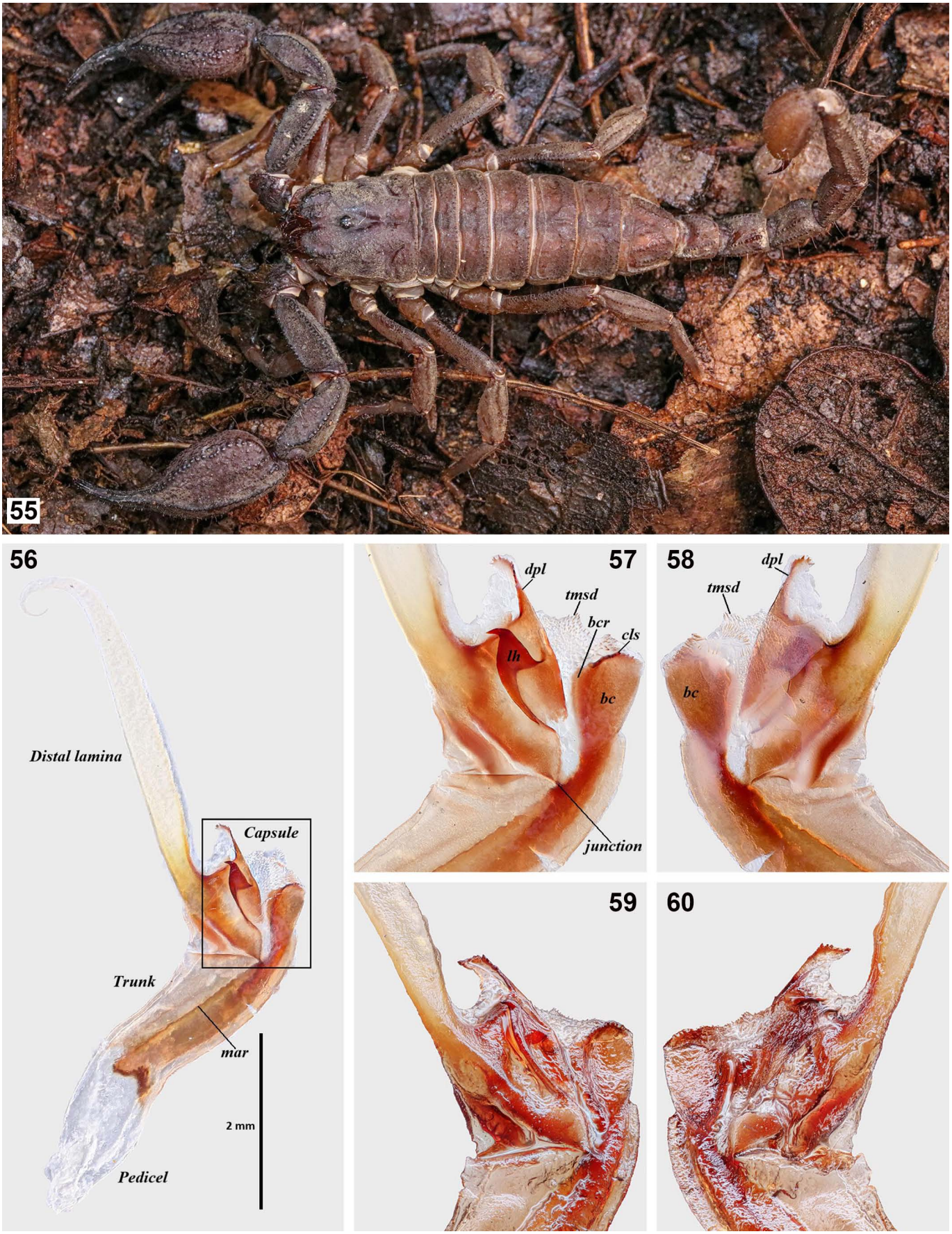

Figures 55–60. *Scorpiops tongtongi*, male and left hemispermatophore. **Figure 55**. Male in vivo habitus under captive condition. **Figures 56–60**. Left hemispermatophore in convex view (56). Capsule in convex (57, 59) and concave (58, 60) views. Capsule exposed in air (59–60) was coated with clove oil in order to reveal the surface texture before the photos were taken. Abbreviations: *dpl* (distal posterior lobe), *lh* (lateral hook), *tmsd* (terminal membrane of sperm duct), *bc* (basal carina), *bcr* (basal crest), *cls* (crown-like structure), *mar* (mid-axial rib), *dc* (distal carina).

Figure 61–**62**. *Scorpiops xui*, male (61) and female with 1st instar offspring (62) in vivo habitus under captive condition.

Figures 63–**64**. *Scorpiops yangi* in vivo habitus under captive condition. **Figure 63**. Male (right) and female (left) in natural resting posture. **Figure 64**. Male (left) and female (right) displaying thanatosis or catalepsy in rigid posture.

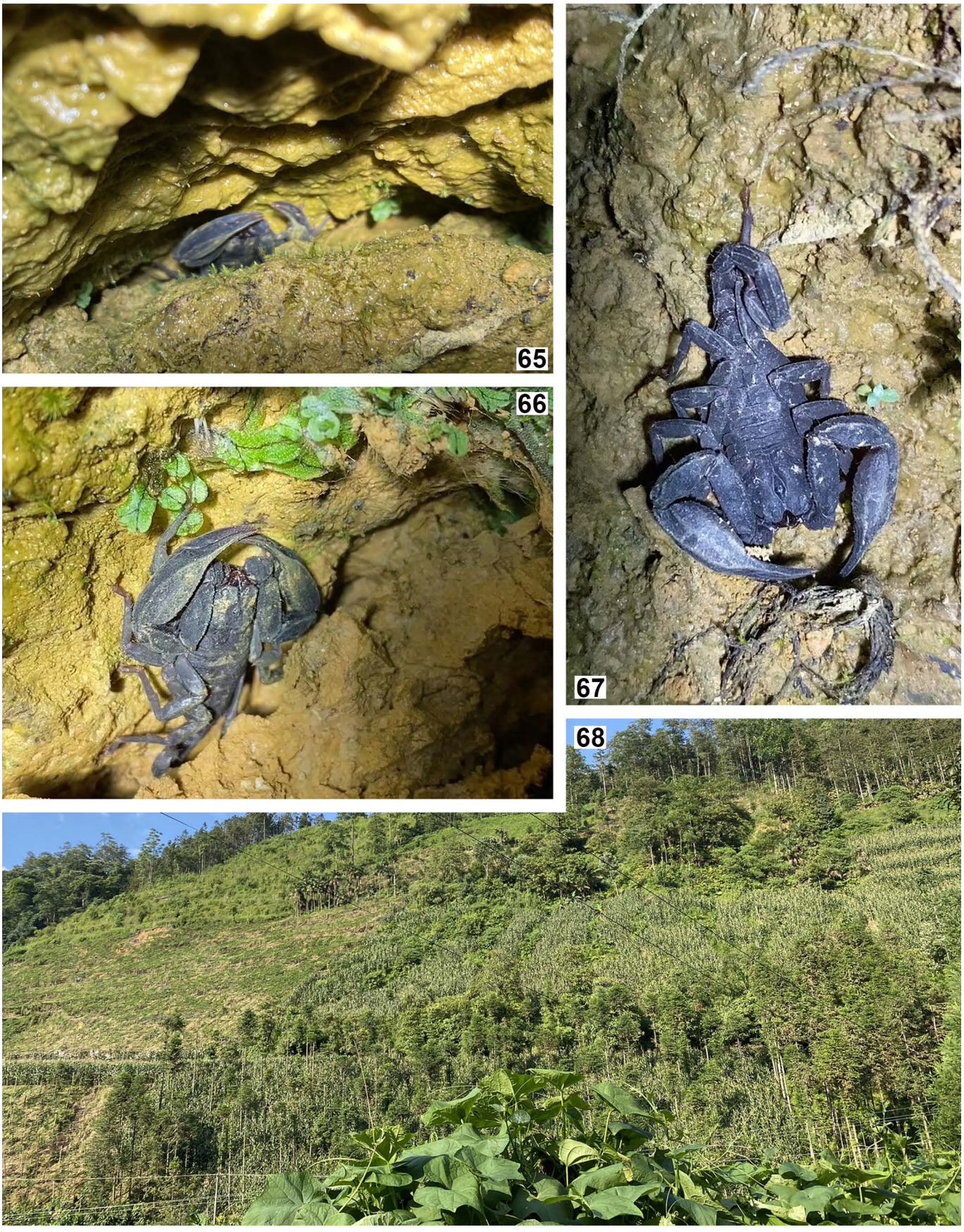

Figures 65–68. *Scorpiops yangi*, topotypes in original habitat from Gulinqing Township.

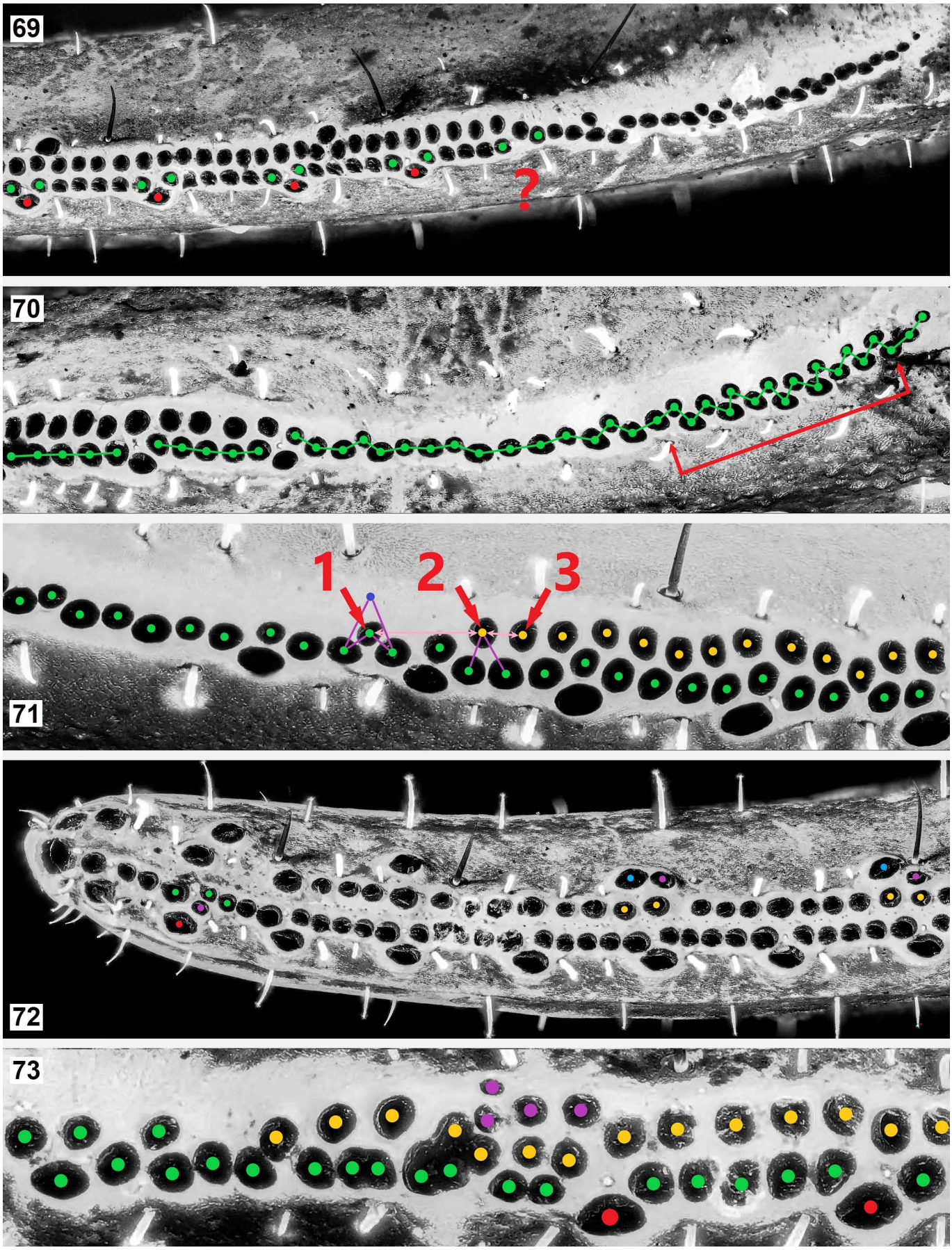

Figures 69–73. Considerations for denticles. **Figure 69**. *Scorpiops* sp. (Menglun), female, left chela, showing the loss of an OD and normal MD-OD-MD combinations. **Figure 70**. *S. validus*, female, left chela, showing the linearity is influenced by the included angle. **Figure 71**. *S. lowei*, female, right chela, showing the differentiation of IAD (yellow) and MD (green). **Figures 72–73**. *Scorpiops* sp. (Menglun), females, showing examples of low-degree proliferations in which the abnormal denticles (purple) flank a certain denticle type as well as their weak influence on the arrangement; in Fig. 73, there are also two denticle-fusion anomalies.

Species & distribution records	TL (mm)	PTC	ID	OD	MD	IAD	P-Vt	C-L/W
S. jendeki (n for C-L/W: 1♂5♀), BS (LL; LY; TC); DH (LCh-WZS; LH); DL; NJ (FG; GS)	♂ 25*–32.2* ♀ 42.1*	♂ 4*–5 ♀ 4–5	5*	9*	50*	10*	♂ 6*–7* ♀ 6–7*	♂ **2.63–2.65** ♀ **2.63–2.83**
S. lowei (n for C-L/W: 8♂8♀) XSBN (MH-Mh)	♂ 37.9–46.0 ♀ 39.7–50.9	♂ (6*)7–8 ♀ [5]6–7	4–8	14–16	71–88	45–59	♂ 9–10 ♀ 8–10(11*)	♂ **3.33–4.03** ♀ **3.32–4.12**
S. puerensis (n for C-L/W: 2♂5♀) PE (LCa; SM)	♂ 46.2–49.8 ♀ 51.6–54.4	♂ 7–8 ♀ 6–8	4–6	9–14	80–92	47–51	♂ 8–11 ♀ 10–11	♂ **3.25–3.39** ♀ **3.31–3.44**
S. shidian (n for C-L/W: 4♂♀) BS (SD-JC, SD-JTB; LY)	♂ 45.7–51.7 ♀ 45.8–52.4	♂ 7–8 ♀ (6*)7–8	6–7	14–16	77–95	44–67	♂ (11*)12–13 ♀ (10*)11–13	♂ **4–4.4** ♀ **3.9–4.33**
S. tongtongi (n for C-L/W: 2♂4♀) DH (YJ-near TBG)	♂ **44** ♀ **40–45**	♂ **7** ♀ **5**–6	**3–5**	**10–12**	86–**96**	**39–52**	♂ **6–7** ♀ 7	♂ **2.71–2.91** ♀ **2.9–3.17**
S. vachoni (n for C-L/W: 4♂2♀) XSBN (MLa-BJ)	♂ 47.2–54.0 ♀ 48.1–54.8	♂ 7–9 ♀ 7–8	7–8	13–15	92–116	53–80	♂ [8]10–11 ♀ 10–11	♂ **3.31–4.11** ♀ **3.54–4.75**
S. validus (n for C-L/W: 4♂4♀) HH (Hh-MZ; LvC; YY)	♂ 43.1–54.3 ♀ 46.2–52.8	♂ (6*)7–8 ♀ 6–7	5–8	11–14	88–109	44–58	♂ 9–10 ♀ (8*)9–11	♂ **3.67–3.97** ♀ **3.43–3.85**
S. xui (n for C-L/W: 1♂4♀) PE (MLi)	♂ 54.1–56* ♀ 58–66*	♂ **7**–8 ♀ 7–8	**5–7**	[**13**] **15–17**	**76–94**	[**45**] **55–65**	♂ 10 ♀ [**9**]10–**11**	♂ **5.08–5.22** ♀ **3.61–4.21**
S. yangi (n for C-L/W: 1♂1♀) WS (MG-GLQ; ?MLP)	♂ 47.8* ♀ 51.3*	♂ 6–7 ♀ 5*–6	[**4**] 6–**7**	**12**–13	**87–94**	**52–60**	♂ 9–10* ♀ 10	♂ **3.92–3.96** ♀ **3.82–3.86**
S. zhangshuyuani (n for C-L/W: 1♂1♀) DH (YJ-TBG)	♂ 42.6 ♀ (49.1*–)53.8	♂ 9 ♀ (7*–)8	5–7	13–15	91–100	70–73	♂ 11–12 ♀ 11	♂ **5.4–5.67** ♀ **4.32–4.33**
***S*. sp. 1** (n for C-L/W: 4♂5♀) XSBN (JH-east of Langcang river)	♂ 42.8–48.8 ♀ 45.7–49.6	♂ [6]7–9 ♀ 7–8	6–8	13–16	80–96	48–63	♂ 10–11 ♀ 10–12	♂ **3.34–3.78** ♀ **3.45–3.7**
***S*. sp. 2** (n for C-L/W: 3♂4♀) XSBN (MLa-MLu)	♂ 45.8–49.4 ♀ 47.8–50.2	♂ 7–9 ♀ 7–8	6–8	13–16	84–104	52–66	♂ [7]10–11 ♀ [9]10–11[12]	♂ **3.17–3.61** ♀ **3.4–3.9**

Table 2. Morphological comparison of *Scorpiops* recorded from Yunnan based on quantitative characters. Abbreviations for locale: **(1)** city and prefecture: **BS** (**Baoshan** City), **DH** (**Dehong** Dai and Jingpo Autonomous Prefecture), **DL** (**Dali** Bai Autonomous Prefecture), **HH** (**Honghe** Hani and Yi Autonomous Prefecture), **JH** (**Jinghong** City), **MZ** (**Mengzi** City), **NJ** (**Nujiang** Lisu Autonomous Prefecture), **PE** (**Puer** City), **TC** (**Tengchong** (county-level) City), **WS** (**Wenshan** Zhuang and Miao Autonomous Prefecture), **XSBN** (**Xishuangbanna** Dai Autonomous Prefecture); **(2)** district and county: **FG** (**Fugong** County), **GS** (**Gongshan** County), **Hh** (**Honghe** County), **LCa** (**Lancang** Lahu Autonomous County), **LCh** (**Longchuan** County), **LH** (**Lianghe** County), **LL** (**Longling** County), **LvC** (**Lvchun** County), **LY** (**Longyang** District), **MG** (**Maguan** County), **MH** (**Menghai** County), **MLa** (**Mengla** County), **MLi** (**Menglian** County), **MLP** (**Malipo** County), **SD** (**Shidian** County), **SM** (**Simao** District), **YJ** (**Yingjiang** County), **YY** (**Yuanyang** County); **(3)** town and village level: **BJ** (**Bujiao** Village), **GLQ** (**Gulinqing** Township), **JC** (**Jiucheng** Township), **Mh** (**Menghai** Town), **MLu** (**Menglun** Town), **TBG** (**Tongbiguan** Township), **WZS** (**Wangzishu** Township); **(4)** infrastructure: **JTB** (**Jingtangba**; Jingtang dam). Other abbreviations: **TL** = total length; **P-Vt** = ventral trichobothria of pedipalp patella; **C-L/W** = length/width ratio of right pedipalp chela. *Note*: the external trichobothria of pedipalp patella and length/depth ratio of telson are excluded for their limited utility within these species; denticle counts can be biased by subjective consideration (Tang, 2022b); C-L/W are all re-calculated based on the "condyle method" but only referential due to artificial measurement errors and method difference (calculated specimens (noted after the name) are fewer than before as some were sent to Charles University in Prague, Czech Republic, for DNA analysis; however, both chelae were measured); abnormal values observed personally (Tang, 2022b & c) are enclosed in brackets, asterisked data (some in parentheses) are taken from papers of other authors (Zhu et al., 2007; Di et al., 2011; Di et al., 2013; Ythier, 2019; Kovařík et al., 2020), and new data are bolded (if the current observations accord with the previous ones in Tang (2022b & c) or original descriptions for *S. xui* and *S. yangi*, they are not bolded).

10/10 OD, >73/>86 MD, 39/40 IAD, 3/3 ID; (3) 11/11 OD, 86/92 MD, 45/42 IAD, 4/4 ID. In the first female, only one ID was identifiable on its left finger, while on its right finger, proliferations were discovered at the distal region, confusing the separation of ID and IAD as well as yielding higher count of MD; this is thus considered abnormal and excluded from the diagnosis. In the second female, the proximal region on both of its fingers was damaged, rendering low count of MD (excluded). Other characters generally the same, except for the chela which is relatively more robust in males.

Affinities. The described features of the adult male further differ *S. tongtongi* from all its Yunnan congeners and will be elaborated below. Tang (2022b: 14) also compared it from a geographically closest neighbor from Myanmar, *S. beccaloniae* (Kovařík, 2005). While *S. tongtongi* was described by a single female specimen, *S. beccaloniae* was based on a male. This thus undermined the credibility of the validity of *S. tongtongi* if the two species were to be compared. However, the author nonetheless applied two sex-independent characters to support her statement: ventral

Species	Overall R of C	Location of CW_{max}	MF lobe	IA	TG	OTC	Fulcra
S. jendeki	♂ Robust ♀ Robust	♂ Proximal half ♀ Proximal half	♂ Absent ♀ Absent	Weak	♂ Dense ♀ Sparse ♂ Small-Large ♀ Very large	short oval	Absent
S. lowei	♂ Moderate ♀ Moderate	♂ Proximal half ♀ Proximal half	♂ Moderate ♀ Weak	Strong	♂♀ Dense ♂ Small ♀ Moderate-Large	elongated rhomboid	Present
S. puerensis	♂ Moderate ♀ Moderate	♂ Proximal half ♀ Proximal half	♂ Strong ♀ Weak-Moderate	Strong	♂♀ Dense ♂ Moderate ♀ Moderate-Large	elongated rhomboid	Present
S. shidian	♂ Slender ♀ Slender	♂ Even ♀ Even	♂ Weak^{ex}-Weak ♀ Absent-Weak^{ex}	Strong	♂♀ Dense ♂ Moderate ♀ Large	elongated rhomboid	Present
S. tongtongi	♂ Robust ♀ Moderate	♂ Proximal half ♀ Proximal half	♂ Strong ♀ Absent-Weak^{ex}	Weak	♂♀ Sparse ♂ Small-Moderate ♀ Large	short oval	Absent
S. vachoni	♂ Moderate ♀ Moderate	♂ Proximal half ♀ Proximal half	♂ Strong ♀ Weak	Strong	♂♀ Dense ♂ Moderate ♀ Moderate-Large	elongated rhomboid	Present
S. validus	♂ Moderate ♀ Moderate	♂ Even ♀ Even	♂ Strong ♀ Weak-Moderate	Strong	♂♀ Dense ♂ Small ♀ Moderate-Large	elongated rhomboid	Present
S. xui	♂ Slender ♀ Moderate	♂ Medial ♀ Even	♂ Weak ♀ Absent-Weak^{ex}	Strong	♂♀ Dense ♂ Small ♀ Moderate-Large	elongated rhomboid	Present
S. yangi	♂ Moderate ♀ Moderate	♂ Even ♀ Even	♂ Moderate ♀ Weak	Strong	♂♀ Dense ♂ Small ♀ Moderate-Large	elongated rhomboid	Present
S. zhangshuyuani	♂ Slender ♀ Slender	♂ Medial ♀ Even	♂ Weak^{ex} ♀ Absent-Weak^{ex}	Strong	♂♀ Dense ♂ Small ♀ Moderate-Large	elongated rhomboid	Present
***S*. sp. 1 (Jinghong)**	♂ Moderate ♀ Moderate	♂ Proximal half ♀ Proximal half	♂ Moderate-Strong ♀ Weak	Strong	♂♀ Dense ♂ Small ♀ Moderate	elongated rhomboid	Present
***S*. sp. 2 (Menglun)**	♂ Moderate ♀ Moderate	♂ Proximal half ♀ Proximal half	♂ Moderate-Strong ♀ Weak	Strong	♂♀ Dense ♂ Small ♀ Moderate	elongated rhomboid	Present

Table 3. Morphological comparison of *Scorpiops* recorded from Yunnan based on qualitative characters (qualitative criteria exemplified in Figs. 97–190 and Tang, 2022b). Abbreviations: R = ratio; C = chela; CW_{max} = maximal width of pedipalp chela; MF = pedipalp movable finger; ex = extremely; IA = internal apophysis of pedipalp patella; TG = tergite granulation; OTC = ocular tubercle coverage. *Note*: Eb_3 position, pectinal lamellae morphology and fulcra development are excluded from this table due to their limited/confusing utility within these species (Tang, 2022b). "Small/moderate/large" depends on visually perceived average granule diameter with respect to the tergite area or posterior width.

patellar trichobothria number and spiniform apophysis of patella. Other characters either were the same or may show substantial overlap in this genus. With the current description of adult male *S. tongtongi*, it is now certain that both species are indeed different. *S. beccaloniae* is more similar to other Yunnan *Scorpiops* (except for *S. jendeki*) by its dark coloration, proportionally larger median ocelli, triangular anteromedian notch of carapace, proportionally narrower pedipalp chela, strong patellar spiniform apophysis, rough cuticle and elongated telson (Kovařík, 2005: figs. 13–14). *S. beccaloniae* also has a higher PTC range (8–9) while both males of *S. tongtongi* are 7. Based on the knowledge of Yunnan *Scorpiops*, if the overall range is 7–9, then encountering specimens with 8 PTC would be of a much higher possibility (e.g., male *S. vachoni*: frequency of 7 PTC ≈ 0.06, frequency of 8 PTC ≈ 0.85, frequency of 9 PTC ≈ 0.09, n = 34).

Ecology and behavior. Specimens of *S. tongtongi* were found sympatrically with *S. zhangshuyuani* in Tongbiguan Township, in a landscape featuring chains of undulating hills. The microhabitat of *S. tongtongi* is characterized by rocks and soils covered with green, short mosses, and they were often found under rocks and rotten logs. Young juveniles (approximately 3~4 instar) were found during the same period (June to July) as subadults and adults. Anecdotal observations reported the occurrence of subadult and adult *S. tongtongi* since March, where some individuals were running on the ground diurnally. Two gravid females examined were dissected with 18 and 22 embryos respectively. This species also appears to have a higher demand for humidity than other Yunnan *Scorpiops*.

The scorpions showed temporary resistance towards conspecifics shortly after they were captured and placed in small containers. However, a case of cannibalism was reported by the collector where an immature individual was consumed by an adult female. Under captive condition, the single adult male exhibited different temperaments with respect to most of the other Yunnan congeners. For example, in comparison with the adult male *S. xui* which remained almost motionless

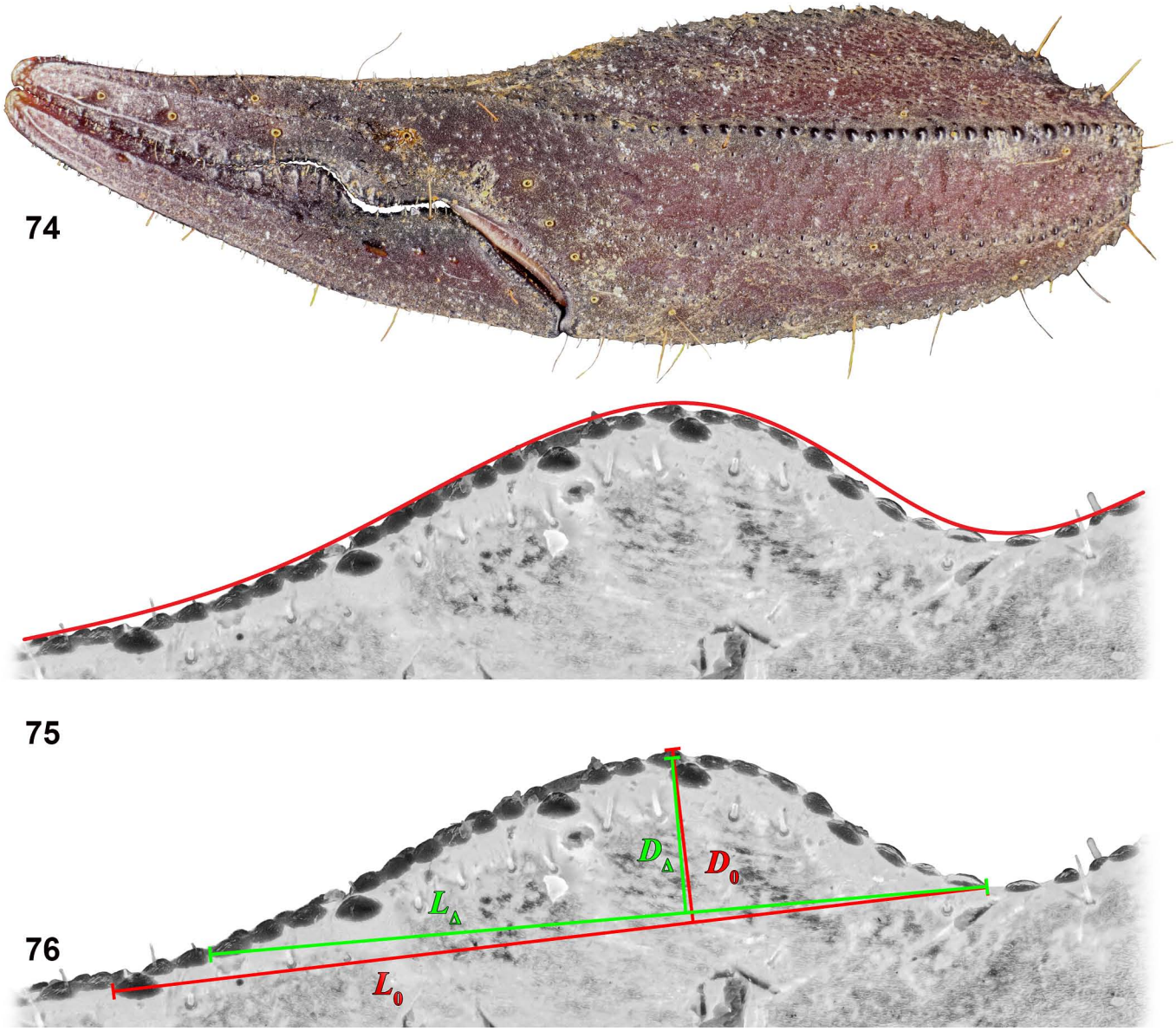

Figures 74-76. Measurement of proximal lobe on pedipalp movable finger. **Figure 74**. *Scorpiops novaki*, female from Zayü County, Nyingchi, Tibet, left chela in external aspect. **Figure 75**. The outline of MF-lobe approximated by manual curve fitting of five dots, showing no obvious P_{in} and P_{te} for its length. **Figure 76**. Denticles on the dentate margin used as the landmarks for P_{in} and P_{te} of length; the apex of lobe arc which decides the depth may be the denticle (red method) or may not (green method); slight deviation may result in the difference in the final ratiometrics (red vs. green).

when being touched, the adult male *S. tongtongi* inclined to flee in response to the tactile stimulation. The two species also showed different sensitivities to vibrations caused by the movement of their containers: *S. xui* appeared to be indifferent while *S. tongtongi* was agitated, constantly moving back and forth, seemed to be deciding the direction of its subsequent escape path.

Furthermore, comparing with the congeners with relatively longer pedipalps, *S. tongtongi* may instead resort to thumping the threat with pedipalps more frequently, similar to the behavior observed in some *Heterometrus* with robust pedipalp chelae (Tang, 2023) and *S. langxian* from Tibet (Tang, pers. obs.). It also wielded its telson more frequently than the congeners. Thanatosis or catalepsy was less easily to be triggered as the scorpions usually tended to fight back or escape when being threatened. However, under particular scenarios, they do manifest a similar posture as observed in *Tityus ocelote* Francke & Stockwell, 1987 and *Ananteris platnicki* Lourenço, 1993 (Triana et al., 2022: figs 2a, c). This usually happens after the scorpion was rapidly flipped or dropped. It is also worth noting that all of the examined Yunnan *Scorpiops* had been observed with cataleptic behaviors (e.g., Fig. 60). Similar behavior was also observed in *Chaerilus conchiformus* Zhu et al., 2008 (a single adult male) and *C. pseudoconchiformus* Yin et al., 2015 (a pair of adults) collected from Bayi District, Nyingchi, Tibet (Tang, pers. obs.).

Discussion

1. Further review on the morphological study of *Scorpiops*

Overview. Most past literature applied the following morphological characters to differentiate *Scorpiops* at the species-level: (1) dimensional and ratiometric (quantitative) characters: total length (TL), length/width ratio of pedipalp chela (chela-L/W); (2) enumerative (quantitative) characters: number of ventral trichobothria on pedipalp chela (chela-Vt), number of external and ventral trichobothria on pedipalp patella (patella-Et and patella-Vt), pectinal tooth count (PTC); (3) qualitative (despite the feasibility of quantification for some characters) characters: coloration, presence/absence or degree of proximal lobe on dorsal edge of pedipalp movable finger (MF-lobe), relative position of trichobothrium *Eb*3 to *Est*, *Db* and *Dt* on pedipalp manus (Eb_3-position), and presence/absence or degree of pectinal fulcra. Coloration could be biased if the specimen has been long preserved in ethanol (e.g., the problem with *S. vachoni* (Qi et al., 2005), which was said to be "yellow brown" in Di et al., 2011: 24). The presence/absence of contraction at the juncture of telson vesicle and aculeus (defined as the "annular ring") was once regarded as a generic character but then refuted in the family-level revision by Kovařík et al. (2020: 8), yet it may sometimes be supportive at the species-level (i.e., some species may exhibit a stronger contraction; cf. Kovařík et al., 2020: fig. 52). Furthermore, Kovařík et al. (2020) introduced three additional diagnostic characters (according to their table 9): delimitation of pectinal lamellae (qualitative), length/depth ratio of telson (telson-L/D) (quantitative), and number of denticles in each row on pedipalp movable finger (quantitative). Tang (2022b & c) also employed several other qualitative characters to differentiate the new species from their congeners: size and density of tergal granules, development degree of carinae, development degree of pedipalp patellar internal apophysis, depth of carapacial furrows and grooves, shape/coverage of median ocular tubercle, and shape of carapacial anteromedian notch. Although Tang (2022b: figs. 230–263) had included comparative photos of the Yunnan *Scorpiops* species, with the upgraded photographic equipment, most of those characters (except for the telson) are illustrated with refined UV photos in Figs. 137–190. Below, the utility of some characters is further reviewed/summarized based mainly on the study upon Yunnan *Scorpiops*. The problem with chela-L/W is particularly discussed in the next chapter.

1.1. The delimitation of pectinal lamellae

This character was considered as a useful character at the species-level, and divided into four categories (Kovařík et al., 2020: 21). However, after examining several specimens of *S. shidian* (Qi et al., 2005), Tang (2022b: 34) considered this character to be unstable as the same species (or the same individual) may exhibit different morphologies (the development of grooves/sulci on the pectines is not always the same); this character could be sexually dimorphic (males usually have more developed grooves).

1.2. Length/depth ratio of telson

Telson-L/D was not elucidated in detail and lacked data of many species (Kovařík et al., 2020: 128–129, table 9). It is true that different species may have different telson profiles which can therefore be used for diagnosis, but it becomes less informative among many Yunnan *Scorpiops* that share a similar general morphology which also have similar telson profiles (cf. Tang, 2022b: figs. 232, 235, 238, 241, 244, 247, 250, 253, 256, 259, 262, 265). After further comparing different *Scorpiops* telsons, I assume that telson-L/D alone could be sometimes overshadowed by another useful character of the telson profile – the location of the convex point on the telson ventral outline (an arc) from the lateral view (the depth used in telson-L/D is usually derived from a perpendicular passing this point).

Two species could share a similar telson-L/D; however, their convex points may be located differently. In some species, this point may be at the middle of the telson ventral outline (e.g., Kovařík et al., 2020: fig. 22), while in others, it may be closer to the aculeus (i.e., distally; e.g., Kovařík et al., 2020: fig. 49) or the anus (i.e., proximally; e.g., Kovařík et al., 2020: fig. 70); this character may be sexually dimorphic. Telson-L/D essentially limits the relative size or degree of slenderness of the telson, but the convex point further determines the shape thereof. Two parameters in combination could provide a more comprehensive description for the telson profile. Elliptic Fourier Analysis (EFA) is a promising technique that can be used to quantify irregular geometric shapes without definite landmark points (Caple et al., 2017; Kuhl & Giardina, 1982). This method provides a more objective result for qualitative descriptors and has previously been implemented to dissect basal pectinal tooth, spiracle and telson profiles in genera *Teruelius* and *Grosphus* (Lowe & Kovařík, 2022: 6–7, 10, 12, 30, 32, 48).

1.3. Relative position of trichobothrium *Eb*3 on pedipalp manus

Eb_3 was categorized into five spatial types in Kovařík et al. (2020: 8), defined by its relative position with respect to *Est*, *Db* and *Dt*. However, according to the exemplar figures associated by the authors in their paper, it seemed rather subjective to define "in distal/proximal half", "in middle", and "at same level".

Figure 16 in Kovařík et al. (2020: 7) was defined as type A (in distal half), and figures 528 as type B (Kovařík et al., 2020: 80) and 365 as type C (Kovařík et al., 2020: 49) (both in middle). The difference is subtle; a straight axis passing Eb_3 must be defined to separate the distal and proximal halves by its mid-point. Figures 528 and 20, as defined in Kovařík et al. (2020), showed Eb_3 "at the same level" with *Dt*. However, in figure 528, Eb_3 seemed to be a bit higher than *Dt* (i.e., more distal to *Dt*), while in figure 20 (Kovařík et al., 2020: 7), *Dt* seemed to be a bit higher than Eb_3 (i.e., more distal to Eb_3). If the same straight axis is taken, a perpendicular passing Eb_3 (and of course the axis) can be used to determine if *Dt* is "at the same level" with Eb_3 (i.e., whether *Dt* is on this

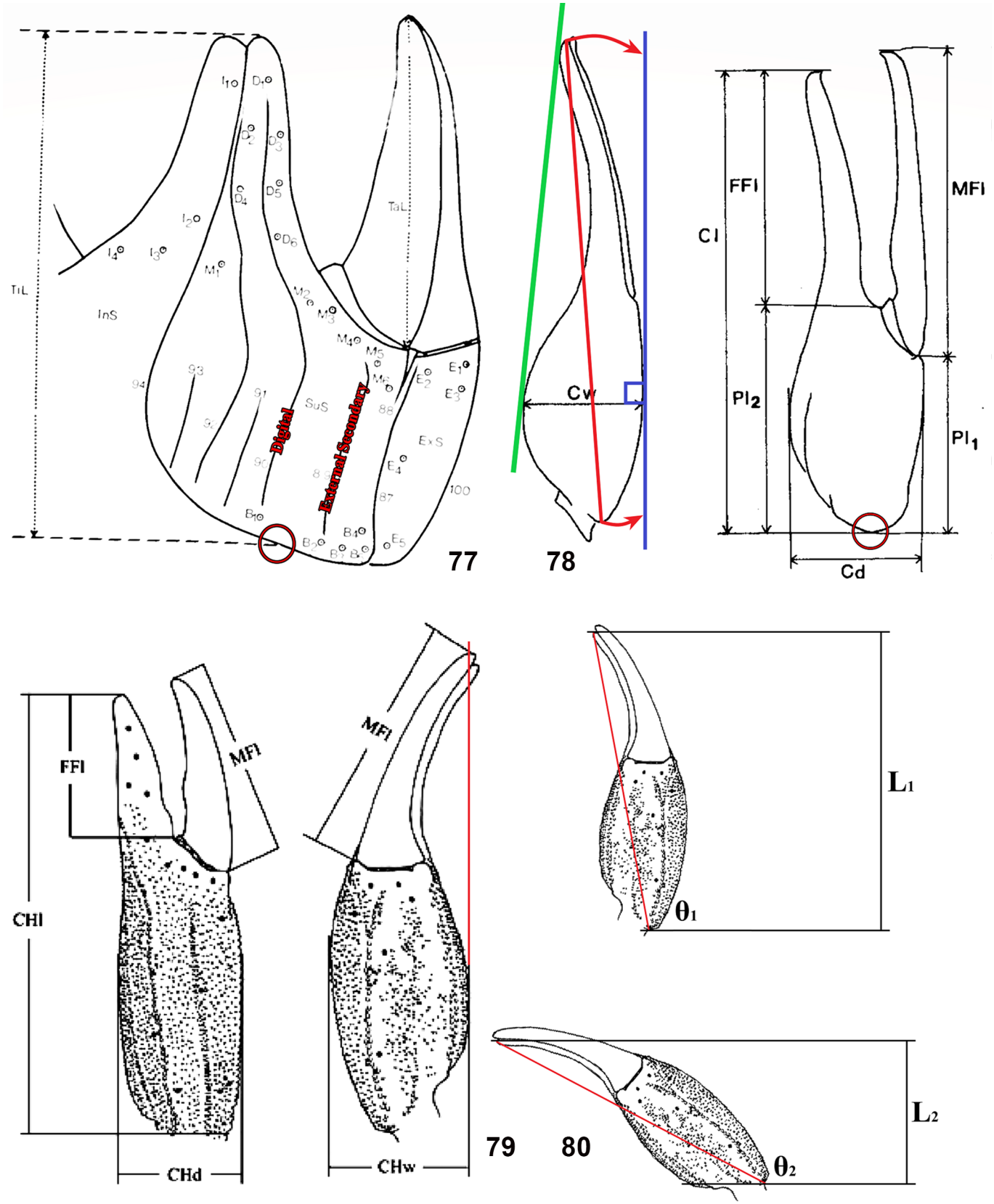

Figures 77–80. Mensurational methods of scorpion chela applied in several *Scorpiops* papers. **Figure 77**. Definition by Stahnke (1970); red circle: region of P_{in} between digital and external secondary carinae. **Figure 78**. Definition by Sissom et al. (1990); red circle: region of P_{in} without clear reference system; red line: axis defined in this paper; green line: the straight line that passing the fingertip and a point of the inner curve arc; blue line: orthogonal to Sissom's chela-W. **Figure 79**. Definition in Sun (2010)'s dissertation; red line: extension of Sun's right bar of chela-W annotation. **Figure 80**. Ambiguity of Sun's method; change of angle influences the length obtained: $\angle\theta_1 < \angle\theta_2$ ($\theta_1 + \theta_2 > 180°$), $L_1 > L_2$.

perpendicular). This is apparently affected by the angle of the position of chela – which is not normalized within a reference system. Figure 18 in Kovařík et al. (2020: 7) was considered type D, i.e., Eb_3 is not at the same level with *Dt*. Indeed, it was not, but how closely the *Dt* approximates Eb_3 (or the other way around) would it be considered as "at the same level" (cf. Kovařík et al., 2020: figs. 18, 20)? This was neither quantified nor standardized (e.g., using the perpendicular method as above discussed).

Nevertheless, if the variation of *Dt* position is not continuous within this genus (i.e., *Dt* does not continuously travel on the entire digital carina), then it is not necessary to rigorously define the position; i.e., there is a spatial gap on this carina between type D and E in which *Dt* will never present. For instance, assuming that figure 20 in their paper marked the highest point *Dt* could be for type E and figure 18 marked the lowest point *Dt* could be for type D, *Dt* is thus impossible to appear in the carina section in between. However, judging from the table 9 in Kovařík et al. (2020), the same species may show different Eb_3-position types, rendering this character not always reliable (e.g., *S. montanus* Karsch, 1879). Furthermore, much like the telson-L/D, many species that are resemblant with each other in other aspects share the same type of Eb_3-position (e.g., most Yunnan species), which prevents this character from being applied to distinguish those species. This means that Eb_3-position could sometimes only be employed as an accessory character, and it appears to be more informative for the multivariate analysis of the entire genus. For the latter purpose, a perhaps more useful method would be analyzing the geometric area connected by *Dt*, *Est*, Eb_3 and *Db* (i.e., using explicit landmark points to define the relative position of Eb_3).

1.4. Trichobothrial count

Three trichobothrial counts are often used to distinguish *Scorpiops*, chela-Vt, patella-Et and patella-Vt. According to table 9 in Kovařík et al. (2020), most *Scorpiops* have 4 chela-Vt, and only few species can be distinguished with this character by showing extremely high counts (8–25), except for *S. irenae* Kovařík, 1994 which only has 3. The *Scorpiops* of Yunnan cannot be distinguished with this character, nor can they be easily distinguished with

patella-Et. The patella-Et of those species do not exhibit distinct disparity, whether in the past studies by other researchers or in my recent studies. All species vary within the range of 17–20, with 17–19 being normal values (mostly 18). The huge overlap eclipsed the utility of this character in practice.

On the contrary, patella-Vt is more applicable. This is because that almost all of the Yunnan *Scorpiops* vary within a larger interval of [8, 13] (excluding the two most distinct species, *S. jendeki* Kovařík, 1994 and *S. tongtongi*), with the average being [9, 11] (Table 2). There are more integers in the interval of patella-Vt (6) than that of patella-Et (4), resulting in a higher interspecific variability. The variation range of many species is restricted in a smaller interval. For example, the interval of *S. shidian* is [11, 13], meaning its patella-Vt number is never lower than 11. This allows it to be fully distinguished from *S. lowei*, as the latter varies within [8, 10]. However, *S. lowei* was recorded with 11 patella-Vt in the past papers (misidentified as *S. kubani*; Di et al., 2011: table 2). But this only appeared in two patellae of one immature female, accounting for 1/32 of all the studied scorpion specimens (64 patellae). Similarly, *S. shidian* had been recorded with 10 patella-Vt once (Di et al., 2011: table 2), accounting for 1/50 of all the studied patellae (25 scorpion specimens). These records may simply represent anomalies. Without doubt, perfect numerical separation is rarely observed.

Although the interspecific variation range for patella-Vt is higher than that for patella-Et, its numerical disparity is still low, and thus the possibility of showing a great proportional overlap is nonetheless high. Within Yunnan *Scorpiops* species, the overlapping value usually involves 2–3 digits, and it is often their respective normal value range that overlaps (normally, most Yunnan *Scorpiops* vary within [9, 11], so this range is highly overlapped among different species). This means that the data obtained from a randomly selected specimen may very likely to be accord with the normal value of two or more different species, impossible for distinguishment. Conversely, non-overlapping value can often be used for exclusion. For instance, for *S. lowei* and *S. puerensis* (Di et al., 2010), their rate of proportional overlap is 75% (3/4 digits; *S. lowei*: [8, 10]; *S. puerensis*: [8, 11]). It may well be impossible to tell them apart based on this character alone. But if one specimen shows 11 patella-Vt, it is then unlikely to be *S. lowei*.

The abnormal value is often accompanied by visible phenotypic anomalies (e.g., great distance indicates loss of trichobothria; Tang, 2022b: fig. 183); therefore, such a scenario is usually not influential for identification as the observer can conjecture and "reconstruct" the lost trichobothria according to their normal positions. Other anomalies include of the shrinkage of trichobothrial diameter and the proliferation in number (e.g., Tang, 2022b: fig. 217).

1.5. Pectinal tooth count

The utility of PTC is similar to that of patella-Vt, but this character is sexually dimorphic. The upper and lower limits of PTC in females are usually lower than those in males, and data of both sexes should be recorded for a more comprehensive analysis. *S. jendeki* is a very special species among Yunnan *Scorpiops*, hence it is not considered here (data in Table 2). With the temporary disregard of *S. tongtongi* and *S. yangi*, only 3 digits (6, 7, 8) account for the variation interval of PTC in most female *Scorpiops* species (often have 7). The numerical decrease contributes to the increase of overlapping rate and the decrease of diverging rate. The same method is applied – to see if one specimen exceeds the upper/lower limits of a certain species. For example, according to Table 2, if the PTC of one specimen is 7–8 on two sides, then it is unlikely to be *S. lowei* or *S. validus* (Di et al., 2010). Similarly, for a specimen with 6–7 PTC, it is unlikely to be *S. vachoni* or *S. zhangshuyuani*. The reason for the constant emphasis upon

Figures 81–**82**. *Scorpiops* cf. *wrzecionkoi*, male from Lhasa, Tibet, right chela in dorsal (81) and external (82) aspects. Green line: shortest distance between fingertip and proximal margin at the tibio-patellar articulation; red line: chela-L or "axis" defined in this paper; blue circle: region where Stahnke (1970) selected as his P_{in}.

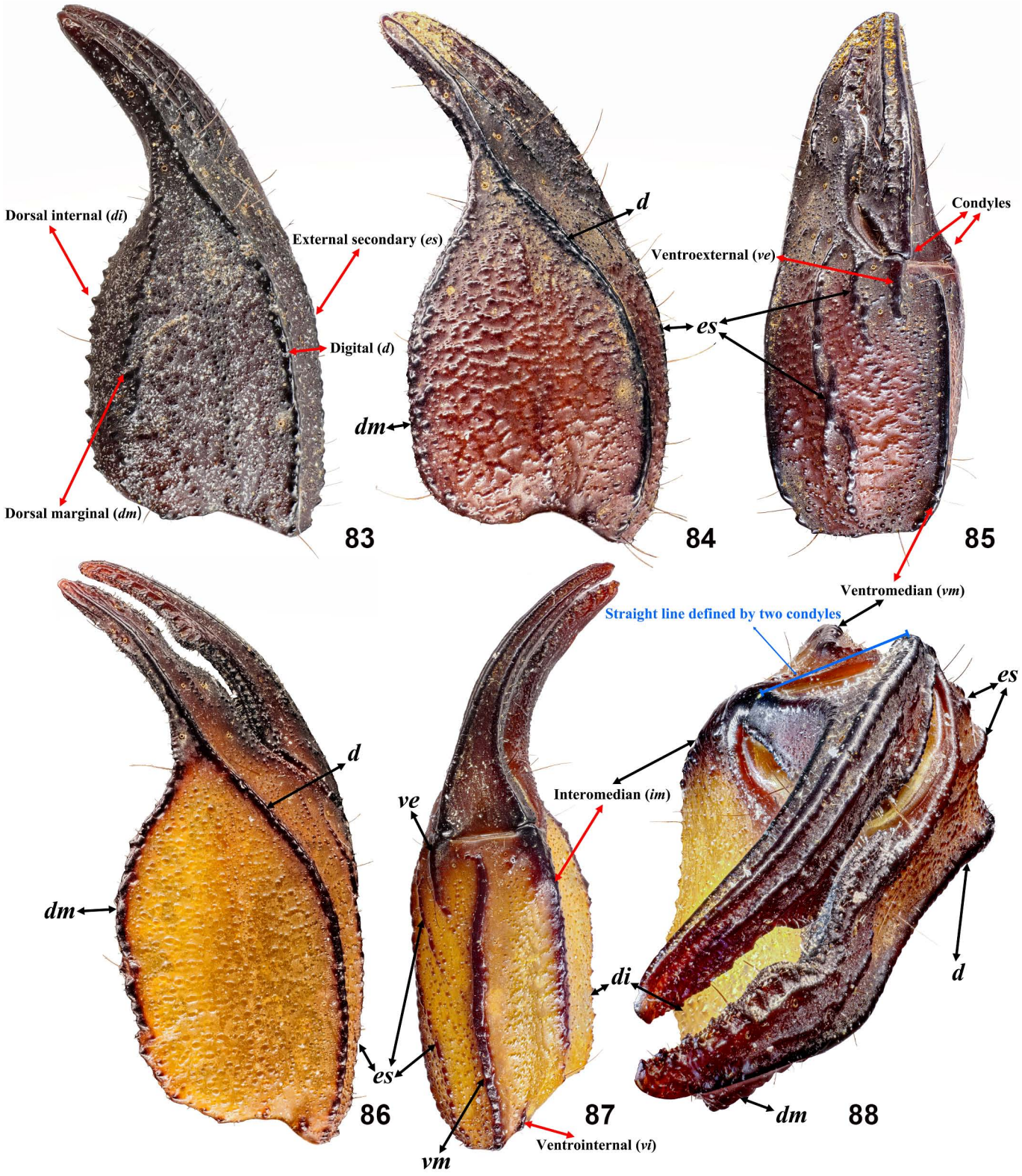

Figures 83–88. Comparison of chelae of *Scorpiops*. **Figure 83**. *S. jendeki*, female, right chela in dorsal aspect with nomenclature of chelal carinae annotated. **Figures 84–85**. *S. langxian*, female from Bayi District, Nyingchi, Tibet, right chela in dorsal (84) and ventro-external (85) aspects, showing two movable finger condyles and a strong ventromedian carina. **Figures 86–88**. *S.* cf. *songi* Di & Qiao, 2020, adult male from unknown locality, right chela in dorsal (86), ventral (87) and front (88) aspects, showing a strong ventromedian carina clearly rising above the two movable finger condyles.

using "unlikely" resides in the fact that the sample size for any certain species examined by any researcher hitherto is not large. Hence it is impossible to conclude whether one species would almost never show a certain value (e.g., whether PTC = 6 is possible for *S. vachoni* females), although such a value would usually be an abnormal one. This highlights the importance of utilizing multiple variables for analysis. The variation interval of males takes in one more digit, 9. Most male Yunnan *Scorpiops* species vary within [6, 9], with the normal state being [7, 8]. By the same token, if one male specimen is recorded 9 PTC, it is unlikely to be *S. lowei*, *S. puerensis*, *S. shidian*, *S. validus* or *S. yangi* (the sample size for *S. xui* is too small, 3 males (two in the original paper and one in this study)). Similarly, if only 6 PTC are recorded, then it is unlikely to be *S. puerensis*, *S. shidian* or *S. vachoni*.

No significant difference was discovered between left and right PTC within recorded data, hence they were pooled together and analyzed. Fig. 200 shows the interspecific discrepancy of mean male vs. female PTC across all ten Yunnan *Scorpiops* and two unidentified populations from Jinghong and Menglun. Data clustering below the diagonal line implies the sexual dimorphism in mean PTC where females have lower PTC than males. Long error bars in female *S. tongtongi*, male *S. xui*, *S. yangi*, female *S. zhangshuyuani* and male *S*. sp. from Menglun were caused by a low sample size; lack of error bars in male *S. jendeki*, *S. tongtongi* and male *S. zhangshuyuani* were due to the consistent records in small samples. It is obvious that most female Yunnan *Scorpiops* have a PTC range of 6–7, while most males fall into the range of 7–8, with *S. jendeki* and *S. zhangshuyuani* being the outliers. It is also apparent that *S. lowei* is well separated from its presumed morphological relatives, *S. vachoni* and the two unidentified populations. Raw data of recorded PTC values for Yunnan *Scorpiops* are available on ResearchGate as supplementary files (https://www.researchgate.net/publication/372719954_Raw_PTC_pectinal_tooth_count_data_of_studied_materials_of_Yunnan_Scorpiops).

The potential obstruction that may occur during the actual recording of PTC is the loss of pectinal tooth/teeth or pectine(s) due to injury. Other cases involve the morphological anomalies in teeth, such as the prominent dilation (e.g., Tang, 2022b: figs. 83, 119), or the incomplete separation of adjacent teeth (e.g., Tang, 2022b: figs. 103, 105). In fact, dilation can be reckoned as a primary stage of incomplete separation, although the latter is usually referred to a tooth with two visible tips, while the former may sometimes be indicated by a small mid-gap at the base of the tooth. In an immature female paratype of *S. lowei*, a rare minimal value was recorded, 5 (Tang, 2022c: fig. 84, right pectine). But this value may well be ascribed to the incomplete separation of two teeth.

1.6. Denticle rows on pedipalp movable finger

Denticle row is a new diagnostic character for *Scorpiops* employed by Kovařík et al. (2020), classified into four types: outer denticle (OD), median denticle (MD), inner accessory denticle (IAD) and inner denticle (ID). These denticle types (dentitions) were initially proposed by Soleglad & Sissom (2001: 33, 35, 37–38) with simple illustrations, and restricted to the distal region of movable finger. They did not discuss how to strictly differentiate denticle rows at the proximity of movable finger, nor had they provided the solution to some anomaly problems. The ambiguity or incompleteness of definition induces the subjectiveness in practice. Tang (2022b) suggested several parameters that can be considered for denticle row classification: denticle size, linearity/continuity of row and interdental spacing. However, some phenotypic anomalies could obstruct the identification.

There are three common scenarios of anomalies: denticle loss (sometimes due to postnatal abrasion; Tang, 2022b: fig. 268, purple arrows), denticle proliferation (e.g., Tang, 2022b: fig. 269, red arrows), and denticle locus disarray (e.g., Tang, 2022b: figs. 85, 182). The determination of denticle loss is the same as that of trichobothria loss, based on its normal locus and spacing. The lost denticle can be reconstructed by the residual trace and the normal size and spacing of the dentition type to which it belongs provided that this margin is not damaged. For example, an OD is usually flanked by two MDs; the distance between these two MDs is usually greater than the normal MD-MD distance. Hence, there must be a loss of MD if there is no denticle between a pair of distant MDs (Fig. 69, red question mark). Denticle proliferation is very common in Yunnan *Scorpiops*; the proliferation of one denticle type may also be accompanied by the loss of another type. For the low degree of proliferation, which could be as low as one or two additional denticles deviated from a certain row (e.g., Tang, 2022b: fig. 268, pink arrow, from its relative position, it cannot be regarded as a subordinate of any denticle row); abnormal denticles usually flank a certain denticle type (e.g., IAD or ID). For additional denticles of a low amount, conservatively they should be discarded during enumeration, because they often do not affect certain denticle rows which will still retain their normal arrangement if one subjectively ignore these denticles (Figs. 72–73, purple dots). Once the amount of the proliferated denticle is increased, it will often lead to denticle locus disarray. In this case, the enumeration of that finger is usually discarded as no denticle type can be classified within a greater range on the movable finger, which would otherwise significantly influence the normality of the data. In the adult male *S. xui* examined in this study, in addition to a proximal section of damaged MD row which thus yielded a low value (64 were identifiable; this data is disregarded), there was also a section of IAD (of only 45 denticles, but the configuration was normal) where those denticles drastically shrunk.

The essence conveyed by the term "denticle row" is the linearity. Hence, the priority for the denticle classification is the degree of linearity. The denticle row can be deemed as a line comprised of multiple discrete dots, and the included angle of the vertex formed by every group of three dots (a triplet) will affect the final linearity. The larger the angle, the higher the linearity; on the contrary, the smaller the angle, the greater the tendency of interlaced arrangement (Fig. 70). If one IAD and two MDs are regarded as a triplet, then their

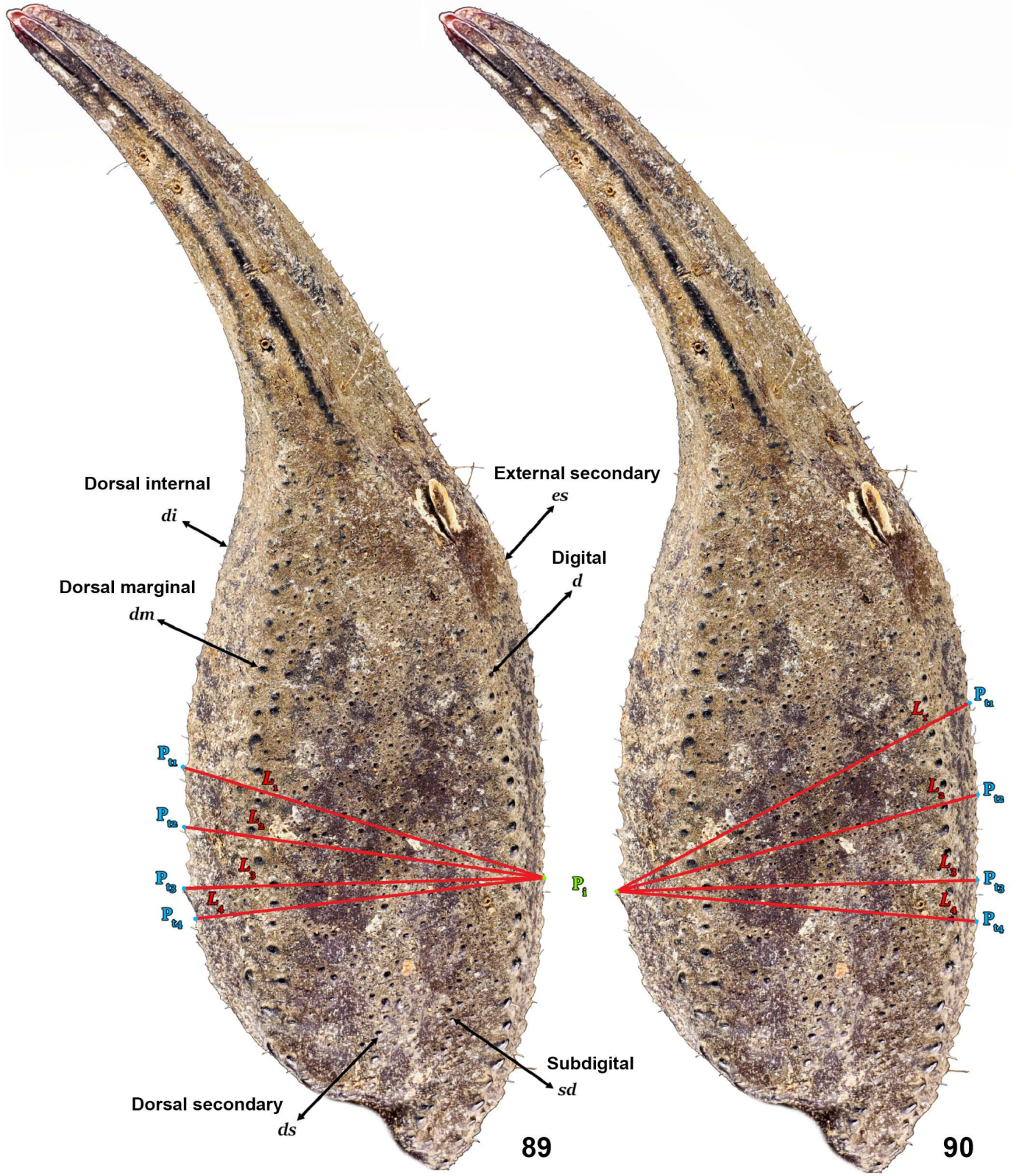

Figures 89–90. *Scorpiops validus*, female, right chela in dorsal aspect. Red lines: options 1 (89) and 2 (90) of chela-W.

included angle is *usually* acute (Fig. 71); if the included angle is obtuse, then there is no IAD within the triplet. This is my usual standard applied for the differentiation of IAD and MD. If a triplet of acute angle is followed by a triplet of obtuse angle at the proximity of the finger, then normally all the subsequent denticles are MD, and IAD is terminated within that triplet of acute angle. In Fig. 71, the female *S. lowei* is marked with three arrows; among which, No.1 refers an MD, and No. 2 and 3 refer to the last two IADs. The determination is based on the included angle of the triplet. But the MD pointed by No.1 is relatively deviated from the main trajectory of MD – its included angle is a bit smaller than other MD triplets. If the included angle is further smaller (i.e., further deviated from other MDs; Fig. 71, blue dot), it will be similar to an IAD. However, the distance between No.1 and No.2 prominently surpassed the normal value of adjacent IAD distance (Fig. 71, pink line). Thus, it is still not reckoned as an IAD. This hence involves another parameter for the denticle identification – interdental spacing. Normally, IADs are all tightly positioned, and so are the MDs, except for the location where an OD occurs (as above discussed). The interdental spacings for both MD and ID are obviously greater, but this spacing may decrease when approaching the distal end.

MD is the primary denticle, while IAD is accessory. This necessitates the prioritized consideration of the linearity of MD. In a case with a female *S. puerensis* (Tang, 2022b: 43, fig. 267), given the included angles, the purple line constituted by three denticles (termed as No. 2, No. 3 and No. 4, from top to bottom, all green) had the highest smoothness (i.e., most linear). But in order to guarantee the linearity of MD, the pink line composed by another set of three denticles (termed as No. 1, No. 2 and No. 3, from top to bottom, No.1 yellow) was selected as the main trajectory. This was because that considering the position, the yellow denticle (No. 1) was an IAD, the green ones (No. 2–4) were MDs, and only MDs would reach the proximity. If the purple line with a higher linearity was recognized, then both No. 2 and No. 3, along with the subsequent denticles, must be homogeneous with No. 4, and would all be considered as IADs, reaching the proximity. This clearly does not meet the definition; IAD must not become the main trajectory. If No. 1 and 3 were regarded as MDs, while No. 2 and 4 as IADs, then the normal interdental spacing would be disrupted: distance 1–3 was greater than 1–2 or 2–3 or 4–2.

In the absence of anomalies, the partition of the four denticle types is usually explicit from the middle to distal region of movable finger (cf. Tang, 2022c: figs. 55–56). But when approaching the whereabouts of MF-lobe, the separation of OD, MD and IAD usually become ambiguous, and particularly in the complex of MD and IAD where they may not form linear rows, but interlace with each other (cf. Tang, 2022c: figs. 42–43). The size of OD is usually larger than those of MD and IAD. However, upon reaching proximity, its size could approximate that of MD (i.e., there is an inconspicuous gradient decrease for the size of OD), impeding the separation. In addition, the major problem for OD identification is its tendency to incorporate into the MD row at the proximal lobe. The final OD is therefore empirically selected according to the common condition within a species (the location where an OD usually terminates), using the specimens showing obvious an OD-MD size difference as standards. However, if the denticle in that position is completely incorporated into the MD row without obvious size difference, no OD is considered, which usually renders a lower count of OD. Whereas OD may become ambiguous proximally, ID may be confused with IAD distally if there is an anomaly. In most Yunnan *Scorpiops,* the most distal IAD shows a clear separation with the subsequent IADs. The anomaly occurs as additional IADs within this section.

IAD usually does not extend to the extreme proximity, because MDs may be arranged in multiple interlaced rows behind MF-lobe (cf. Tang, 2022b: figs. 270–271; fig. 270 showed a female *S. validus* with interlaced multiple rows, while fig. 271 showed a female *S. zhangshuyuani* with one explicit row). Interlaced arrangement prevents a single denticle "row" to be formed; denticles close to the inner side cannot be classified as IADs, nor can those close to the outer side be allocated to MDs. They should all be regarded as MDs. But where should the IAD terminate? For example, in the female holotype of *S. tongtongi*, explicit partitions were never appeared between MDs and IADs (Tang, 2022b: figs. 21–22). Since its MDs also presented an interlaced arrangement at the proximity, the two distinct rows for MD and IAD cannot be identified, precluding a potential interpretation for this condition – IADs accompanied MDs towards the proximity. Therefore, the final IAD was designated as the denticle at the same level as the final OD, treating all the subsequent denticles as MDs. However, the two rows can nonetheless be clearly separated in some species despite their aggregation at the proximity (cf. Kovařík et al., 2020: fig. 119).

1.7. Proximal lobe on dorsal edge of pedipalp chela movable finger

The MF-lobe is a very useful specific diagnostic character. There are three general cases: (1) both sexes barely exhibit evident MF-lobes; (2) males have obviously more prominent MF-lobes; (3) both sexes possess strong MF-lobes. Hence, this character is usually addressed in two ways: "with/without" and "degree". This character is not quantified in the descriptions by most authors, but using qualitative descriptors (with, without, prominent/strong, moderate, weak) instead; the definition of "present/absent" is therefore rather subjective. In some species, MF-lobes are indeed absent (e.g., Kovařík et al., 2020: figs. 200, 202, 220, 424, 526, 680, 698, 700, 702). However, other species do have MF-lobes by comparing with those that certainly lack thereof, despite the fair weakness (e.g., Kovařík et al., 2020: figs. 188, 194, 196, 212, 230, 256, 276). Since those qualitative descriptors were not incorporated into a quantified spectrum of degree, those species with weaker MF-lobes were often also described as "absent" (similar to the rounding in math). A quantification method was proposed in Tang (2022b): evaluate the development degree of MF-lobe by its length/depth (height) ratio (lobe-L/D). However, this method suffers from problems during the measurement.

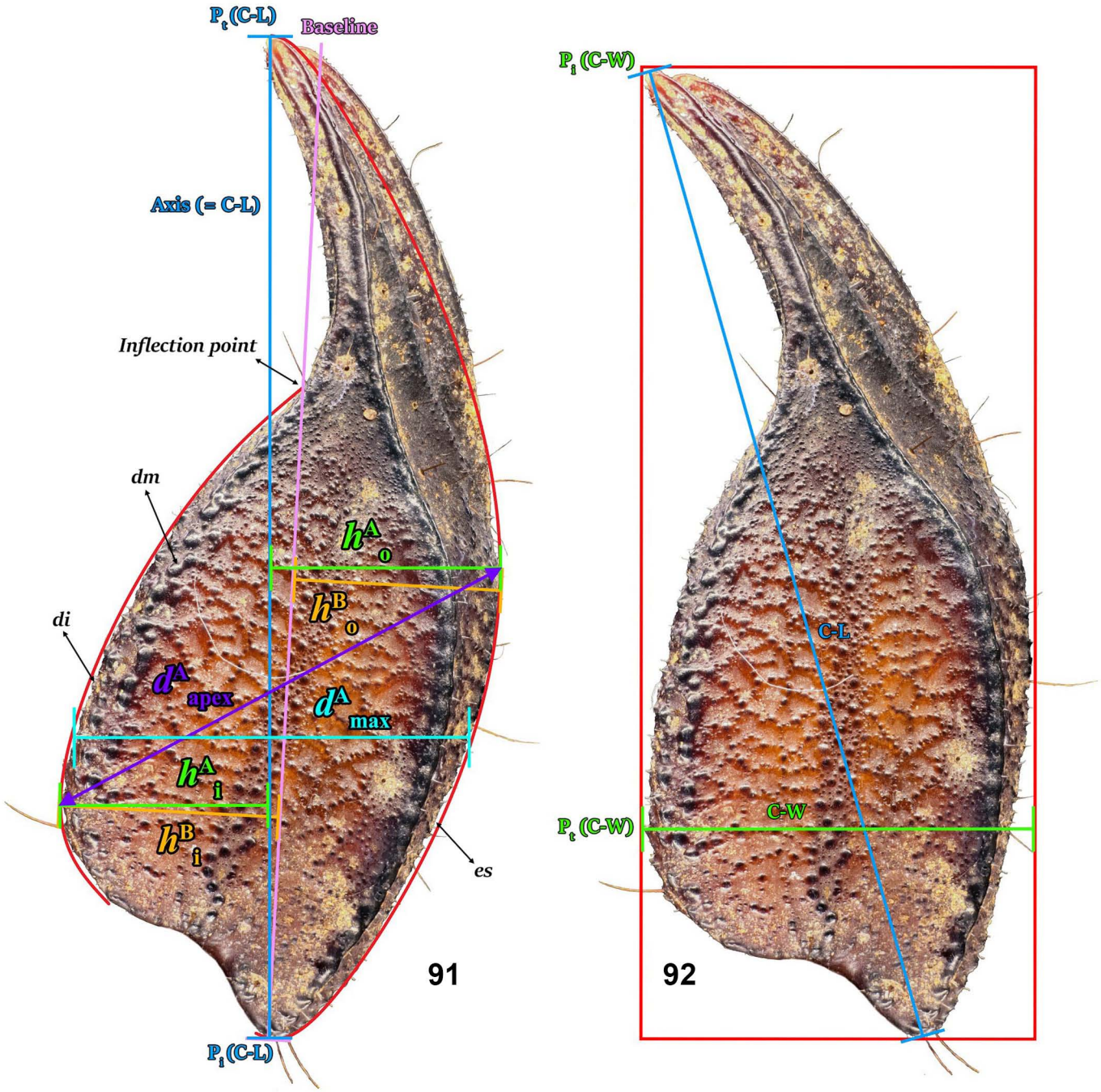

Figures 91–**92**. *Scorpiops atomatus*, female from Gyaca County, Shannan, Tibet, right chela in dorsal aspect. **Figure 91**. Comparison of "axis" and "baseline" methods. Red curves: rough fitting of chela outline; blue line: axis (chela-L in this paper); cyan line: maximal distance and orthogonal to axis; green lines: orthogonal to axis and passing the apexes of both arcs; purple line: connection between to apexes; pink line: baseline of the inner arc; yellow lines: orthogonal to baseline and passing the apexes of both arcs. **Figure 92**. "Squeezing method"; red rectangle confined the chela using four points. The left side of this rectangle is determined by P_{in} (chela-W) (or P_{te} (chela-L)) and P_{te} (chela-W); its right side is a parallel line tangential to the outer arc.

All dimensional measurements include two basic steps, selecting the initial (P_{in}) and terminal points (P_{te}). The value of lobe-L/D that reflects the development of MF-lobe is influenced by the choice of these two points for both the horizontal length and the vertical depth. Since the MF-lobe is essentially risen from the dentate margin of the pedipalp movable finger, one cannot determine its depth before ascertaining its baseline (the straight line that its length is on). Apparently, its length is a part of this margin (how much the MF-lobe covers thereon); therefore, its depth is dependent on its length and one of its points must be on this length. However, there is no obvious P_{in} or P_{te} for this length, as the outline of MF-lobe is fitted onto the dentate margin as a smooth curve rather than a polygonal line (Fig. 75); P_{in} and P_{te} are thus ambiguous at the two convex regions. Using the same MF-lobe as the example and measuring its length and

Figures 93–96. Application of "condyle method" upon a modified caliper (93–95) using the right chela of an adult male *S. xui* as the example, and pinned specimens of *S. tongtongi* (96). In reality, to avoid the deviation caused by the curvature of chelal fingers, the chela needs to be positioned in a vertical direction (Fig. 94); this obviously depends on the width of the L-shaped plate. The chela does not have to be orthogonal to a horizontal plane since the rotation around the pitch axis does not affect the width measured, as long as the roll and yaw axes are fixed (thus defining a 2D plane) based on the rod (however, this could be difficult by manual measurement).

depth twice (Fig. 76), the length and depth obtained from the first trial are termed L_0 and D_0, and those from the second trial are termed L_Δ and D_Δ. If $L_\Delta \neq L_0$, then $D_\Delta \neq D_0$. It is very possible that $L_\Delta/D_\Delta \neq L_0/D_0$, yielding different lobe-L/D ratios. This brings up the problem. Scorpions are small creatures, the final ratios calculated are usually integers with one or two significant digits. However, since these integers are usually the same (e.g., one species is 2.16 and the other is 2.32) or

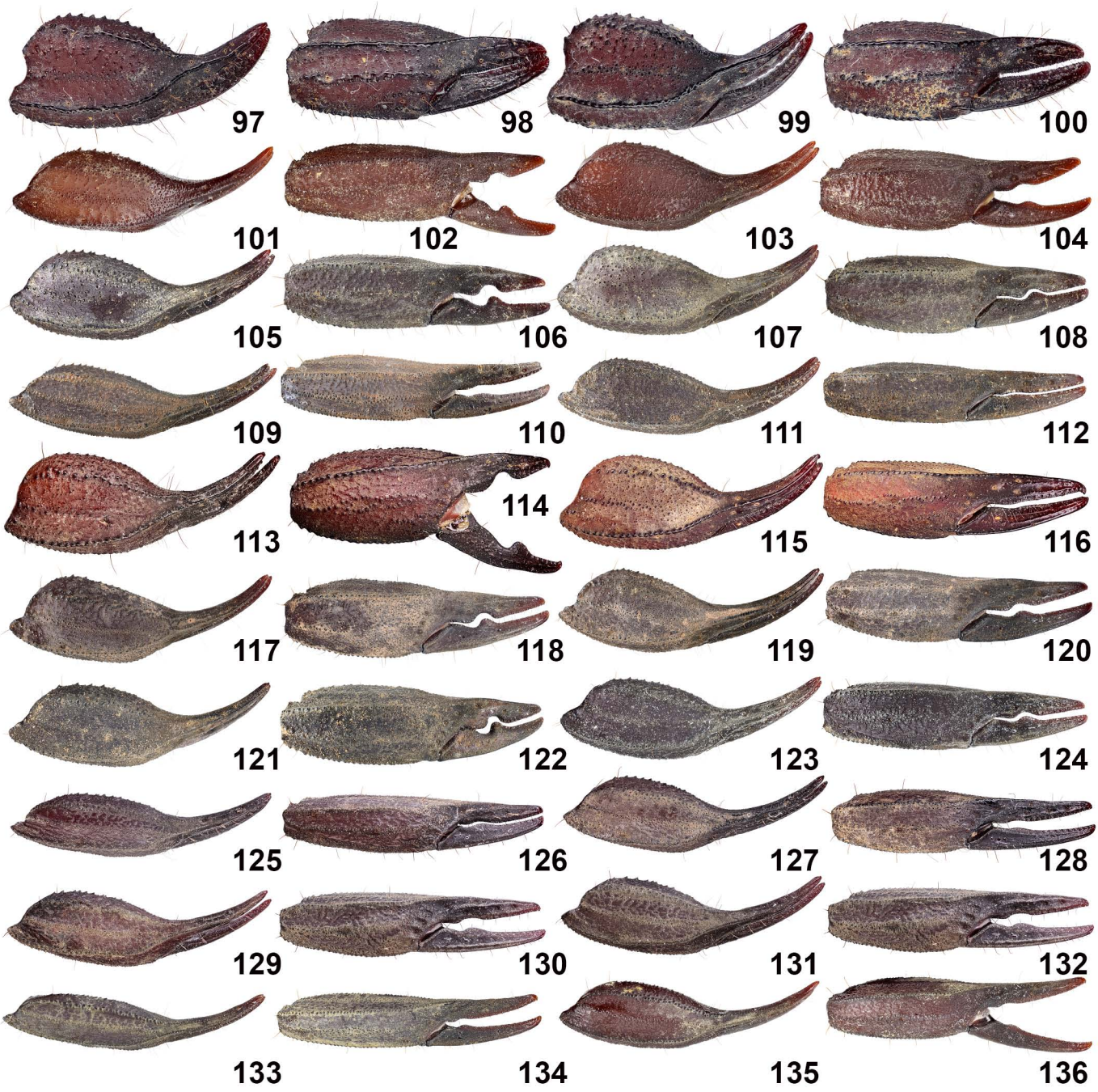

Figures 97–**136**. Comparison of adult Yunnan *Scorpiops* chelae under white light. **Figures 97**–**100**. *S. jendeki* Kovařík, 1994, male (97, 98) and female (99, 100). **Figures 101**–**104**. *S. lowei* Tang, 2022, male (101, 102) and female (103, 104). **Figures 105**–**108**. *S. puerensis* (Di et al., 2010), male (105, 106) and female (107, 108). **Figures 109**–**112**. *S. shidian* (Qi et al., 2005), male (109, 110) and female (111, 112). **Figures 113**–**116**. *S. tongtongi* Tang, 2022, male (113, 114) and female (115, 116). **Figures 117**–**120**. *S. vachoni* (Qi et al., 2005), male (117, 118) and female (119, 120). **Figures 121**–**124**. *S. validus* (Di et al., 2010), male (121, 122) and female (123, 124). **Figures 125**–**128**. *S. xui* (Sun & Zhu, 2010), male (125, 126) and female (127, 128). **Figures 129**–**132**. *S. yangi* (Zhu et al., 2007), male (129, 130) and female (131, 132). **Figures 133**–**136**. *S. zhangshuyuani* (Ythier, 2019), male (133, 134) and female (135, 136).

adjacent (e.g., one species is 1.91 and the other is 2.14) among congeners, the data disparity (morphological difference) is highly dependent on the digits after the decimal place. Thus, for lobe-L/D, the artificial measurement error resulted from the slight deviation of the location of the length selected will greatly affect the subsequent determination of the difference.

Denticles on the dentate margin could be used as the landmarks for P_{in} and P_{te} of the length. They fit onto the outline of MF-lobe and are discrete enough to be selected. Although now there is an objective standard for the two points, it remains a problem of which denticle marks the P_{in} or P_{te} of the MF-lobe. This is still chosen subjectively by human visual

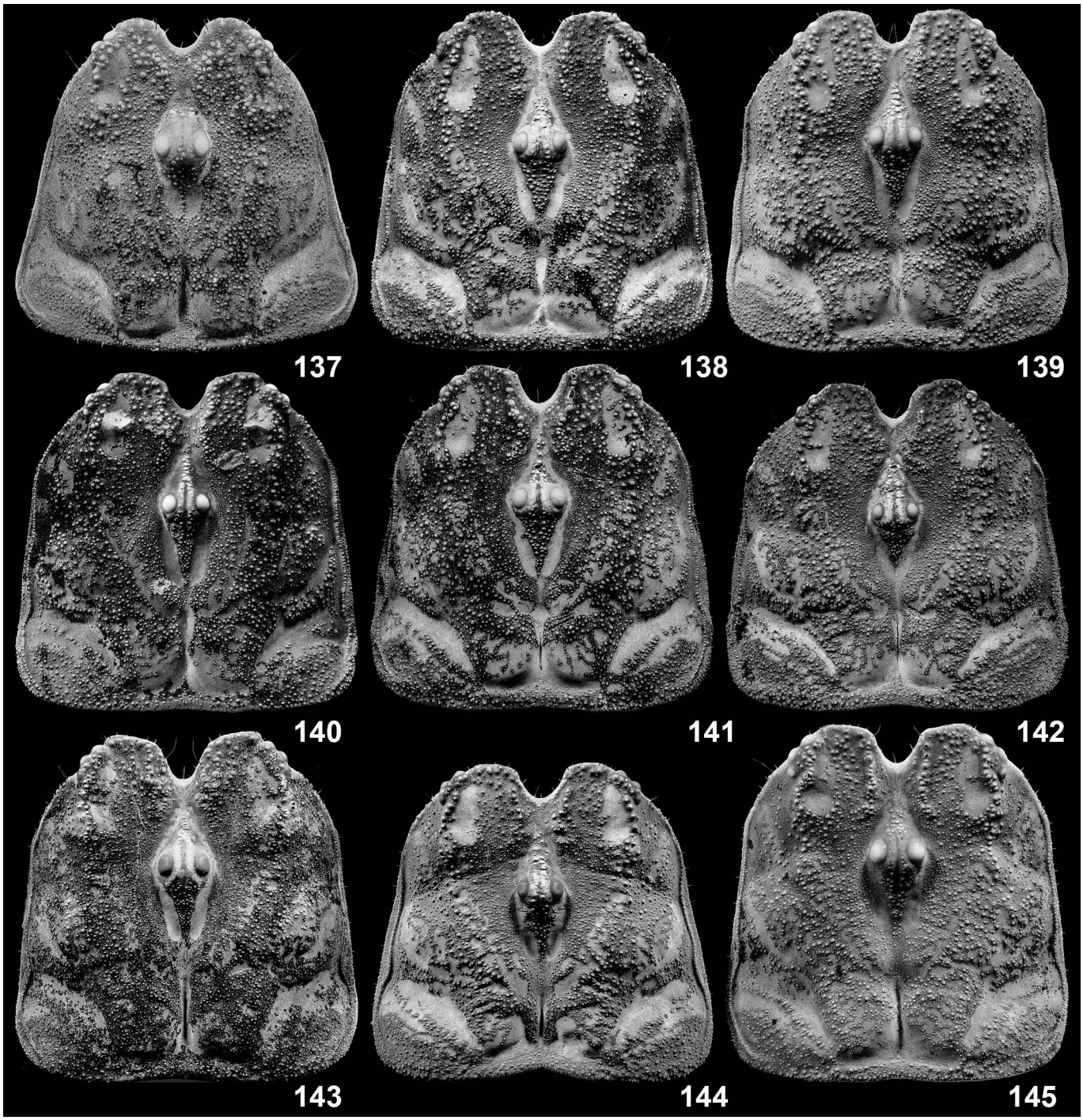

Figures 137–**145**. Carapace morphosculpture comparison between males of *Scorpiops jendeki* (137), *S. lowei* (138), *S. puerensis* (139), *S. shidian* (140), *S. vachoni* (141), *S. validus* (142), *S. xui* (143), *S. yangi* (144) and *S. zhangshuyuani* (145) under UV light. Scale normalized by posterior width.

perception, unless the outline of the dentate margin can be processed in computer programs by curve fitting, allowing the determination of the two convex points (the same points as P_{in} and P_{te}) located before and behind the MF-lobe.

The measurement of depth becomes clear if the length is determined: P_{in} can be set as the apex of MF-lobe and P_{te} is on the length; the straight line determined by those two points should be vertical to the length. The only problem is how the apex of MF-lobe should be determined. Denticles exist on the surface of the dentate margin, so there are two options: (1) take the height of the denticle into account (option chosen in Tang, 2022b); (2) ignore the denticle and set P_{in} on the surface of the dentate margin. However, denticles usually do not have great thickness, so there may not be significant differences between the two options.

Another problem with this method is its utility across the entire genera. For the species/sex (usually females) with very weak lobes, the error will be even greater, because the

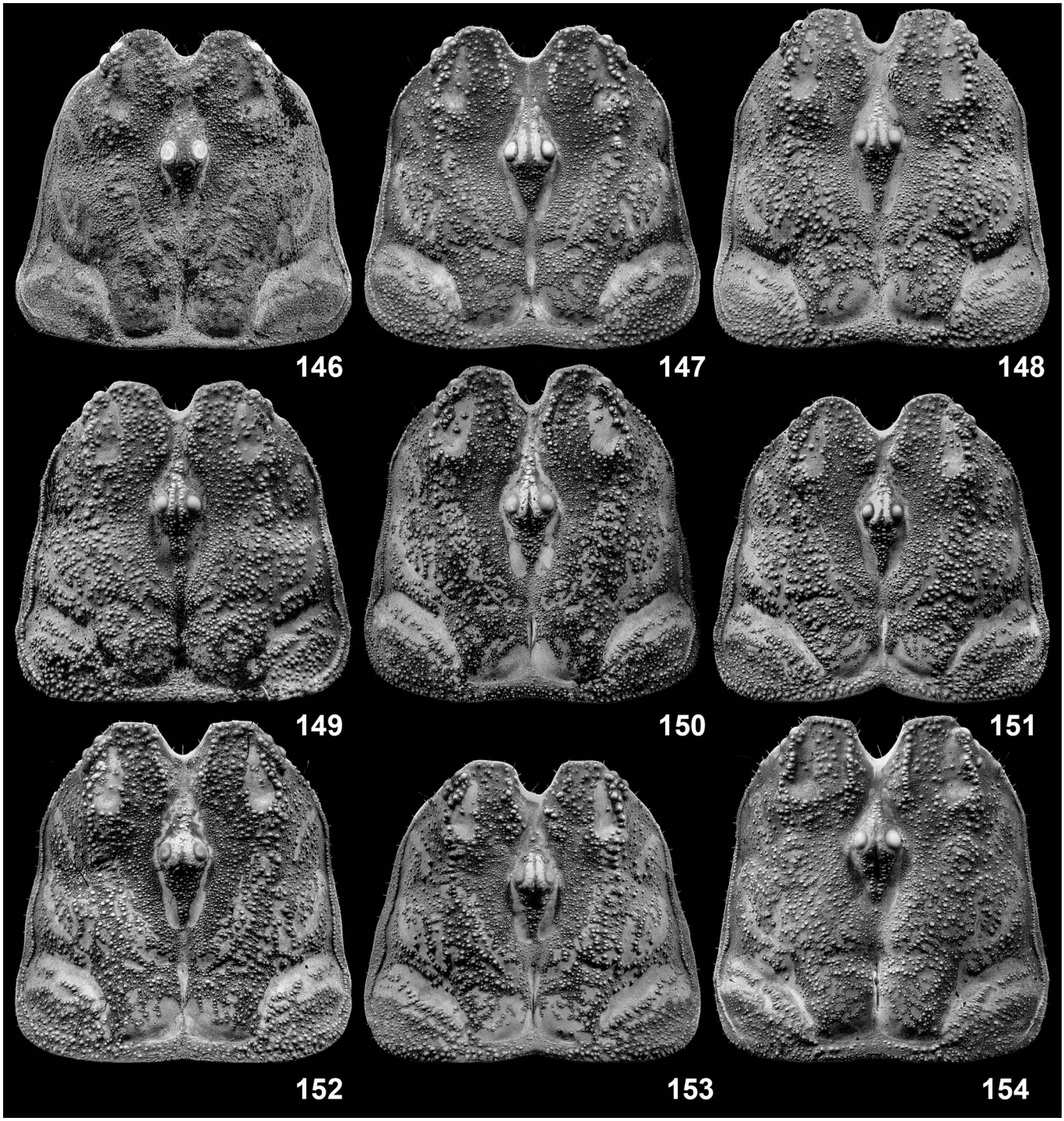

Figures 146–154. Carapace morphosculpture comparison between females of *Scorpiops jendeki* (146), *S. lowei* (147), *S. puerensis* (148), *S. shidian* (149), *S. vachoni* (150), *S. validus* (151), *S. xui* (152), *S. yangi* (153) and *S. zhangshuyuani* (154) under UV light. Scale normalized by posterior width.

outline of the lobe converges more greatly to the outline of the dentate margin (cf. Tang, 2022b: fig. 273). This further affects the choice of P_{in} and P_{te} for the length of MF-lobe. Therefore, this ratiometric value is not used in this study. Providing photos of comparison for common diagnosis (not for multivariate analysis) is probably more practical than using ratiometrics.

Conclusion. The strong overlap of various characters among the *Scorpiops* species gives rise to the heavy reliance upon the sample size and accurate information of origin for the identification of some species. Adequate specimens from the same origin may prevent the specimen data from being within the overlapping range that hinders identification. Additionally, data obtained from adequate specimens may also reflect some trends to some extent.

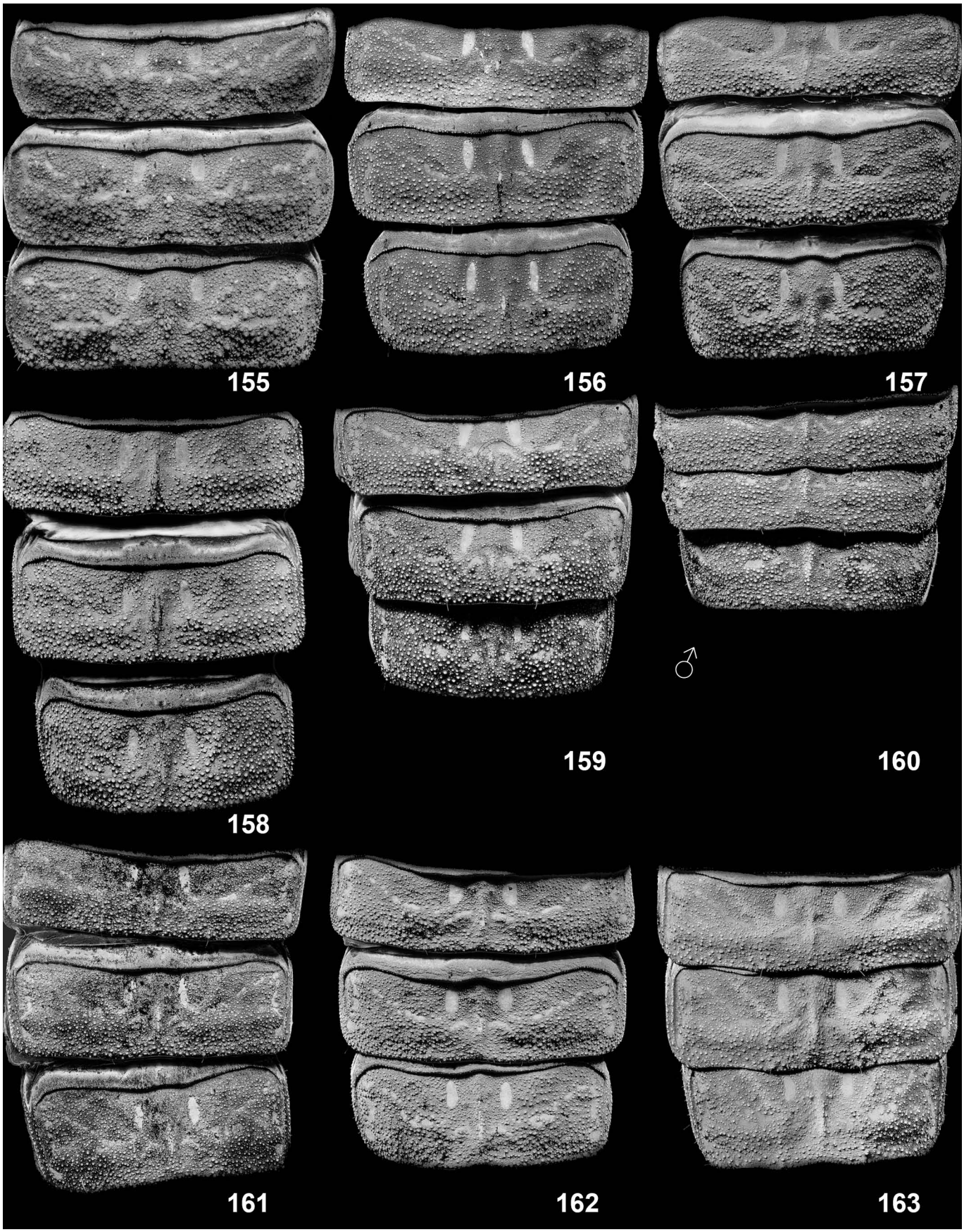

Figures 155–163. Tergites IV–VI morphosculpture comparison between males of *Scorpiops jendeki* (155), *S. lowei* (156), *S. puerensis* (157), *S. shidian* (158), *S. vachoni* (159), *S. validus* (160), *S. xui* (161), *S. yangi* (162) and *S. zhangshuyuani* (163) under UV light. Scale normalized by maximum Feret width at this angle.

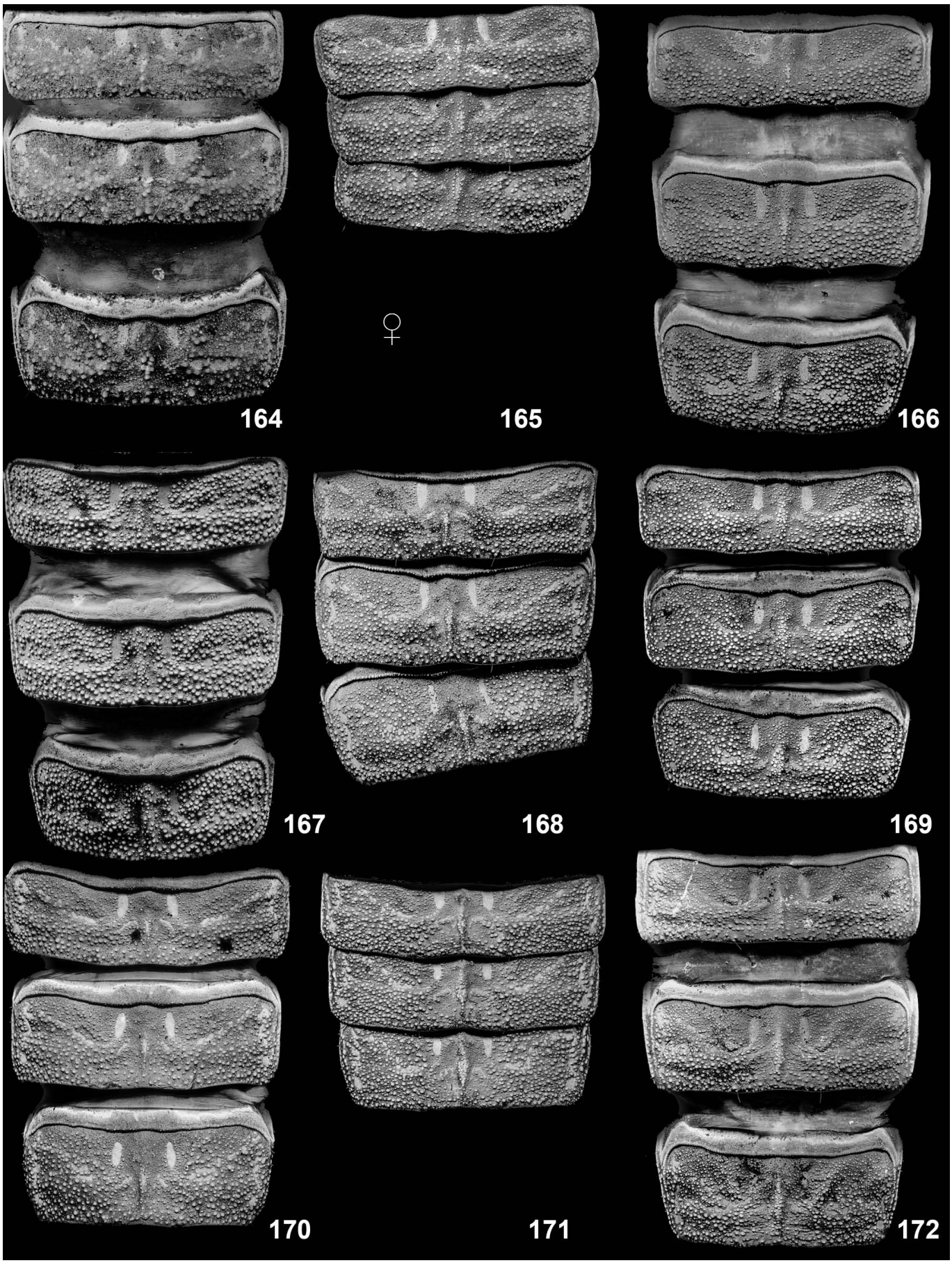

Figures 164–**172**. Tergites IV–VI morphosculpture comparison between females of *Scorpiops jendeki* (164), *S. lowei* (165), *S. puerensis* (166), *S. shidian* (167), *S. vachoni* (168), *S. validus* (169), *S. xui* (170), *S. yangi* (171) and *S. zhangshuyuani* (172) under UV light. Scale normalized by maximum Feret width at this angle.

S. lowei is geographically distant from *S. kubani*, and the only congener between is *S. vachoni* which is clearly different from both species. Tang (2022c) examined some *Scorpiops* populations on the east side of Lancang River (a river between *S. lowei* and *S. vachoni*), from Jinghong City (*S*. sp. 1) and Menglun Town (*S*. sp. 2), distributing very closely to *S. lowei*. The examination upon those populations was aimed to preclude the existence of any transitional population between *S. lowei* and *S. kubani*, thus to confirm the differential characters found between the two species were not the intraspecific variations of the same species. Both populations did not show obvious overall differences from either *S. lowei* or *S. vachoni*, and were as much different from *S. kubani*. Some diagnostic characters were overlapped, but nonetheless different. The robustness of chela and the prominence of MF-lobe of the males in both populations were somewhat stronger than those of male *S. lowei*. More evident differences presented in PTC, dentitions, and patella-Vt. The PTC for females of *S. lowei* was 6–7 (male 6–8), while that for both populations was 7–8 (male 7–9). Their dentition counts for both MD and IAD were higher than those of *S. lowei*, despite a certain degree of overlap (Table 9). The dentition count also showed a transitional increasing pattern in the direction of "*S. lowei* → *S*. sp. 1 → *S*. sp. 2 → *S. vachoni*" (consistent with the geographic direction: west to east, north to south). The normal patella-Vt variation range for *S. lowei* was 8–10, while that for both populations was 10–12. Overall, the two unidentified populations were more similar to *S. vachoni*, but they cannot be readily identified as the latter due to the lack of the knowledge of its distributional limit. Some characters also showed a certain degree of disparity. For example, ΣIAD value of both populations was 48–66, but that for *S. vachoni* was 53–80; ΣMD value of both populations was 80–104, but that for *S. vachoni* was 92–116. However, due to the huge overlap, relying solely on the morphological characters is insufficient.

As what have been expatiated, for morphological identifications, variations occur in both ratiometric and enumerative characters. Some species are mutually overlapped in some degrees, but there could be a general tend – the upper limit of one species is higher than that of the another. This may not be sufficient, as this could also be the overall variation range of the same species. A relatively credible conclusion can be inferred by taking multiple characters into consideration.

2. Measurement of pedipalp chela length and width

Overview. Chela-L/W is the most common diagnostic character used for *Scorpiops*. Although I do not recommend this method, the definition must be addressed in order to reduce the inconsistencies between authors. Those inconsistencies may lead to either the overlap that masks the interspecific difference, or the exaggerated separation thereof. To calculate the ratio, the measurement of length and width is required in the first place, which again brings up the problem of selecting P_{in} and P_{te}. The measurement method varies among different authors; confusions and inconsistency in the data occur in this genus (Tang, 2022b: 21). Current researchers mostly follow the measurement methods proposed by Stahnke (1970: 303–304) or Sissom et al. (1990: 217–218; used in most Chinese papers). However, during the actual performance, both methods are challenged by the uncertainties of subjective definition.

2.1. Measurement of chela length

Both Stahnke (1970) and Sissom et al. (1990) delimited their chela-L by the distance between a location at the proximal margin of chela (here as P_{in}) and the tip of the fixed finger (here as P_{te}). According to the definition by Stahnke (1970: 304), "*Shortest distance from proximal margin at point of tibio-patellar articulation, approximately through trichobothrium B_1, to distal tip of finger*", in combination with his figure 5 (Stahnke, 1970: 303), the P_{in} he defined appeared to be between the digital and external (= "exterior") secondary carinae of the chela (Fig. 77). On the other hand, the P_{in} selected by Sissom et al. (1990: fig. 11.1 D) was not indicated by any carina, but seemed to be located at the apex of the arc observed from the external view (Fig. 78). In reality, this apex could be either the proximal end of the digital carina or that of the external secondary carina, and may as well be in between the two carinae, depending on the shape of the chela and/or the angle at which the chela is positioned. Since the chela-L was not explicitly explained by Sissom et al. (1990), the problem with Stahnke's definition is addressed first.

Problems are concerned with the precise selection of P_{in}. From which aspect should this "articulation" be observed and determined? Assuming that this "articulation" is selected on the manus margin rather than the small joint structure extended from the manus but partially hidden in the intersegmental membrane (which would be even more difficult to select a point on its surface), as illustrated in Fig. 81: should it be observed from the dorsal aspect, then it is obviously not the location of the P_{in} selected by Stahnke (Fig. 82, blue circle), but at the base of the dorsal secondary carina (this depends on the chela shape though, which could be further internal in some species).

Illustrations for the measurement method are confusing in some papers, because chela-L was not indicated by a straight-line segment across the chela, but annotated by one external to the chela profile. The first problem is associated with the shape of the scorpion chela. The outer margin is rarely straight, but curved irregularly. So, is chela-L defined as the straight-line segment that is perceived from the view of a certain angle, or the curve segment that fits onto the outline of the outer margin? By common sense, it should obviously be the former. This leads to the next question. For example, in a figure illustrated in Sun (2010) (Fig. 79), the line segment of chela-L was drawn from the external view. Indeed, when observed from the lateral side of a curve segment on the horizon, it is displayed as a straight-line segment which may represent chela-L. However, by rotating this curve segment around its yaw axis, the length of this straight-line segment will change correspondingly. Although Fig. 80 used an extreme condition to elucidate this problem more clearly,

the ratiometrics are dependent on the measurement of each parameter and the digits after the decimal place are sensitive to the slight deviation. Nevertheless, no paper has defined at what angle the chela should be positioned.

A simple method of clearly illustrating the measurement chela-L would be drawing a straight-line segment across the chela – the maximal distance between the tip of the fixed finger and the apex of the curved proximal outline of manus from the dorsal aspect (Fig. 81). This line segment accords with the maximum Feret diameter of the whole chela, and will be referred to as the "axis" in the next section. The problem that may occur during manual measurement would be the variation of the yaw and pitch axes of the chela if it is positioned in dorsal view. In theory, the yaw axis should be adjusted to ensure the line segment that represents the length is orthogonal to the two opposing surfaces of the caliper jaws. It is imprecise for human eye to locate both P_{in} and P_{te} on a small specimen in reality, and the line segment can vary if the chela is rotated around its yaw axis. The pitch axis is also influential, which changes the included angle between the line segment and the horizontal plane defined by the parallel edges of the opposing caliper jaws; the larger the angle, the smaller the length (= the hypotenuse of a right triangle). A possible solution would be using a thin rectangular bar that is orthogonal to the opposing caliper jaws as the reference line. The lateral surface is used to adjust the yaw axis, while the ventral surface is used for leveling the pitch axis. Nevertheless, since the lateral outline is curved and the dorsal surface is uneven in scorpion chela, this can only be done visually rather than fitting the chela onto both surfaces.

2.2. Measurement of chela width

The measurement of chela-W suffers from even greater problems. As defined in Stahnke (1970: 304), "*Greatest interior to exterior marginal width*", the measurement of chela-W clearly requires to locate P_{in} and P_{te} on the "inner" and "outer" margins of the chela. The two margins viewed by the observer are dependent on how the chela is placed (which will be further discussed), but chela-W is conventionally taken from the "dorsal aspect". Carinae can be utilized as landmark margins; however, not all the scorpion chelae are carinate. Stahnke (1970) did not use carinae to define chela-W, nor did Sissom et al. (1990) illustrate any carinae. The figure drawn by Sissom et al. (1990: 218) was very similar to figure 13E in Cain et al. (2021) in their revision of Levant *Buthacus*, a genus that lack prominent carinae on their chelae, but differed by the angle of chela placement. It appears that Cain et al. (2021: 18) obtained the chela-W after they placed the chela at a specific angle at which the fixed finger fully covers the movable finger (but not in Sissom et al., 1990). However, the selection of maximal chela-W seems to be subjectively perceived without an objective reference. Nevertheless, *Scorpiops* are carinate species and these carinae can serve as the "landmarks" for the delimitation. Four methods are proposed and evaluated here, namely "baseline method", "axis method", "squeezing method" and "condyle method", using different reference systems, with two premises firstly clarified below.

The first problem is associated with the carina morphology. For species with granulated carinae on the pedipalp manus, before measuring the distance between the inner and outer margins (if the margins are defined by those carinae), one must consider whether the height of the granule should be included in chela-W, which neither Stahnke (1970) nor Sissom et al. (1990) discussed. The size of the carinal granule at the same or similar location may vary due to interspecific differences or postnatal damage (e.g., abrasion). If two individuals of two species had the same chela-L/W ratio when granules were disregarded, the species with larger granules will most certainly yield a smaller chela-L/W if it was measured again with granules included (i.e., chela-W is increased). Variations as such could mask or amplify the interspecific difference, but this is more likely to result from a combination with many other variables as granules are relatively small. In this paper, all the measurement methods discussed included the granule height.

The second problem lies in the selection of landmark carinae. For genus *Scorpiops*, there are four carinae associated with the inner and outer margins, namely dorsal internal (*di*, = D5 in Soleglad & Sissom (2001: 41)), dorsal marginal (*dm*, = D4 in Soleglad & Sissom (2001: 41)), digital (*d*, = D1 in Soleglad & Sissom (2001: 41)) and external secondary (*es*, = E in Soleglad & Sissom (2001: 41)) carinae (Fig. 83), from inner to outer. When viewed from the dorsal aspect, the visible carinae are determined by the shape of chela (interspecifically variable) and the precise angles of observation and/or placement of chela (human errors). In some species, the chela manus is flattened and its internal surface is concealed (Fig. 86), thus resulting in the concealment of *di* (which is also usually weak) by *dm*; *dm* hence becomes the mere available carina left as the proxy of "inner margin". On the contrary, the chela appears cubic from front aspect in many Yunnan *Scorpiops* with elongated pedipalps, which *di* is therefore revealed and marks the "inner margin" as it is external to *dm* (Fig. 89). In species with rounded and robust chela, *es* is usually clearly visible and consistently external to *d* along its length (Fig. 84); it hence signifies the "outer margin" in order to obtain a maximal chela-W. However, in species with weaker *es*, *es* may converge to the outline of *d* at the proximal section, although this is also affected by the angle of view. The choice of inner margin is simple: choose *di* if it is visible; if it is not, then choose *dm*. Given that the external surface of chela is usually convex, *es* would be selected as the outer margin in most cases as it is often exposed.

(1) Measurements restricted within the dorsal profile of chela

If chela-W is taken from the dorsal aspect and all the measurements are applied upon the chela surface, the "dorsal plane" of the chela must be first defined. Unlike many buthid species which show a globous chela, *Scorpiops* species present a more cubic chela as it is carinate. The surfaces between each pair of those carinae can be considered as "planes". Assuming the "dorsal plane" is defined as the flattest plane with the maximum area visible when a scorpion is placed in its natural

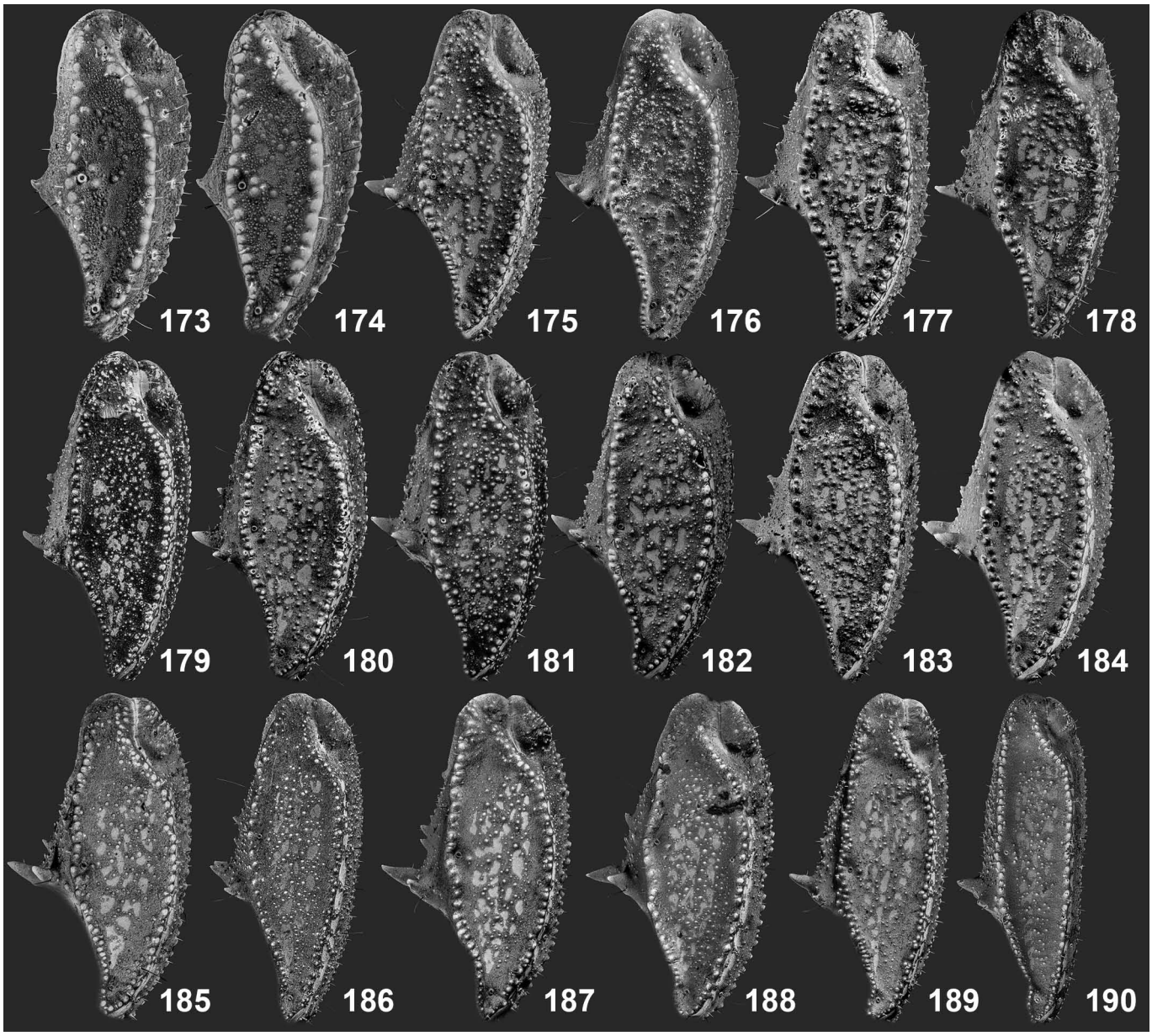

Figures 173–**190**. Right pedipalp patella comparison between adult *Scorpiops* spp. under UV light. **Figures 173**–**174**. *S. jendeki*, male (173) and female (174). **Figures 175**–**176**. *S. lowei*, male (175) and female (176). **Figures 177**–**178**. *S. puerensis*, male (177) and female (178). **Figures 179**–**180**. *S. shidian*, male (179) and female (180). **Figures 181**–**182**. *S. vachoni*, male (181) and female (182). **Figures 183**–**184**. *S. validus*, male (183) and female (184). **Figures 185**–**186**. *S. xui*, male (185) and female (186). **Figures 187**–**188**. *S. yangi*, male (187) and female (188). **Figures 187**–**188**. *S. zhangshuyuani*, male (189) and female (190). Scale normalized by maximum Feret length at this angle.

posture (i.e., dorsum revealed), its two boundaries will be delimited by the carinae *dm* and *d* as both *di* and *es* are lower than thereof (therefore not on the same plane with *dm* and *d*). This leads to the placement of the chela: adjusting the dorsal plane of chela parallel to a horizontal plane; and the angle of observation: sight trajectory orthogonal to the dorsal plane. However, the dorsal plane is not always ideally flattened but may be irregularly convex. This prevents one from firmly attaching it to a horizontal plane to ensure parallel. Therefore, the adjustment is often visually determined and less accurate. A mathematical correction procedure is to fit an ellipsoid to the silhouette of the chela in lateral view (defined by a sight trajectory that is parallel to the condylar axis). The pitch angle that needs to be adjusted can be the angle of the major ellipsoid axis of the fit, and needs to be rotated out to zero to level the chela. The major ellipsoid axis angle can be measured in software (e.g., ImageJ). Then physically replicate the same chela pitch angle holding the pedipalp by the patella with a 3D clamp. This requires a lateral photo of the chela in the first place (note: the major ellipsoid axis does not equal the chela-L as the former is influenced by the inward curvity of the finger with respect to the yaw axis that is orthogonal to the condylar axis). Since it may cause significant deviation when measuring the length after the roll angle is adjusted, it is better to leave

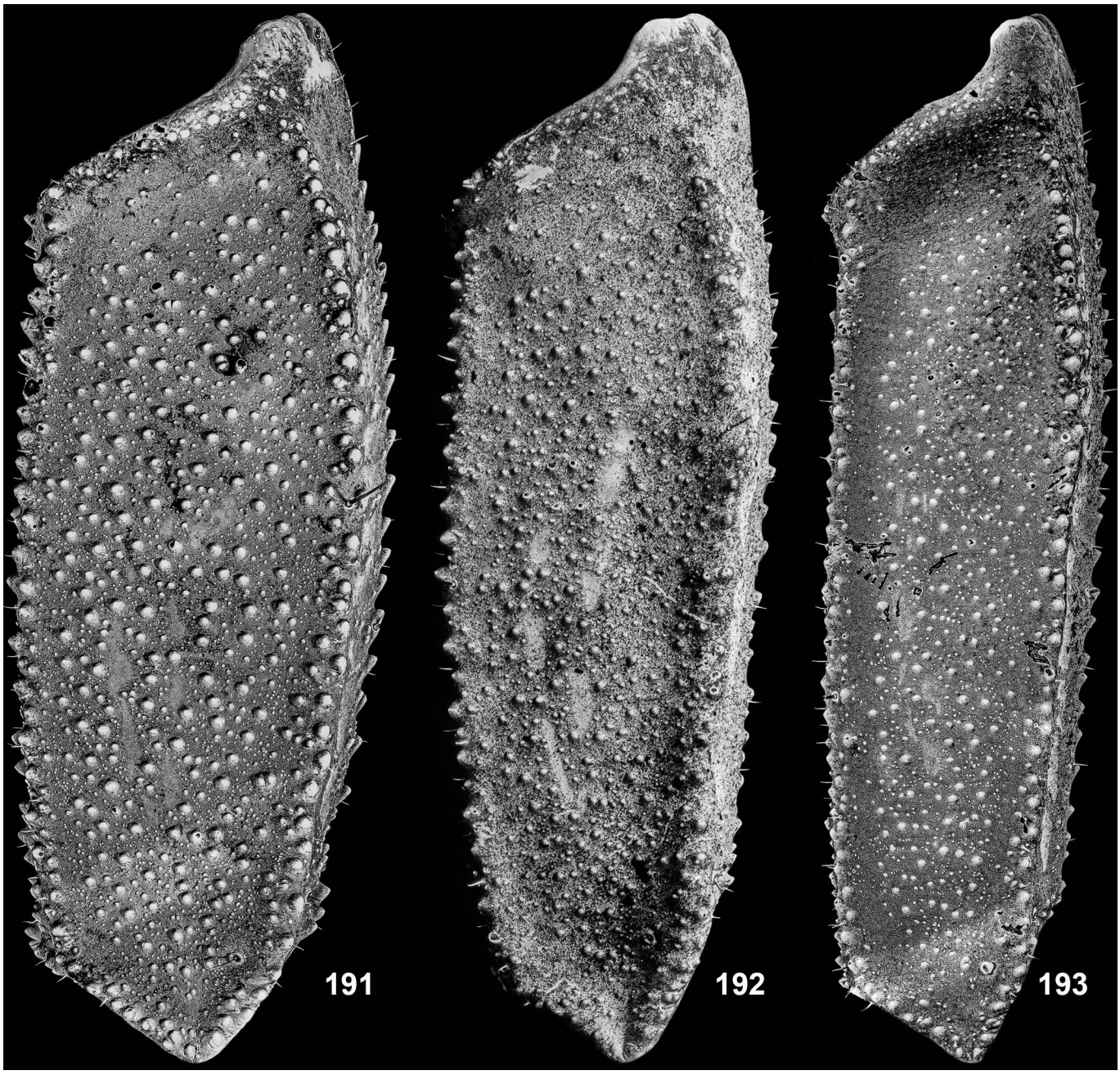

Figures 191–**193**. Right pedipalp femur comparison between males of *S. shidian* (191), *S. xui* (192) and *S. zhangshuyuani* (193) under UV light in dorsal view. Scale normalized by maximum Feret length at this angle.

the chela untouched, and take a photo in dorsal view (defined by a sight trajectory that is orthogonal to the condylar axis) to obtain the length in computer. However, the length obtained is in pixel, and in order to obtain a value in millimeter, it requires another parameter that has a functional relationship with the length and can be definitely obtained in both pixel and millimeter scales. This method is also time consuming in terms of the steps and adjustment it demands. In addition, the major ellipsoid axis can be affected by the upward curvity of the finger which is interspecifically variable. Therefore, it may only be recommended for an analysis that requires relatively precise data.

Since the inner and outer margins (below, as inner and outer arcs; Fig. 91, red curves) are often curved in many *Scorpiops* species, the visually judged maximal width can be easily biased. This necessitates carinal granules to be selected as the definite landmarks. If both *di* and *es* are visible (a common condition for all Yunnan *Scorpiops*), *di* is selected as the inner arc and *es* as the outer arc. To obtain the maximal distance (as defined by Stahnke, 1970), at least one of the points must be selected as the apex of the arc (this depends on the arc defined which will be further discussed). Assuming the granule height is taken into consideration with P_{in} determined visually, four width options are given (Figs. 89–90): (1) case

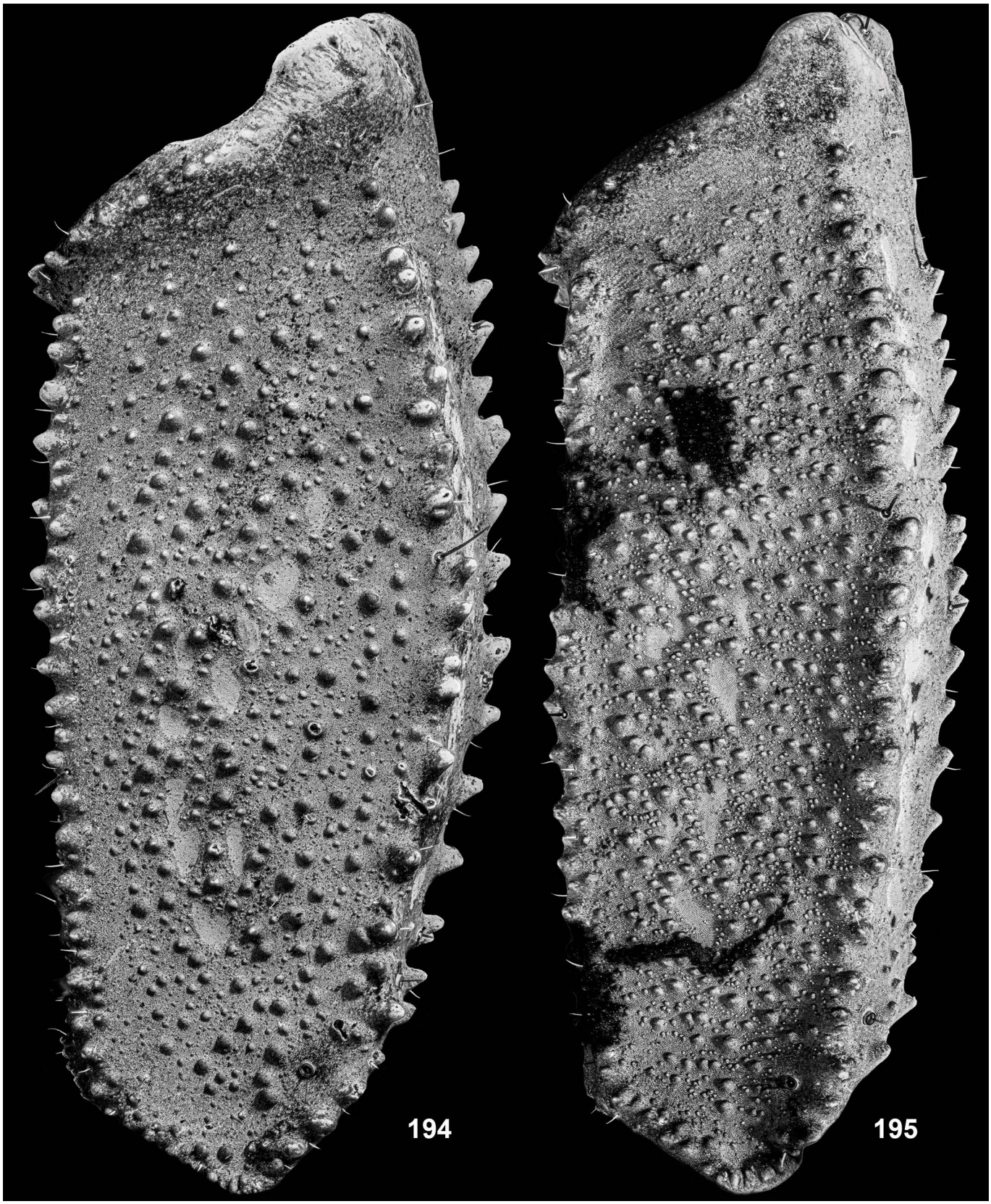

Figures 194–**195**. Right pedipalp femur comparison between males of *S. validus* (194) and *S. yangi* (195) under UV light in dorsal view. Scale normalized by maximum Feret length at this angle.

1: P_{in} on *es*; (2) case 2: P_{in} on *di*. Apparently, in both cases, L_3 is the most appropriate distance to represent chela-W by intuition. However, those different options are intentionally illustrated to be distinctive. In reality, the up/downward deviation from L_3 caused by the change of P_{te} could be slighter, but this error nonetheless contributes to a probably influential change of the value after the decimal place, which would yield a ratiometric value that masks the interspecific difference (i.e., presented as the overlap of chela-L/W between species). Case 2 is more sensitive to deviation as there are no prominently enlarged granules on *es* that would usually be considered as the landmark points; on the other hand, in case 1, some species may have multiple enlarged spiniform granules of similar heights. The exact reason accounting for the free variation of the location of P_{in} and P_{te} lies in the fact that there is no defined reference system with respect to the selection of landmark granules. This further results from the dorsal profile of a scorpion chela not being a relatively regular geometric shape. If it is axisymmetric (e.g., rectangle or rhombus), the width will then be easily determined by the latitudinal axis. The outline of the scorpion chela is usually an arc, and human eyes are not sophisticated enough to determine the apex of an arc. Therefore, it is difficult to reproduce the method as both P_{in} and P_{te} selected are free to move along the arcs. Two methods, baseline and axis methods provide a definite reference system for the arcs and thus their apexes.

Both the baseline and axis methods require two measurements to obtain chela-W, the heights of the inner and outer arcs. A baseline must present to determine an arc's P_{in} and P_{te} and therefore obtain its height by drawing a perpendicular passing its apex (a line segment with the maximum length). The inner margin of the chela is undulate from dorsal aspect: it is concave at the manus region but convex from the base of the fixed finger. This results from an inflection point approximately located between the manus and finger, causing the finger to curve inwards. A baseline of the inner arc is defined by this point and the P_{in} of chela-L ("axis") (Fig. 91, pink line). Since the fingertip is more internal to this inflection point, the outer arc that is dependent on the curvity of finger will be intersected by this baseline. Hence, this baseline is only for the inner arc. As illustrated in Fig. 91, the chela-W obtained by the baseline method equals $\Sigma h^B = h^B_i + h^B_o$ ("*h*" for height, "B" for baseline, "i" for inner, "o" for outer). As above discussed, the axis (Fig. 91, blue line) is the chela-L defined in this paper, from the proximity of manus to the fingertip. For the same reason, it will intersect the inner arc. As illustrated in Fig. 91, the chela-W obtained by the axis method equals $\Sigma h^A = h^A_i + h^A_o$ ("*h*" for height, "A" for axis, "i" for inner, "o" for outer). The axis method is essentially a variant of the baseline method as the axis itself is also the baseline of the outer arc. However, it is clear that the height of one of the two arcs in either method is not obtained with respect to its baseline as there is none. What about using the baseline method for the inner arc and the axis method for the outer arc? Chela-W = $\Sigma h = h^B_i + h^A_o$. This will result in a repeated measurement in the region between the baseline and the axis. The contrary algorithm (i.e., chela-W = $\Sigma h = h^A_i + h^B_o$) results in a lack thereof. Furthermore, both methods are relatively difficult to be performed and the errors will be greater as it involves two independent measurements.

Another method would be drawing a straight line orthogonal to either the baseline or the axis and moving it across the entire manus plane, intersecting with the inner and outer arcs, and deeming the line segment with the greatest length as chela-W. This line segment is subject to the yaw axis and does not seem to fit with the width of a chela in common sense as it is oblique (Fig. 91, cyan line, derived from the apexes in the axis method as an example). It is also visually inaccurate to determine the maximal length intersected. Additionally, the line segment obtained by connecting the two apexes is also not an appropriate representative for chela-W because it is even more oblique (Fig. 91, purple line, using the axis method as an example) and its value will be greater (the sum of the hypotenuses of two right triangles).

(2) Measurements surrounding the profile of chela

The "squeezing method" (Fig. 92) is more convenient and preferrable comparing to the above ones. The measurement of chela-W is still conducted after the chela is placed dorsally; however, it does not start directly upon the dorsal profile. The first step is to draw a straight line passing a point on the outline of the fingertip (P_{in}), and rotate it around the yaw axis of P_{in} to make it tangential to the inner arc apex, deriving P_{te}. Then, draw its parallel straight line and make it tangential to the outer arc apex. The distance between the two straight lines is thus defined as chela-W, which seems to accord with an intuitive cognition for the width of chela; this width equals the minimum Feret diameter of the whole chela. It confines the entire chela within a rectangular space, defining chela-W by measuring the width of the rectangle. This would easily give chela-L/W by measuring pixels if the above steps are conducted in computer – both the pixel length of the maximum and minimum Feret diameters can be easily obtained at a more accurate degree. Chela-W is a two-dimensional measurement. In Euclidean geometry, a straight line must be defined by at least two points (or, two points can determine a straight line) and it is infinitely continuous. An ordinary digital image displayed on a computer is usually represented by discrete points, i.e., pixels; thus, a line in an image is not strictly a Euclidean geometry. However, it can be approximated as such in many cases. This allows people to convert pixels in to millimeters when measuring specimens on a computer. The examiner can crop out the chela from the original image into a rectangular image that firmly confines the chela by adjusting its angles in computer software like Photoshop. To obtain the actual chela-W in millimeters, one only needs to measure chela-L on the real specimen (which causes fewer errors) and then calculate chela-W in proportion to the chela-L/W derived from the pixel measurement (chela-W^{mm}= chela-L^{mm}/(chela-L/W^{pixel})).

However, this method has its limitation. The chela-W derived is dependent on the morphology of the pedipalp finger – the inward curvity of the finger will influence the width of the rectangle that confines the chela profile. In species with a

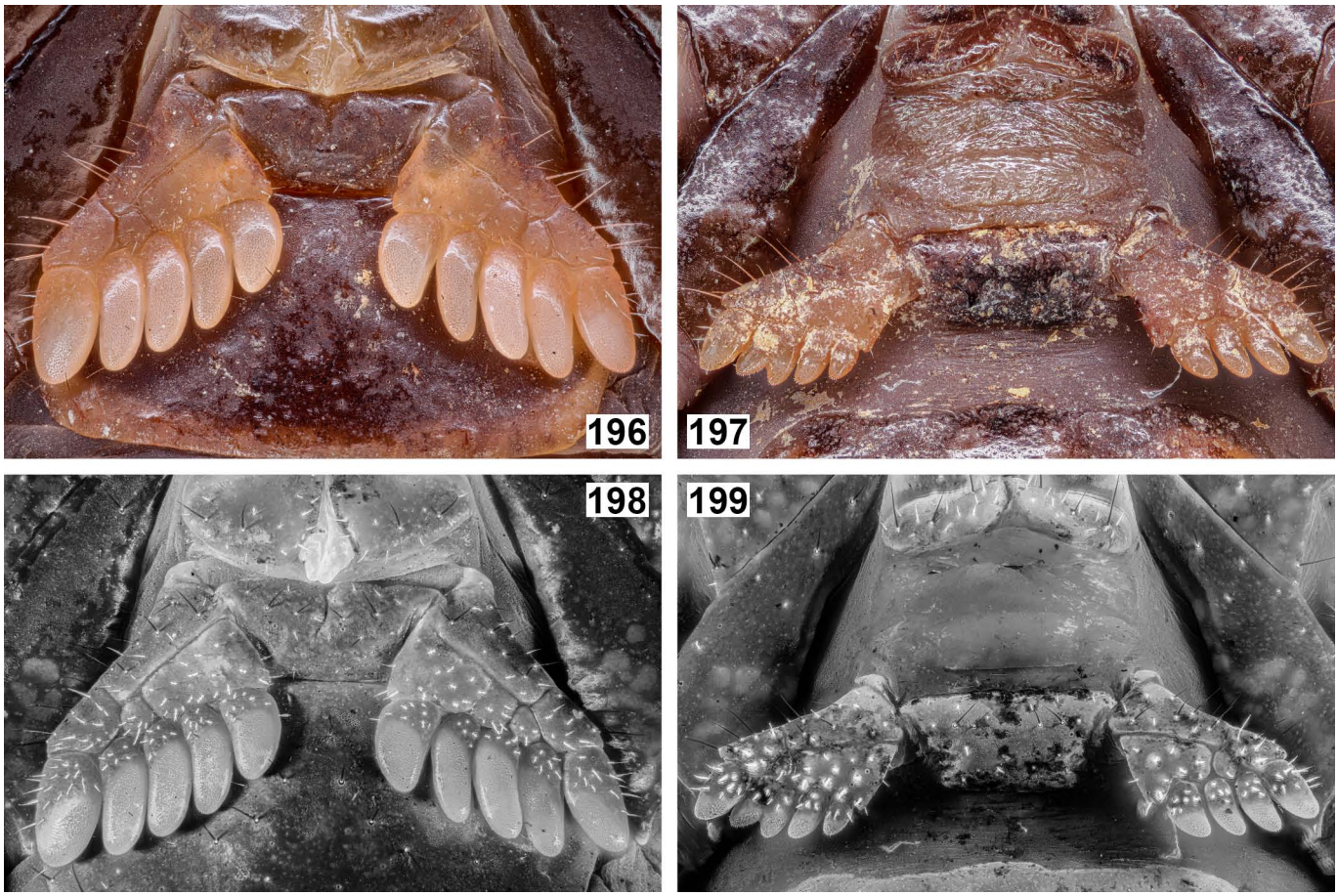

Figures 196–199. *Scorpiops jendeki*, male (97, 98) and female (99, 100) pectines. **Figures 196–197**. Under white light. **Figures 198–199**. Under UV light.

more curved fixed finger, the minimum Feret diameter derived from this rectangle will be greater than an intuitively perceived chela-width (i.e., the manus width that is independent of the finger) (e.g., Kovařík et al., 2020: fig. 253, *S. grandjeani* (Vachon, 1974), figs. 261, 263, *S. citadelle* (Kovařík, 2013), fig. 271, *S. asthenurus* Pocock, 1900). The aim of this paper is to establish a general measurement method for the genus *Scorpiops*. Although most *Scorpiops* species do not show conspicuous differences between the two widths (the Feret width derived from the "squeezing method" and the intuitive width of the manus), those exceptions rendered this method to be less applicable.

The fourth method involves an alteration in the placement of chela, deriving the "condyle method". Not all scorpions have carinate chela or share the same curvity of fingers, but all species possess a pair of ventral condyles at the base of their movable finger. This universal morphological character can be utilized as the landmark points to define a straight line ("condylar axis"). Many authors may place the scorpion specimen in its natural posture as would occur in vivo, which causes variable torsions around the proximal-distal axis of the chela (the "roll axis") due to specific adaptations. This renders the chela placement less well-defined but leveling the condylar axis (the "pitch axis") could cancel this torsion effect. Fitting condylar axis to the horizontal plane and then stabilizing the chela on this surface by randomly attaching at least one point (e.g., granules, which the largest would be the first one(s) to make contact) on its ventral side allows one to place the chela on a horizontal plane firmly and definitely. However, this method is not applicable if the ventromedian carina (*vm*, = V2 in Soleglad & Sissom (2001: 41)) of the chela is highly developed as in many *Scorpiops* species (Figs. 85, 87–88). The strong *vm* is "higher" (or lower, depending on the view aspect) than the condylar axis, it will be "pressed" into the horizontal plane (assuming it is soft) if employing the above method. Only a solid plane can firmly stabilize the chela; however, the raised *vm* prevents the attachment of the chela ventral surface (defined by the condylar axis and at least one point) to the plane unless it is crushed. Moreover, this may even be impossible to be applied as the two condyles could be way below (or above, depending on the view aspect) the highly developed *vm* in some *Scorpiops* species. It is also not ideal to define a plane by the two condyles and a point on the distal section of *vm*. If this plane is made horizontal, it would cause the proximal part of the chela posterior to that point to tilt upward (i.e., rotation around the pitch axis). Depending on the development of *vm*, the tilting angle may vary. Nevertheless, this does not affect the measurement chela-W, but only the photography of the dorsal profile of chela. Should one place the chela at the angle that allows the fixed finger

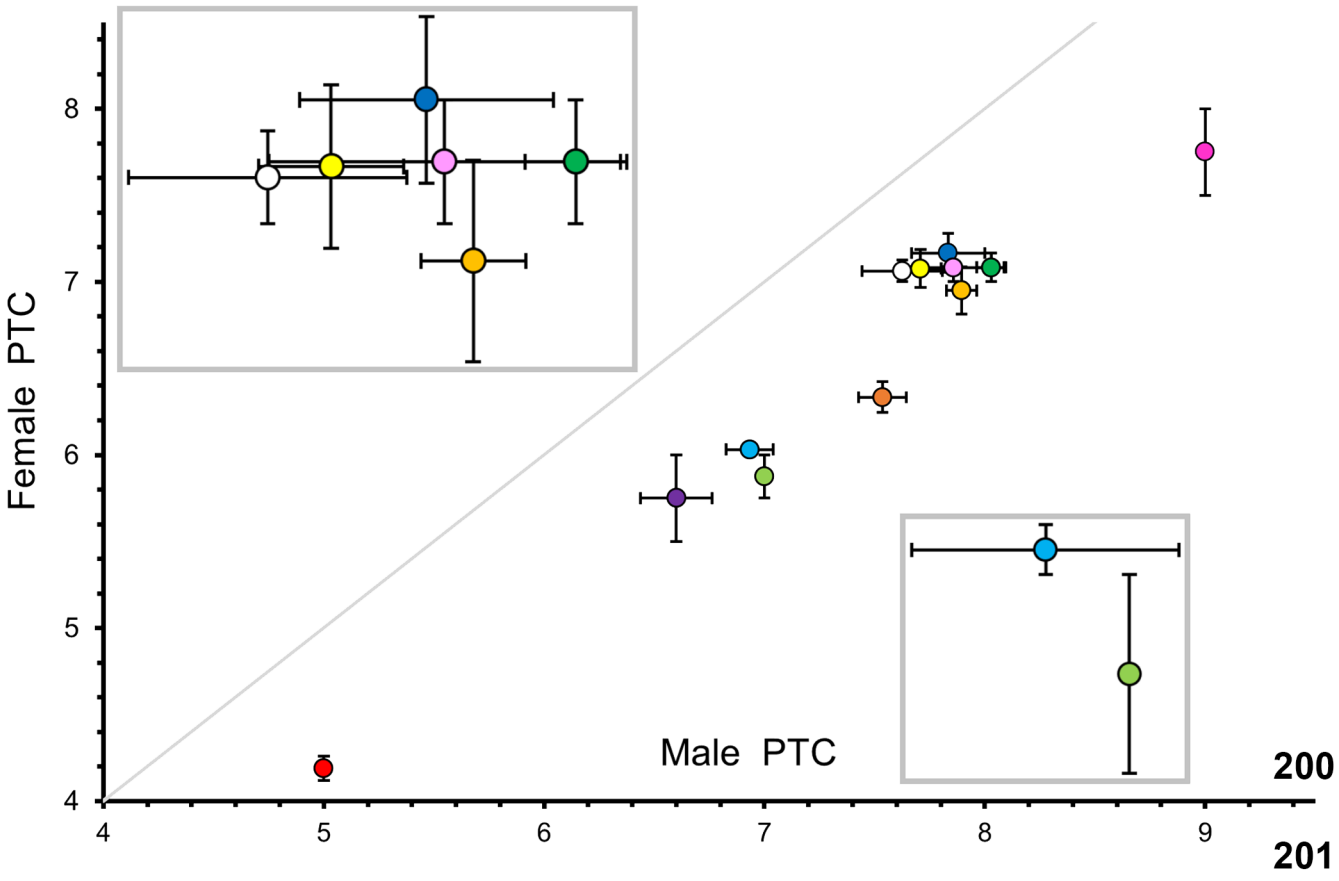

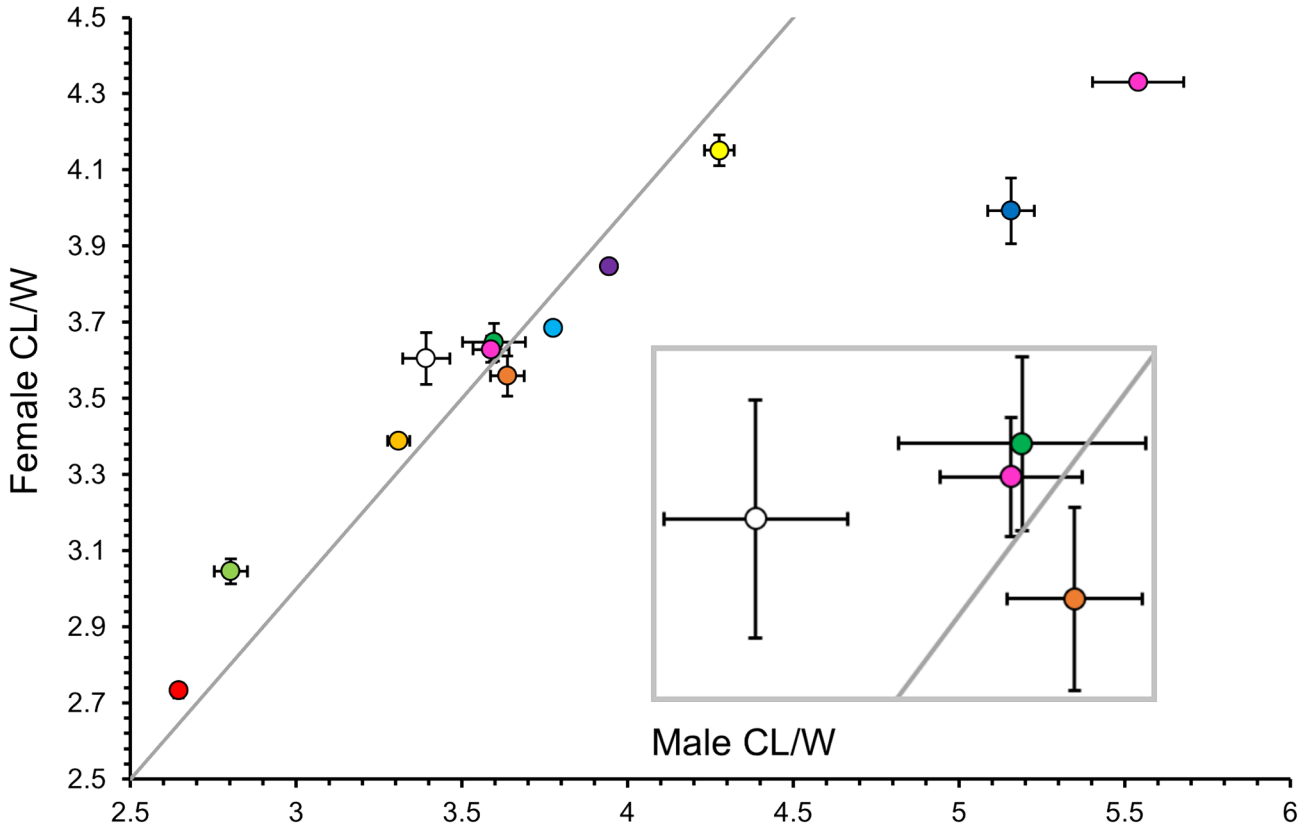

Figures 200–**201**. Bivariate scatter plot comparing males (abscissa) vs. females (ordinate) with standard error bars; gray line is diagonal. **Figure 200**. Mean PTC comparison (raw data available on ResearchGate); clustered values amplified in grey rectangles. **Figure 201**. Mean chela-L/W comparison; clustered values amplified in grey rectangles. Symbols: *S. jendeki* (●); *S. lowei* (●); *S. puerensis* (●); *S. shidian* (●); *S. tongtongi* (●); *S. vachoni* (●); *S. validus* (●); *S. xui* (●); *S. yangi* (●); *S. zhangshuyuani* (●); *S.* sp. (Jinghong) (●); *S.* sp. (Menglun) (○).

to fully conceal the movable finger? In some buthid species with globous chelae, this orientation is geometrically identical to leveling the condylar axis, so that one could confirm the leveling by observing the coverage of movable finger by fixed finger from the top. But in many *Scorpiops*, the movable finger is slanted outward and the fixed finger cannot fully cover the movable finger even if the condylar axis is leveled.

If the condylar axis is parallel to an axis in a two-dimensional space and the sight trajectory is orthogonal to the condylar axis (i.e., the roll and yaw angles are fixed), the chela-W remains constant. The view angle is non-influential to the chela-W as long as the sight trajectory only rotates around the condylar axis (= pitch axis) and remains orthogonal to it. Therefore, the width can be measured from the ventral aspect which exposes the condylar axis allowing adjustment and does not require it to be fitted onto a plane defined by a point on *vm*. For a photographic measurement by calculating the pixels, if the photo is taken from the ventral aspect, the final chela-W yielded will be sensitive to the location of the maximal width if there is a pitch rotation around the condylar axis (i.e., the dimension perceived is negatively correlated with distance). However, this error can be reduced by the photo stacking procedure which would obtain a final image stacked from photos of different focal distances. In addition, the sight trajectory must be orthogonal to the condylar axis (rendering the former as a yaw axis) to ensure a fixed roll angle. For a manual measurement performed by a caliper, the subsequent problems would be accurately adjusting the condylar axis, orienting it to be orthogonal to the opposing surfaces of the two jaws, as well as parallel to the shared plane of the jaws. This can be achieved by technically modifying the caliper jaws.

Two criteria must be met: (1) the condylar axis must be parallel to the straight line that is orthogonal to the opposing surfaces of the jaws to ensure fixed yaw and roll angles; (2) the lateral planes must have enough surface area (larger than the inner and outer surfaces of the chela) to instantly make contact with the most convex points of the two surfaces of chela to ensure that the planes are tangential. The original caliper only has a pair of very flattened jaws, which may not be sufficient to automatically locate the highest convex points. Although the examiner could rotate the chela to identify these points, this dynamic process may cause larger errors. In this study, a modification is designed to satisfy those requirements (Fig. 93). The modification involves five independent parts: a thin cylindrical metal rod with a square plane base, a L-shaped metal plate with five screw holes and a penetrating cylindrical tunnel (plate 1), a L-shaped metal plate with four screw holes and a non-penetrating cylindrical tunnel (plate 2), and two L-shaped metal plates each with four screw holes (plate 3 & 4). The rod enters the tunnel on plate 1 and stopped by its square base. A L-shaped plastic cover can also be used to further stabilize the rod by accommodating the rod's square base in a corresponding square depression on one side and a hole on the other side for a screw to nail it on the lateral surface of plate 1. The plate 1 and 3 clamp the fixed caliper jaw by four screw holes; similarly, the plate 2 and 4 clamp the movable caliper jaw. The rod continues to enter the tunnel on plate 2. When assembled on to the caliper jaws, the two vertical planes of plate 1 and 2 face each other, creating a larger surface area for locating the convex points. The condylar axis can be leveled by attaching it to the thin rod which is designed orthogonal to the opposing surface of the two vertical planes. The rod essentially passes through the tunnel of plate 2 and its length can be tailored to satisfy the widest scorpion chela.

Despite the modification being applied, human errors during manual measurement nonetheless generate prominent instability upon the digits after the decimal place. However, with the orientation of the chela strictly defined, the measurement could be performed by more advanced techniques, such as the 3D scanning. The only drawback of the condyle method is its limited function in conveying interspecific differences. When viewing from the front, assuming both the length of the condylar axis and the maximal coronal-sectional width of the manus (a transverse axis of the lateral dilation of chela; ≈ minimum Feret diameter or intuitively perceived chela-W) are constant, the size of the vertex formed by their respective straight lines (i.e., by the proximal-distal axis of the chela) decides the final chela-W. The larger the vertex (<90°), the smaller the condyle-defined chela-W; this vertex is interspecifically variable. Since the line segment representing the maximal coronal-sectional width may not necessarily be parallel to the condylar axis, the condyle-defined chela-W will be smaller than an intuitively perceived chela-W. This method essentially changes the roll angle and tilts the dorsal plane of the chela laterally to one side (usually the external side), which may result in reducing the width of a dorsoventrally flattened chela. If two species have the same chela-L but the chela-W of one species is greatly reduced by this method, approximating the chela-W of the other species, the ratio of chela-L/W may not be able to clearly separate the two species, and may even render overlap. Furthermore, it may have greater influence on the width/depth of chela that could represent the relative flatness. Despite this limitation, the condyle method is a universal approach for all scorpion species. A standardized method that only depends on one variable (whether the pitch axis is leveled) and disregards the specificity of adapted morphologies (e.g., flattened chela specialized for crevice-dwelling) ensures the stability in measurement that would not be tailored for certain taxa (which may cause greater inconsistency). On the other hand, although the chela-L/W derived from this method could be less informative in interpreting the morphological differences, supplementary morphometrics like maximum or minimum Feret diameters can always be additionally provided for the interested taxa that may require data as such for the interspecific analysis.

However, could any of these methods be the actual one applied by the previous authors? It does not seem likely for the first two methods which are counterintuitive in terms of the chela-W obtained and rather complicate during practice. Retrospective investigation on the illustration in Sun (2010) did not confirm this assumption for the squeezing method as

well. By extending the right vertical bar upwards that delimited one side of chela-W, it did not meet the tip of the fixed finger (Fig. 79). This indicates that chela-W in that method was not orthogonal to the straight line that passes two points on the inner side of the chela as defined in the squeezing method. Similarly, looking back to the illustration by Sissom et al. (1990), the chela-W was not orthogonal to either that line or the axis of the chela (Fig. 78). It was only orthogonal to a straight line external to the chela. Assuming that the outer margin of the chela is a smooth arc, then the straight line that is tangential to it passes only one point which is not strictly chosen. Multiple lines can be drawn within a tiny segment of this arc, passing different points by rotating the chela around its yaw axis, rendering different chela-W (as it is orthogonal to a specific straight line). In reality, the outer margin is granular in *Scorpiops*, which means there are plentiful "granule candidates" to be set as the two landmark points that define a straight line. However, the landmark points were never selected in the past literatures. What about the condyle method? It cannot be determined from the illustration of either Sun (2010) or Sissom et al. (1990) as it is uncertain whether the condylar axis was orthogonal to the sight trajectory in the former and whether it was parallel to the chela-W illustrated in the latter. The illustration provided by Stahnke (1970) was different but judging by his text definition of chela-W, "*Greatest…width*", it appears that it accorded more with the minimum Feret diameter.

Conclusion. Even with so many problems and possible solutions raised here, few authors have explicitly explained how they measured chela-L and chela-W of *Scorpiops*, but simply claimed that they had followed either Stahnke (1970) or Sissom et al. (1990) in their "Methods" section. In Tang (2022b), this problem was also not addressed in depth, and the demonstrative figure for chela measurement still suffered from the definition of chela width. In fact, all the discussed methods hold a certain degree of feasibility. However, the lack of explanation prevents one from determining if the previous authors used the same method, or whether those methods would yield accurate results, rendering the ratiometric data in the diagnostic table less useful. Thus, given that problems often present in the measurement method and accuracy, rather than emphasizing on the accurate ratio variation range of a species, a visual presentation based on adequate photos of specimens is more preferrable to be included in the species comparison, also allowing readers to measure chela-L/W themselves. Precise measurements can be accomplished in computer after generating a three-dimensional model by scanning hardware and photogrammetry software (Segre et al., 2023). However, such technology is currently premature and yet to be widely adopted. Therefore, chela-L/W of all studied Yunnan *Scorpiops* were updated with the condyle method (Table 2). According to Fig. 201, it is obvious that most Yunnan *Scorpiops* show weak sexual dimorphism in this aspect (approximating the diagonal line), with *S. xui* and *S. zhangshuyuani* being the outliers. *S. jendeki* has the lowest chela-L/W, followed by *S. tongtongi*, which is prominently separated from the third robust species, *S. puerensis*. *S. lowei* differs from *S. puerensis* and *S. vachoni* by showing a reversed sexual dimorphism, albeit the overlapping variation (standard error bars).

On the other hand, Tang (2022b: 31–32, 34) argued that quantified chela-L/W alone may not be sufficient to convey the morphological difference in chelae between species. Many morphologically similar species share a wide range of ratiometric overlap; with the addition of various measurement problems, its usability is curtailed during practice. The shape of chela from dorsal aspect could appear differently in two species that are overlapped or approximate in chela-L/W to some extent (Tang, 2022b: 31): "*In qualitative terms, the dorsal chela shape of* S. puerensis *appears oval, while that of* S. validus *appears rectangular. This dorsal profile is delimited by the external carina and dorsal internal carina; thus, in* S. puerensis*, the distance between the two carinae increases progressively towards the proximal end, while in* S. validus*, the two carinae are essentially parallel.*" Here, this character is defined as the location of the maximal chela width (CW_{max}) on the dorsal surface of manus. Quantification could again lead to technical errors; therefore, the most intuitionistic method is the direct presentation of figures. Among Yunnan *Scorpiops*, in species with CW_{max} near the proximity (in the proximal "half"; this is not rigorously quantified), the inner margin of their manus is slanted internally towards the proximity (Figs. 97, 99, 101, 103, 105, 107, 113, 115, 117 and 119). For those with a weakly curved or less oblique inner margin which usually occurs in species with relatively elongated chelae, their CW_{max} may be ambiguous (but nonetheless somewhat near the proximity) because the inner and outer margins of the manus are nearly symmetrical (or parallel, if they both are almost straight), and they are considered to exhibit an "even" distribution of chela-W (Figs. 109, 111, 121, 123, 127, 129 and 135). Sometimes, the CW_{max} is located medially on the manus, which leads to an impression of smoothly curved inner margin (Figs. 125 and 133).

3. Comments on the *Scorpiops* in China

3.1. Morphological comparison of *Scorpiops* spp. from Yunnan

Male specimens are crucial for identification of most *Scorpiops* found in Yunnan as they often show sex-dependent traits in the pedipalp that allow differentiation. Ten species have been described from Yunnan (excluding two recorded populations), and all of them are endemic to China (although *S. tongtongi* is also likely to be found in Myanmar). As a prevailing knowledge among Chinese aficionados, those species are often equivocally referred to as the "Yunnan/Vietnam flat rock scorpion" under the umbrella name "*Euscorpiops vachoni*" (now *Scorpiops vachoni*) which was, on the contrary, an enigmatic species before Tang (2022b) illustrated with new materials. It is then confirmed that many specimens from Yunnan are incorrectly identified. Exact geographic information (the origin of the specimens) is important and can often be used for instant identification; however, it is not

always available. In this section, this information is considered absent, attempting to distinguish those species based solely on the phenotypic characters. For the ease of morphological identification, the ten described species can be parsed into three groups based mainly on the chela morphology: (1) *S. jendeki* and *S. tongtongi*; (2) *S. lowei, S. puerensis*, *S. vachoni*, *S. validus* and *S. yangi*; (3) *S. shidian*, *S. xui* and *S. zhangshuyuani*. In Tang (2022b: 22, 24), *S. tongtongi* was included in the second group due to the only female specimen available, while *S. yangi* was allocated to the third based on the original sketch. These groups are subjectively categorized for quick species identification. Each species will be discussed and compared with other congeners. Detailed information can be found in Tables 2 and 3, and the keys below.

The first group easily stands out from the remaining species by their relatively robust pedipalp chela in at least males, relatively sparsely granulated tergites in females, short and oval median ocular tubercle, costate-granular patella carinae, weak pedipalp patellar internal apophysis, low patella-Vt count (always <8), absence of fulcra and more bulbous telson. In terms of the median ocular tubercle, species in Groups 2 and 3 all have densely granulated superciliary carinae. *S. jendeki* and *S. tongtongi* differ from each other in the following aspects: (1) size: smaller vs. larger; (2) carapace: triangular vs. quadrate; (3) coloration: blackish vs. brownish; (4) PTC: lower vs. higher; (5) movable finger denticle count of MD and IAD: prominently lower in *S. jendeki*; (6) proximal lobe in adult males: absent vs. present; (7) tergites: basally covered with small granules and adorned by moderate to large granules vs. basally smooth and adorned by small to moderate granules; (8) superciliary carinae of median ocular tubercle: moderately granulated vs. completely smooth. *S. jendeki* clearly differs from other Yunnan congeners in combination of above listed characters. However, *S. tongtongi* resembles the second group more due to their more similar chela shape; on the other hand, it can be easily distinguished from the third group by its robust chela apart from other mentioned differences. Chelae of female *S. tongtongi* may somewhat resemble those of *S. lowei* and *S. puerensis*, while those of males are more robust than the species in the second group. Nevertheless, besides the mentioned differences, females of *S. tongtongi* can be easily differentiated from the second group by the lack of proximal lobe (or extremely weak). In addition, both sexes of *S. tongtongi* possess proportionally larger telson vesicle (especially in males) than the remaining species.

The date for the name "*Scorpiops jendeki*" is hereby corrected as "1994" rather than "2000" (erroneously followed Di et al. (2013) as "Kovařík, 2000" in Tang (2022a: 14; 2022b: 5, 14, 21; 2022c: 21)). The type series of *S. jendeki* included only six females when it was described as a subspecies of *S. hardwickii* (Kovařík, 1994: 62–66; incorrectly spelled as *S. hardwickei*), although in Kovařík et al. (2020: figs. 34, 115, 213–214), the holotype was documented as a "male". Only one female had 5 teeth on its left pectine (paratype No. 5; Kovařík, 1994: 65). Kovařík (2000: 180) further examined one male and two females when elevating it to species level. In his table 3 (Kovařík, 2000: 178), *S. jendeki* was recorded with 2 times for 5 teeth in male, 5 times for 5 teeth and 11 times for 4 teeth in females. Given that the sums of pectines examined (18 pectines) and specimens listed (9 specimens) accord with each other, it is reasonable to believe that both subsequent females examined had 5 teeth on both of their pectines. Di et al. (2013: 90–94) redescribed this species based on 3 females and 1 immature male (specimen nos. YNLL0801–4, as "Material examined"). However, their diagnosis was confusing as they claimed to have examined 6 specimens (unless "specimen" stood for "patella"): "…*Patella with 17 external trichobothria (5* eb*, 2* esb*, 2* em*, 4* est*, 4* et*) (Fig. 127) and 6–7 ventral trichobothria (**6 specimens**, Fig. 128)*…". In the next sentence, they used the plural form for "male": "…*Both **males** and females have fingers of pedipalps straight, without any flexure*...". It is only reasonable if they considered both the immature male they examined and the male examined by Kovařík (2000); for a species without a proximal lobe in adult males, the immature males thereof would also show no lobe. In their table 3 (Di et al., 2013: 85), only two females (YNLL0801–2) was provided with their PTC (both 4 on either pectine). No illustration was provided for the immature male they examined (I hereby assume that the immature male also had 5 teeth on both pectines); they also considered this species as "…*Sexual dimorphism is not distinct*…". The authors did not justify the method for their sex identification upon their immature specimen or discuss any characters that can be applied to distinguish male from female. Subadult male *Scorpiops* have been dissected with weakly sclerotized and only partially developed hemispermatophores (e.g., Kovařík et al., 2015: fig. 3), which could be an evidence for the sex of an immature specimen if it is at its penultimate instar. Prior to the examination of *S. jendeki* in this study, the genital papilla is known to present in all male Yunnan *Scorpiops* and is age-independent. This sexually dimorphic character is now also confirmed for *S. jendeki*; additionally, the pectines of the male are also larger than those of the females (Figs. 196–199). The apparently heavily skewed sex ratio in this species resulted in rare male specimens available for examination.

The second group includes five species that are somewhat similar to each other, often causing misidentifications. They can be distinguished from the third group by their more robust pedipalp chela and relatively stronger proximal lobe in both sexes, but similar in the following aspects: (1) PTC range (ca. 6–9); (2) denticle count range; (3) patella-Vt count (slightly higher in the third group by reaching 12–13); (4) coloration: appears greyish black in vivo (but authentically reddish black to brownish black when moistened and revealed by liquid); (5) strong patellar internal apophysis; (6) elongated telson; (7) elongated and rhomboid median ocular tubercle; (8) pectinal fulcra present. The second group can be further divided into two subgroups: (1) CW_{max} located in the proximal half and chela-L does not conspicuously exceed carapace length: *S. lowei*, *S. puerensis* and *S. vachoni* ; (2) chela-W even throughout entire dorsal plane and chela-L conspicuously exceeds carapace length: *S. validus* and *S. yangi*.

Within the first subgroup, *S. lowei* is generally smaller among these species (and the entire second group) and is also recorded with relatively low count of MD (may fall below 80). Patella-Vt of *S. lowei* rarely reaches 11 while 11 is recorded as a normal value from the other two species. The proximal lobe of male *S. lowei* is also relatively weaker than the other two species in general (Fig. 102 represents the strongest condition in this species observed; other examples can be found in Tang 2022b & c) and therefore rendering weaker sexual dimorphism in this aspect. Females of *S. lowei* also possess the second weakest lobe in the second group, surpassed by that of *S. yangi* and followed by those of *S. vachoni*. *S. lowei* further differs in particularly from *S. puerensis* by a higher count of OD and from *S. vachoni* by a lower count of PTC. In addition, *S. lower* usually has a more reddish coloration than all the other Yunnan *Scorpiops* (except for *S. tongtongi*), which can be intensified after its fixation in ethanol. *S. puerensis* possesses the most robust chela in the second group, although it may not be as large (in relation to body size) as those of *S. validus* and *S. yangi* (especially the males thereof). It further differs from *S. vachoni* (and *S. validus*) by a lower count of MD. The proximal lobe of male *S. puerensis* is stronger than that of male *S. vachoni* (and similar to that of male *S. validus*). Females also have relatively strong lobe when compared with *S. lowei* and *S. vachoni*. *S. vachoni* is recorded with the highest range of MD and IAD, and the highest average of PTC and ID. It is the only species in the second group that reaches 9 PTC in at least one sex. Its patella-Vt also does not fall below 10 normally. Those higher morphometrics supported the revalidation of *S. validus* from *S. vachoni*. The internal margin of the chela is also rather oblique in *S. vachoni*, giving it a distinguishable chela shape.

In terms of the second subgroup, both species are usually easily recognizable by their relatively large and slender chela when compared to the first subgroup. *S. validus* and *S. yangi* appear similar and are recorded with overlapping range of PTC and patella-Vt, although it is plausible that the latter would generally have a lower count. The two species are primarily distinguished by the development of proximal lobe on the movable finger which is stronger in the former. Males of *S. validus* possess the strongest lobe in the entire second group. It is also interesting to note that most of the female *S. validus* examined (plus data in other papers) yielded 6 PTC (of 31/32 pectines), while only few female *S. puerensis* had 6 PTC (of 4/20 pectines) with 7 being the mode (of 13/20 pectines). Only two females and five males of *S. yangi* have been examined (including the pair examined in this study). One female had been recorded with only 5 teeth on its right pectine. Given the dearth of samples, comparison between the two species by their PTC may not be reliable for now. Similarly, only two specimens (four fingers) of *S. yangi* have been examined in this study, and their dentition count did not clearly differ from that of *S. validus*. However, during the present investigation, it appears that adult male of *S. yangi* has more elongated pedipalp femur (Figs. 194–195) and chela (Fig. 201).

The third group encompasses three species with slender chela in at least males. *S. shidian* differs from the other two species by showing no prominent sexual dimorphism in chela ratiometrics. Females of *S. xui* possess the most robust chela in this group, approximating those of *S. validus* and *S. yangi* (but smaller in size). *S. zhangshuyuani* stands out by having the most slender pedipalp in males (also among all Yunnan *Scorpiops*). Femur and patella of male *S. zhangshuyuani* are obviously more slender than those of *S. shidian* and *S. xui* (Figs. 191–193). All of those three species show weak proximal lobe. The lobe morphology is similar between *S. shidian* and *S. xui*, while although it is also weak in *S. zhangshuyuani*, the lobe covers only a small section on the movable finger. *S. zhangshuyuani* is also recorded with the highest PTC (9) in this group for males. The three species share similar range for OD and ID, but that for MD and IAD is higher in *S. zhangshuyuani*. *S. xui* possess the lowest amount of patella-Vt, while both *S. shidian* and *S. zhangshuyuani* often have at least 11 patella-Vt. *S. yangi*, being the species with relatively slender chela and weakest proximal lobe in the second group, can be further distinguished from the third group as follows: (1) proximal lobe stronger; (2) chela more robust; (3) relatively lower patella-Vt count, especially when compared with *S. shidian* and *S. zhangshuyuani*; (4) lower count of OD when compared with *S. shidian* and *S. xui*; (5) lower count of MD and IAD when compared with *S. zhangshuyuani*; (6) lower count of PTC.

3.2. *Scorpiops zhui* and "*S. jingshanensis*" from central China

Chongqing and Hubei are two adjacent provinces. *S. zhui* Lv et al., 2023 was described from Wushan and Wuxi counties of Chongqing. This species is distinctive in terms of its morphology and geographic location. It is characterized by the prominent sexual dimorphism of pedipalp chela: more robust in males with a developed lobe on the movable finger. However, many other characters including PTC and patella-Vt renders a similarity with many Yunnan *Scorpiops*, especially with *S. lowei*, *S. puerensis* and *S. vachoni* if taking the overall morphology into consideration. Apart from having a lower range of patella-Et, *S. zhui* can be well separated from the above three species based on two characters (cf. Tang, 2022b): (1) male chela obviously more robust when comparing with *S. lowei* and *S. vachoni*; (2) female finger lobe extremely weak to absent when comparing with all the three species (especially with *S. puerensis*). The single species from Hubei was "*S. jingshanensis* Li, 2016", a *nomen nudum* proposed in a Chinese book without redescription (Tang, 2022a: 2). The materials of this species were represented by a pair of initially unnamed immatures. Given the geographic proximity, the authors of *S. zhui* compared their new species with "*S. jingshanensis*" by three characters but appeared to be insufficient as the two trichobothrial counts were very close between the two species. Based on their statement in the comparison, the two species differ as follows (the latter data refer to "*S. jingshanensis*"): (1) chela-Vt: 5 vs. 4; (2) patella-Vt: 10 vs. 8. However, according to their complete dataset, chela-Vt was recorded as 4–5 for *S.*

zhui, and patella-Vt was 8–11, both overshadowed the known data of "*S. jingshanensis*" which were derived from a very low sample size (2 specimens). Nevertheless, according to the photos of "*S. jingshanensis*" in Li (2016), the chela of that species is very rounded and is clearly different from *S. zhui*. Their immaturity indicates that the mature individuals would only be even more robust. Therefore, "*S. jingshanensis*" appears to be a valid species albeit its invalid name, and thus hereby included as a member of the Chinese *Scorpiops* species.

3.3. Dubious *Scorpiops* from Xizang

The *Scorpiops* fauna of the Xizang Province is the most diverse and complicated. To this day, 18 species have been described/recorded: *S. asthenurus* Pocock, 1900, *S. atomatus*, *S. bhutanensis* Tikader & Bastawade, 1983, *S. hardwickii*, *S. ingens* Yin et al., 2015, *S. kamengensis* (Bastawade, 2006), *S. langxian* Qi et al., 2005, *S. leptochirus* Pocock, 1893, *S. lhasa* Di & Zhu, 2009, *S. lourencoi* Lv & Di, 2022, *S. lii* (Di & Qiao, 2020), *S. luridus* Qi et al., 2005, *S. margerisonae* Kovařík, 2000, *S. novaki* (Kovařík, 2005) (junior synonym from Xizang: *Euscorpiops karschi* Qi et al., 2005), *S. petersii*, *S. songi* Di & Qiao, 2020, *S. tibetanus* (junior synonym from Xizang: *S. pococki* Qi et al., 2005), and *S. wrzecionkoi* Kovařík, 2020. Several species deserve special attention.

To begin with, four species were recorded from a politically controversial area, Arunachal Pradesh (India) or Southern Tibet (China). The type locality of *S. asthenurus* was in Kalimpong (near Darjeeling, West Bengal, India; Pocock, 1900: 74), but it was recorded from "Arunachal Pradesh" by Bastawade (2006: 454), where *S. kamengensis* was originally described from (Bastawade, 2006: 457). The original description of *S. leptochirus* stated that the specimen was of unknown origin (Pocock, 1893: 326), but was subsequently complemented by two additional specimens as "N. E. Bengal" (female) and "Assam" (male) (Pocock, 1894: 79). However, in Pocock (1900: 70), this species was stated to be from "Assam: Tura in the Gáro Hills"; another record was from Sadiya town, Tinsukia district, Assam. Tura is a municipality of West Garo Hills – a district in the state of Meghalaya rather than Assam. Nevertheless, Bastawade (2006: pl. map 1) further reported this species from "Arunachal Pradesh"; in Kovařík et al. (2020: 127), this species was as well marked in this area on the map. *S. longimanus* (Pocock, 1893) was also reported from China without explicit location ("Southern Tibet occupied by India"; type locality in Sylhet, Bangladesh) in a Chinese dissertation (Sun, 2010: 142), but it was then ignored in recent papers. However, Bastawade (2006: 454) did mention the occurrence of this species in Namdapha, Changlang district ("Arunachal Pradesh"), which therefore appears to be the source of that record. Be as it may, this specific area is never considered a part of the Southern Tibet, which may account for the exclusion of this species from the Chinese *Scorpiops* checklist in the subsequent papers. Considering the Southern Tibet as a part of China, it is reasonable to include *S. asthenurus*, *S. kamengensis* and *S. leptochirus* as members of the Chinese *Scorpiops*.

Two species are dubious in terms of their records in China, *S. hardwickii* and *S. petersii*. The type locality of *S. petersii* is in India (Shimla, Himachal Pradesh; Pocock, 1893: 325). Kishida (1939: 45) was the first to record its distribution in China, from Xizang and Xikang (also Sikang or Hsikang). Di et al. (2013: 72) examined an unidentified specimen from Lhasa, but it was not proved to be conspecific with *S. petersii* as most characters were shared with *S. hardwickii* except for the unusually larger size. Presumably, this specimen belongs to a large species described from Lhasa in 2015, *S. ingens* Yin et al., 2015. In the description of that species, the authors pointed out that "*Although* S. petersii *also above 75.0 mm, its carapace is not densely granulated, granules on its mesosoma are widely spaced, with the distance between them far greater than their size (Kovařík 2000: 193), while the granules are dense on the carapace and mesosoma of* S. ingens *sp. n.*" (Yin et al., 2015: 55). However, the cognition of *S. petersii* was based on previous studies of Indian specimens, rather than the professed materials from China. It seems that there are no credible Chinese specimens of this species. In addition, although the term "*Scorpiops hardwickii* complex" keeps appearing in literatures, the record of its nominal species in China, *S. hardwickii*, was only reported once from Nyenchen Tanglha Mts., Lhasa (Kovařík, 2000: 176). No Chinese author has ever been able to study any specimen confirmed as *S. hardwickii* from Lhasa (at most referred to as *S.* sp. of "*hardwickii*" complex). In the map by Kovařík et al. (2020: 127), *S. hardwickii* is south to *S. petersii* in proximity (the type locality of this species is in an unknown area of Himalaya). Both *S. hardwickii* and *S. petersii* appear to be extremely far from their records in Xizang (and Xikang) with respect to their type localities. A more plausible assumption is that these old records were erroneous and misidentified, and those specimens may represent either some of the subsequently described species or new species yet to be described.

Finally, several species are associated with the "widespread" *S. tibetanus*. The type locality of this species ("Tsangpo Valley, Chaksam Ferry"), as clarified by Lv & Di (2022: 204) in their redescription of this species, is most probably from Qushui County (of Lhasa). Tang (2022c: 21) incorrectly considered its type locality as the Shigatse City where all the previously examined specimens by the Chinese authors originated from (e.g., Di et al., 2013: 75). Kovařík (2000: 196) previously added both Lhasa and Shigatse as new localities of this species in China. The type locality of *S. pococki* is Gyaca County of Shannan City, other localities (further specified based on the coordinates provided) included in the original description were Bayi District (as "Nyingchi"), Chengguan District (as "Lhasa"), Nêdong District (of Shannan), Samzhubzê District (as "Xigazê" (Shigatse)), and Zayü County (of Nyingchi). In his dissertation, Sun (2010: 133) also reported this species from Mainling County (of Nyingchi) and Maizhokunggar County (of Lhasa). The synonymization of *S. pococki* with *S. tibetanus* in Kovařík et al. (2020) hence greatly expanded the distribution of the latter species in Xizang. Lv & Di (2022: 198, 205) limited the

distribution of this species within Qushui and Gyaca (the latter represents the type locality of *S. pococki*) and agreed that *S. pococki* is a junior synonym of *S. tibetanus*.

S. atomatus was also synonymized with *S. tibetanus* by Kovařík et al. (2020), but no types were studied. Tang (2022a) retained it as a valid species and Lv & Di (2022) formally revalidated this species, both emphasized its smaller size. Lv & Di (2022) also described a new species from Shigatse, *S. lourencoi*. In combination of the diagnostic features proposed by the authors and my additional observations, the three species can be readily distinguished as follows: (1) *es* on chela: formed by discrete granules that are relatively larger than others in *S. atomatus*, very strong and resulted from granule-fusion in *S. tibetanus* (male in particular), not obviously visible and all granules on the same surface are of equal size (large) in *S. lourencoi*; (2) pectine morphology: relatively long with relatively short teeth in *S. atomatus*, relatively short with relatively long teeth in *S. tibetanus*, both pectine and teeth relatively short in *S. lourencoi*; (3) PTC: *S. tibetanus* (♂4–7 ♀4–7) can be separated from *S. atomatus* (♂10–11 ♀8–9) and *S. lourencoi* (♂8–11 ♀7–8) by a generally lower count; (4) IAD: *S. atomatus* (8–9) can be separated from *S. tibetanus* (10–25) and *S. lourencoi* (10–14) by a lower count; (5) patella-Vt: *S. tibetanus* (6–8) can be separated from *S. atomatus* (8–10) and *S. lourencoi* (8–9) by a generally lower count; (6) TL: *S. atomatus* (35–45 mm) < *S. lourencoi* (45–50 mm) < *S. tibetanus* (50–57 mm); (7) chela-L/W and sexual dimorphism: weak sexual dimorphism with females slightly narrower in *S. atomatus* (♂2.3 ♀2.5), strong sexual dimorphism with females conspicuously narrower in *S. lourencoi* (♂1.9 ♀2.4), no sexual dimorphism with both sexes moderate in ratio in *S. tibetanus* (♂2.0 ♀2.0); (8) chela surface granule size: *S. atomatus* < *S. tibetanus* < *S. lourencoi*. However, with the discovery of a new species from Shigatse, it is highly likely that the previous records of either *S. tibetanus* or *S. pococki* from this area were misidentified. It may also be necessary to re-investigate the other populations of *S. tibetanus* (i.e., previous records of *S. pococki*).

One last species remains in doubt, *S. langxian*, which was described from Nang County (type locality) and Bayi District (as "Baishuwang town") in Nyingchi City. Upon comparing the morphological data of *S. langxian* (data from Kovařík et al., 2020) and *S. tibetanus* (data from Lv & Di, 2022), the two species cannot be clearly differentiated: (1) TL (in mm): 52–60 vs. 50–57; (2) chela-L/W: 1.9–2.2 (both sexes) vs. 2.0 (both sexes); (3) patella-Vt: 6–7 vs. 6–8; (4) patella-Et: both 17; (5) PTC: ♂7–8 ♀6 vs. ♂4–7 ♀4–7; (6) denticle rows: ID 4 vs. 4–5, OD 8 vs. 8–9, MD 55 vs. 45–62, IAD 25 vs. 10–25; (7) telson-L/D: ♂2.6 ♀2.7 vs. ♂2.64 ♀2.60; (8) both species with developed MF-lobes in both sexes; (9) both species with P3-type pectines, fulcra absent; (10) both species with D-type Eb_3-position. The overall habitus and coloration are also identical (cf. MNHN-RS-RS8626 and MNHN-RS-RS8627). It therefore seems reasonable to suggest that *S. langxian* is probably a junior synonym of *S. tibetanus*. However, it also appears that female *S. langxian* has an apparently broader manus (this is inconsistent with the chela-L/W value which may be again resulted from the problem with measurement; i.e., if *S. langxian* is broader, then its lower value should be even lower to deviate from 2.0). Similarly, male *S. langxian* appears to have a more bulbous telson than *S. tibetanus* (cf. Kovařík et al., 2020: figs. 36, 46); however, their telson-L/D values are extremely similar. Again confusingly, in Kovařík et al. (2020), male *S. langxian* (fig. 218) had a more pronounced MF-lobe than *S. tibetanus* (fig. 240) but was identical with the male *S. tibetanus* in Lv & Di (2022: fig. 58). The male *S. tibetanus* in Kovařík et al. (2020) was probably a female (also judging from the shape of the chela; male *S. tibetanus* was more quadrate in profile).

Key to the known *Scorpiops* species of Yunnan, China, based on studied material and literature

1. Pedipalp chela relatively robust in at least males; tergite with sparser granulation at least in females; ocular tubercle short and oval; patellar carinae costate-granular; internal apophysis of pedipalp patella weak; patella-Vt never exceed 7; fulcra absent; telson bulbous. **2**
– Pedipalp chela relatively slender in at least one sex; tergite with denser granulation; ocular tubercle elongated and rhomboid; patellar carinae granular; internal apophysis of pedipalp patella strong; patella-Vt greater than or equal 8; fulcra present; telson elongated. **3**

2. Size smaller; carapace more triangular; coloration blackish; PTC 4–5 (♂ & ♀); MD ca. 50, IAD ca. 10; pedipalp MF-lobe absent in adult males; tergite granules denser in male; superciliary carinae of median ocular tubercle moderately granulated. ..... ***S. jendeki***
– Size larger; carapace more quadrate; coloration brownish; PTC 7 (♂) 5–6 (♀); MD ca. 86–95, IAD ca. 39–52; pedipalp MF-lobe present in adult males; tergite granules sparser in male; superciliary carinae of median ocular tubercle completely smooth. ..... ***S. tongtongi***

3. Pedipalp chela slender in at least adult males. **4**
– Pedipalp chela moderate and may be more robust in adult males. **6**

4. Pedipalp chela-L/W without significant sexual dimorphism, chela of adult males may be only slightly more slender than that of adult females; pedipalp MF-lobe extremely weak, nearly absent in adult females; PTC 7–8 (♂ & ♀; ♀ rarely 6); patella-Vt usually greater than 10 (11–13; rarely 10). ..... ***S. shidian***
– Pedipalp chela-L/W significantly sexually dimorphic, chela of adult males obviously more slender than that of adult females. **5**

5. Pedipalp of adult males moderately slender, patella and femur less slender; proximal lobe covers a greater section on movable finger; PTC 7–8 (♂ & ♀); MD may fall below 80, IAD below 70; patella-Vt 10–11 (rarely 9). ..... ***S. xui***

– Pedipalp of adult males extremely slender, including patella and femur; proximal lobe covers a smaller section on movable finger; PTC 9 (♂) 7–8 (♀); MD may reach 100, IAD above 70; patella-Vt 11–12. ..... ***S. zhangshuyuani***

6. Small to moderate body size, TL barely exceeds 50 mm. **7**
– Moderate to large body size, TL never below 40 mm and may approximate 60 mm. **8**

7. TL may below 40 mm; pedipalp MF-lobe moderate in adult males; PTC of males never reaches 9, that of females never above 7; ID may below 6 (4–8), MD never above 90; patella-Vt usually 8–10 (rarely 11). ..... ***S. lowei***
– TL always above 40 mm; pedipalp MF-lobe moderate to strong in adult males; PTC of males may reach 9, that of females never below 7; ID never below 6 (6–8), MD may approximate 100; patella-Vt usually 10–12. .... ***S.* sp. 1&2** (Tang, 2022c)

8. Chela proportionally smaller; chela-L does not greatly exceed carapace length; CW_{max} always located in proximal half. **9**
– Chela proportionally larger; chela-L conspicuously exceed carapace length; CW_{max} inconspicuous, CW even throughout entire dorsal plane (more so in males). **10**

9. Pedipalp MF-lobe weak to moderate in adult females; PTC of males never reaches 9, that of females may reach 6; ID never above 6, OD may reach 9, MD never exceed 100 (ca. 80–90), IAD barely above 50 (ca. 47–51). ..... ***S. puerensis***
– Pedipalp MF-lobe weak in adult females; PTC of males may reach 9, that of females never below 7; ID never below 7, OD never below 13, MD may exceed 100 (ca. 90–120), IAD easily above 50 (ca. 53–80). ..... ***S. vachoni***

10.Pedipalp MF-lobe strong in adult males and moderate in adult females; pedipalp femur proportionally wide in adult males, with retrodorsal carina obviously curved. .. ***S. validus***
– Pedipalp MF-lobe moderate in adult males and weak adult females; pedipalp femur proportionally narrow in adult males, with retrodorsal carina less curved. ..... ***S. yangi***

Acknowledgements

My gratitude goes to Chenkai Tang (唐晨凯; *S. tongtongi*), Hang Qiu (邱航; *S. xui*) and Qingquan Jia (贾清权; *S. yangi*) for their help in the acquisition of specimens, and Leonhard Liu for his assistance in partial image matting. I would also like to thank Dr. Graeme Lowe for his insightful and constructive comments on the text. Credit for the manufacture of caliper modification goes to Xingchengcheng Automation Technology Co., LTD (Kunshan, China). I thank two anonymous reviewers for their comments.

References

BASTAWADE, D. B. 2006. Arachnida: Scorpionida, Uropygi, Schizomida and Oncopodid Opiliones (Chelicerata). *Zool. Surv. India. Fauna of Arunachal Pradesh, State Fauna Series*, 13: 449−465.

CAIN, S., E. GEFEN & L. PRENDINI. 2021. Systematic revision of the sand scorpions, genus *Buthacus* Birula, 1908 (Buthidae C.L. Koch, 1837) of the Levant, with redescription of *Buthacus arenicola* (Simon, 1885) from Algeria and Tunisia. *Bulletin of the American Museum of Natural History*, 450: 1–134.

CAPLE, J., J. BYRD & C. N. STEPHAN. 2017. Elliptical Fourier analysis: fundamentals, applications, and value for forensic anthropology. *International Journal of Legal Medicine*, 131: 1675–1690.

DI, Z.-Y., Y.-W. HE, Y.-L. WU, Z.-J. CAO, H. LIU, D.-H. JIANG & W.-X. LI. 2011. The scorpions of Yunnan (China): updated identification key, new record and redescription of *Euscorpiops kubani* and *E. shidian* (Arachnida, Scorpiones). *ZooKeys*, 82: 1–33.

DI, Z.-Y., X.-B. XU, Z.-J. CAO, Y.-L. WU & W.-X. LI. 2013. Notes on the scorpions (Arachnida, Scorpiones) from Xizang with the redescription of *Scorpiops jendeki* Kovařík, 2000 (Scorpiones, Euscorpiidae) from Yunnan (China). *ZooKeys*, 301: 51–99.

LOWE, G., & KOVAŘÍK, F. 2022 . Reanalysis of *Teruelius* and *Grosphus* (Scorpiones: Buthidae) with descriptions of two new species. *Euscorpius*, 356: 1–105.

KISHIDA, K. 1939. Arachnida of Jehol. Scorpiones. *Report of the first scientific expedition to Mandchoukuo under the leadership of Shigeyasu Tokunage*. June–October 1933, 5, 1, 4 (10): 1–66.

KOVAŘÍK, F. 1994. *Scorpiops irenae* sp. n. from Nepal and *Scorpiops hardwickei jendeki* subsp. n. from Yunnan, China (Arachnida: Scorpionida: Vaejovidae). *Acta Societatis Zoologicae Bohemoslovenicae*, 58 (1–2): 61–66.

KOVAŘÍK, F. 2000. Revision of family Scorpiopidae (Scorpiones), with descriptions of six new species. *Acta Societas Zoologicae Bohemicae*, 64: 153–201.

KOVAŘÍK, F. 2005. Three new species of the genera *Euscorpiops* Vachon, 1980 and *Scorpiops* Peters, 1861 from Asia (Scorpiones: Euscorpiidae, Scorpiopinae). *Euscorpius*, 27: 1–10.

KOVAŘÍK, F. 2009. *Illustrated catalog of scorpions. Part I. Introductory remarks; keys to families and genera; subfamily Scorpioninae with keys to* Heterometrus *and* Pandinus *species*. Prague: Clairon Production, 170 pp.

KOVAŘÍK, F., G. LOWE, M. STOCKMANN & F. ŠŤÁHLAVSKÝ. 2020. Revision of genus-group taxa in the family Scorpiopidae Kraepelin, 1905, with description of 15 new species (Arachnida: Scorpiones). *Euscorpius*, 325: 1–142.

KOVAŘÍK, F. & A. A. OJANGUREN AFFILASTRO. 2013. *Illustrated catalog of scorpions. Part II. Bothriuridae; Chaerilidae; Buthidae I. Genera* Compsobuthus*,* Hottentotta*,* Isometrus*,* Lychas*, and* Sassanidotus. Prague: Clairon Production, 400 pp.

KOVAŘÍK, F., SOLEGLAD, M. E., LOWE, G., PLÍŠKOVA, J., & ŠŤÁHLAVSKÝ, F. 2015. Observations on growth and maturation of a male *Alloscorpiops wongpromi* (Scorpiones: Euscorpiidae). *Euscorpius*, 206: 1–19.

KUHL, F. P. & G. R. GIARDINA. 1982. Elliptic Fourier features of a closed contour. *Computer Graphics and Image Processing*, 18: 236–258.

[LI, W.-X. 2016] 李文鑫 (Lǐ Wén Xīn). 2016. 蝎生物学与毒素('Scorpion Biology and Toxins').科学出版社. ISBN: 9787030507355 (in Chinese).

LV, H.-Y & Z.-Y DI. 2022. *Scorpiops lourencoi* sp. nov., the revalidation of *Scorpiops atomatus* Qi, Zhu & Lourenço, 2005, and the redescription of *Scorpiops tibetanus* Hirst, 1911 (Scorpiones, Scorpiopidae) from China. *ZooKeys*, 1132: 189–214.

LV, H.-Y, W. R. LOURENÇO & Z.-Y DI. 2023. *Scorpiops zhui* sp. n., a new species of Scorpiops Peters, 1861 from Chongqing, China (Scorpiones: Scorpiopidae). *Zootaxa*, 5257: 40–48.

MONOD, L., L. CAUWET, E. GONZÁLEZ-SANTILLÁN & S. HUBER. 2017. The male sexual apparatus in the order Scorpiones (Arachnida): a comparative study of functional morphology as a tool to define hypotheses of homology. *Frontiers in Zoology*, 14: 51: 1–48.

MNHN-RS-RS8626. *Scorpiops langxian* Zhu, Qi & Lourenço, 2005. Paratype(s). *Muséum National d'Histoire Naturelle, Paris, France* (accessed 9. V. 2023). https://science.mnhn.fr/institution/mnhn/collection/rs/item/rs8626?listIndex=6&listCount=9

MNHN-RS-RS8627. *Scorpiops pococki* Zhu, Qi & Lourenço, 2005. Paratype(s). *Muséum National d'Histoire Naturelle, Paris, France* (accessed 9. V. 2023). https://science.mnhn.fr/institution/mnhn/collection/rs/item/rs8627?listIndex=7&listCount=9

POCOCK, R. I. 1893. Notes on the classification of scorpions, followed by some observations on synonymy, with descriptions of new genera and species. *Annals and Magazine of Natural History*, (6), 12: 303–330.

POCOCK, R. I. 1894. A small contribution to our knowledge of the scorpions of India. *Annals and Magazine of Natural History*, (6), 13: 72–84.

POCOCK, R. I. 1900. *Arachnida. The Fauna of British India, including Ceylon and Burma*. Published under the authority of the Secretary of State for India in Council. London: W. T. Blandford, xii, 279 pp.

PRENDINI, L., V. L. EHRENTHAL & S. F. LORIA. 2021. Systematics of the relictual Asian scorpion family Pseudochactidae Gromov, 1998, with a review of cavernicolous, troglobitic, and troglomorphic scorpions. *Bulletin of the American Museum of Natural History*, 453: 1–149.

QI, J.-X., M.-S. ZHU & W. R. LOURENÇO. 2005. Eight new species of the genera *Scorpiops* Peters, *Euscorpiops* Vachon, and *Chaerilus* Simon (Scorpiones: Euscorpiidae, Chaerilidae) from Tibet and Yunnan, China. *Euscorpius*, 32: 1–40.

SEGRE, P. S., J., D. J. IRSCHICK & J. A. GOLDBOGEN. 2023. A three-dimensional, dynamic blue whale model for research and scientific communication. *Marine Mammal Science*, 39(2) (Early View): 1–8. https://doi.org/10.1111/mms.13007

SISSOM, W. D., G. A. POLIS & D. D. WATT. 1990. Field and laboratory methods. Pp. 215–221 in: Polis, G. A. (ed.). *The Biology of Scorpions*. Stanford, CA: Stanford University Press.

SOLEGLAD, M. E. & V. FET. 2003a. The scorpion sternum: structure and phylogeny (Scorpiones: Orthosterni). *Euscorpius*, 5: 1–34.

SOLEGLAD, M. E. & V. FET. 2003b. High-level systematics and phylogeny of the extant scorpions (Scorpiones: Orthosterni). *Euscorpius*, 11: 1–175.

SOLEGLAD, M. E. & W. D. SISSOM, 2001. Phylogeny of the family Euscorpiidae Laurie, 1896: a major revision. Pp. 25–111 *in* Fet, V. & P.A. Selden (eds). *Scorpions 2001. In memoriam Gary A. Polis*. Burnham Beeches, Bucks: British Arachnological Society.

STAHNKE, H. L. 1970. Scorpion nomenclature and mensuration. *Entomological News*, 81(12): 297–316.

SUN, D. 2010. *Taxonomy and Status of Resources of the Scorpiones from China (Chelicerata: Arachnida)*. Dissertation, 274 pp. Hebei University. Hebei Province, China (unpublished).

TANG, V. 2022a. Scorpions of China: an updated checklist with comments on some taxonomic issues (Arachnida: Scorpiones). *Euscorpius*, 355: 1–18.

TANG, V. 2022b. A new species of genus *Scorpiops* Peters, 1861 from Yunnan Province, China, with a preliminary review on its congeners in Yunnan (Scorpiones: Scorpiopidae). *Euscorpius*, 360: 1–45.

TANG, V. 2022c. Reanalysis of the Yunnan population of *Scorpiops kubani* (Kovařík, 2004) with a description of a new species, *Scorpiops lowei* sp. n. (Scorpiones: Scorpiopidae). *Euscorpius*, 361: 1–22.

TANG, V. 2023. Non-aggressive competition between males of *Srilankametrus yaleensis* (Kovařík et al., 2019) (Scorpionidae), and other types of agonistic behavior observed in scorpions. *Euscorpius*, 368: 1–17.

TRIANA, F., F. BONILLA, A. ALFARO-CHINCHILLA, C. VÍQUEZ, C. DÍAZ, C. & M. SASA. 2022. Report of thanatosis in the Central American scorpions *Tityus ocelote* and *Ananteris platnicki* (Scorpiones: Buthidae). *Euscorpius*, 359: 1–5.

VACHON, M. 1974. Etude des caractères utilisés pour classer les familles et les genres de Scorpions (Arachnides). 1. La trichobothriotaxie en Arachnologie. Sigles trichobothriaux et types de trichobothriotaxie chez les scorpions. *Bulletin du Muséum National d'Histoire Naturelle, Paris*, (3), 140 (Zool. 104), mai-juin 1973: 857–958.

YIN, S.-J., Y.-F. ZHANG, Z.-H. PAN, S.-B. LI & Z.-Y. DI. 2015. *Scorpiops ingens* sp. n. and an updated key to the *Scorpiops* from China (Scorpiones, Euscorpiidae, Scorpiopinae). *ZooKeys*, 495: 53–61.

YTHIER, E. 2019. A new species of *Euscorpiops* Vachon, 1980, from China (Scorpiones, Scorpiopidae). *Bulletin de la Société entomologique de France*, 124(2): 189–196.

ZHU, M.-S., L. ZHANG & W. R. LOURENÇO. 2007. One new species of scorpion belonging to the genus *Euscorpiops* Vachon, 1980 from South China (Scorpiones: Euscorpiidae, Scorpiopinae). *Zootaxa*, 1582: 19–25.